NASA CR- 143692

ATLANTIC
SCIENCE CORPORATION

Scientific Research
Scientific Consultation
Computer Services

(NASA-CR-143692) INVESTIGATION OF THE IONOSPHERIC FARADAY ROTATION FOR USE IN ORBIT CORRECTIONS (Atlantic Science Corp., Indialantic, Fla.) 113 p HC $5.25 CSCL 03B

N75-17873

Unclas
G3/46 11060

GENERAL OFFICE: 1701 North A1A • Indialantic, Florida 32903 • Telephone: 305/723-8779
BRANCH OFFICE: P.O. Box 636 • Seabrook, Maryland 20801 • Telephone: 301/459-1692

INVESTIGATION OF THE IONOSPHERIC FARADAY ROTATION FOR USE IN ORBIT CORRECTIONS

ASC 74-F-016

INVESTIGATION OF THE IONOSPHERIC FARADAY ROTATION FOR USE IN ORBIT CORRECTIONS

by

Sigrid K. Llewellyn
Rodney B. Bent
George Nesterczuk

NASA Contract NAS5-21972

December 1974

Atlantic Science Corporation
P. O. Box 3201
Indialantic, Florida 32903

TABLE OF CONTENTS

LIST OF FIGURES

LIST OF FIGURES (con't)

LIST OF TABLES

1.0 Computation of the Faraday Factor

For use in orbit corrections, the Faraday rotation which is effected by both the earth's magnetic field and the ionosphere, has to be reduced to the ionospheric influence alone. The equations relating the Faraday rotation angle along the angular path to the vertical electron content are as follows:

$$\Omega = \frac{K}{f^2} \int_0^{h_u} B \cos\theta \sec\chi N \, dh = \frac{K}{f^2} \overline{M} \int_0^{h_u} N \, dh = \frac{K}{f^2} \overline{M} N_T = \frac{I}{F} N_T$$

where

Ω	=	rotation angle in radians
K	=	2.36 = constant
f	=	frequency in hertz
B	=	magnetic field strength in gauss
θ	=	angle between direction of propagation and magnetic field
χ	=	zenith angle
N	=	electron density in e/m^3
h	=	height above surface of earth in m
$\overline{M}$	=	mean value of ($B \cos\theta \sec\chi$)
N_T	=	vertical total electron content in e/m^2 column
F	=	Faraday rotation factor in $1/(m^2$ radians)
h_u	=	upper integration limit

In practice the measured amount of polarization twist, Ω, is converted to an equivalent vertical total electron content by removing $B \cos\theta \sec\chi$ from under the integral sign and replacing it with a mean value. Then:

$$\Omega = \frac{K}{f^2} \overline{M} \int_0^{h_u} N dh$$

where $\overline{B \cos\theta \sec\chi} = \overline{M}$ is computed in the following manner. A typical N(h) profile is assumed and calculations of the mean value $\overline{M}$ are found by computing:

$$\overline{M} = \frac{\int_0^{h_u} B \cos\theta \sec\chi \, N \, dh}{\int_0^{h_u} N \, dh}$$

The integrals are evaluated in computer mode by generating the electron density N and the function ($B \cos \theta \sec \chi N$) at various height intervals and numerically integrating. Both Simpson's parabolic rule and Gaussian quadrature have been used. The electron density at each height h is calculated by the worldwide Bent Ionospheric profile model (Reference 1). Each parabolic and exponential segment of the profile was integrated separately with a varying number of points to achieve maximum accuracy. A total of 23 points was used to evaluate the integrals by Gaussian quadrature. The components of the magnetic field strength are obtained by a spherical harmonic analysis routine as described by Chapman and Bartels (Reference 2) which uses the coefficients of Epoch 1960 given by Jensen and Cain (Reference 3). The assumption of straight line propagation through a spherically stratified ionosphere was made. No bending corrections were calculated as this would have required a prohibitive amount of computer time, and at a frequency of 140 MHz, bending is a second order effect. Given the straight line propagation assumption the zenith angle at each height h then becomes a function of the ground elevation angle, and the angle θ is calculated using the station and satellite positions and the direction of the magnetic field.

In the following investigations the Faraday rotation factor F is the computed quantity, giving the direct conversion from angular measurement to vertical content, $N_T = F\Omega$. A frequency of f=137 MHz is used to compute $F = f^2/K\overline{M}$, and the conversion factor is expressed in units of $1/m^2$ degrees.

2.0 Influence of Various Parameters on the Faraday Factor

The effects of many different conditions on the Faraday factor have been investigated to gain a better understanding of the variations and to test out the possibilities for mapping the factors. Variations with local time and season have been looked into as well as with magnetic latitude, elevation and azimuth angles. Typical day to day fluctuations of sudden increase and decrease in the ionospheric density and height have been imposed on the Faraday factor. The conditions and effects of the angle between the direction of propagation and the magnetic field have been examined. The influence of the high altitude topside extension of the ionospheric model and the importance of the upper integration limit in computing the factors have been studied.

2.1 Diurnal and Seasonal Influence

Test data was generated at 4 hour intervals for three different stations spaced at 10, 39, and 80 degrees magnetic latitude. Table 1 summarizes the computed values of f_oF2, vertical electron content, and Faraday rotation factors resulting from integrations carried out to 1000, 2000, and 3000 km in height. Normal diurnal influences are causing changes of 2 to 6% in the Faraday factors.

Figure 1 shows the predicted monthly mean diurnal curves of the Faraday factors for the station Honolulu observing the ATS1 satellite during March, June, September, and December of 1968. The very definite changes of the factors with season amount to 3.1% considering the diurnal mean values for June and December, and are as high as 8.5% at 20 hours.

2.2 Effect of Sudden Changes in Critical Frequency and Ionospheric Height

The day to day changes that occur in the ionosphere cause increases and decreases in critical frequency that typically amount to $\pm$ 25% of the monthly mean and also shifts in the ionospheric height of the order of $\pm$ 100 km. Such conditions were simulated for the three stations at 10, 39, and 80 degrees

magnetic latitude, and the Faraday factors along the vertical paths were examined. Deviations of $\pm$ 25% from the predicted f_oF2 greatly effect the electron content, but only have a very small influence on the Faraday factor. 1.3% was the maximum change in the factor and most of the cases showed less than 1% variation; an example is given in Figure 2. Raising and lowering the height of a fixed ionospheric profile has no effect on the electron content, but causes a noticeable change in the Faraday factor from 4 to 6% of the original value. Figure 3a is a plot of the diurnal variation of the factors for the predicted profile height as well as for profiles 100 km higher and lower.

These first results were strictly for cases where the signal is received along the vertical path. In addition, however, a number of selected tests were performed for angular incidence with elevation angles ranging from 0 to 74 degrees. The striking results deviate considerably from the vertical case and are summarized in Figure 3b and Tables 2a-c. Time, station, and observation angle information are tabulated along with the critical frequency, the height at the maximum electron density, the vertical electron content, and the Faraday factor. For the situations where f_oF2 and the height were increased or decreased, the percentage differences of the new electron content and Faraday factor with respect to the basic predicted values are listed. Again, changes in f_oF2 greatly effect the vertical content by up to 80%, but only have a minor influence on the Faraday factor, causing mostly a percent difference of less than 2% and a maximum deviation of 6.3%. The percent differences in the Faraday factor due to height changes are, however, very large in many instances. For one 0° elevation case the variation is about $\pm$ 33%, for a 60° elevation case it is $\pm$ 19%, and for Huancayo observing ATS3 at 74° elevation the height changes cause $\pm$ 12 % variation in the Faraday factor. Several cases also yield smaller percentages of $\pm$ 5 to $\pm$ 7%.

The large variations of the Faraday factor with height seem to be related with the angle θ between the direction of propagation and the magnetic field. In separate columns of Table 2 values of the angle θ are listed for heights of 100 and 1000 km, and changes of up to 55° in θ can be noted over this interval. For the vertical incidence θ only varies by less than 1% and

the Faraday factors by 4 to 6% for the height test. For large variations in θ which can occur along an angular path, and for close approaches of θ to 90 degrees, but not so close as to yield the Faraday equation invalid, the height changes cause great variations in the Faraday factor.

2.3 Effects of Magnetic Latitude, Elevation and Azimuth

The diurnal curves of the Faraday factors for magnetic latitudes spaced at 10, 39, and 80 degrees and for observations along a vertical path are plotted in Figure 4. The diurnal variation of the factor is small compared to the changes with magnetic latitude. The Faraday factor basically increases in a non-linear fashion with decreasing magnetic latitude, yielding a large discrepancy between the values for mid and polar latitudes and the values close to the equator. The daily mean value of 15.1×10^{14} at 10 degrees that is much larger than the values of 3.8 and $3.0 \times 10^{14}/m^2$ deg. at 39 and 80 degrees respectively.

For the same three stations the Faraday factors along a multitude of angular paths were examined at fixed times, selected such that the hourly factors approximately reflected the diurnal mean values. Data was generated at 8 different azimuth angles starting at 0 degrees and increasing in 45 degree steps. For the magnetic latitudes of 80, 39, and 10 degrees, Figures 5a, b, and c show the variation of the Faraday factor with azimuth at elevation angles of 5, 10, 30, 45, 60 and 90 degrees elevation. The curves for every single elevation angle are of a sinusoidal type with an amplitude that is 0 for the 90 degree elevation curve and consistantly increases with decreasing elevation. The smallest values of the Faraday factors at any fixed elevation are obtained between 135 and 180 degrees azimuth and the maximum values are reached between 315 and 360 degrees azimuth for the three stations that were selected on the 279.4 degree geographic longitude line. The minimum and maximum values are to be expected more exactly in the southern and northern direction for stations along the longitude line that connects the geographic and magnetic poles, since along it the azimuth angles with respect to both coordinate systems would be in closer agreement. In the same manner the minimum and maximum

values of the Faraday factors could occur at azimuth angles deviating more from the southern and northern direction for stations along geographic longitude lines further displaced from the magnetic pole. The maximum difference in the Faraday factors between the 5 and 90 degree elevation angles increases from 1.0×10^{14} to 2.4×10^{14} to $12.8 \times 10^{14}/m^2$ deg. for 80, 39 and 10 degrees magnetic latitude respectively. The variation with azimuth is the dominant influence on the Faraday factor except at very high elevations, encompassing the whole scale of possible values. This variation is due almost totally to the changing magnetic field angles for different azimuths.

Tables 3a-c present the variation of the Faraday factors with azimuth for the same three stations at elevation angles of 90, 45, and 10 degrees. Critical frequency and vertical electron content are listed as well and the integration in the computations is carried out to three different heights, 1000, 2000, and 3000 km.

2.4 Variation of the Angle Theta and Directional Changes in Polarization Twist

Several cases in Tables 3a-c are marked by an asterisk, denoting that the Faraday factors are not useable. In the same instances there are missing points in Figures 5b and c. The angle θ between the direction of propagation and the magnetic field passed through 90 degrees along the path, at the height indicated behind the asterisk, yielding the Faraday equation invalid. Equivalent to such a mathematically undefined case is a physical wave that experiences polarization in one direction from the satellite down to a certain height along the path and polarization in the opposite direction below that height. The polarization twist measured is smaller than the total absolute amount of polarization since contributions in reversed directions cancel out. Thus the measurement is not representative of the ionosphere between the satellite and the station, and the Faraday rotation equipment is of no use in these particular instances.

To further investigate at which locations and in which directions these undefined cases occur, graphs of the angle θ at heights between 100 and 1000 km along the wave path were plotted for 8 directions in azimuth starting with

0 degrees and increasing in 45° intervals, and for 6 elevation angles of 0, 15, 30, 45, 60, and 75 degrees. The data was produced for a multitude of stations at magnetic latitudes from 0 to 90 degrees at 15° steps along the magnetic longitude lines of 0, 90, 180, and 270 degrees. Figures 6a-d show the graphs selected at 0, 30, 60, and 90 degrees magnetic latitude and 0° magnetic longitude, and Figure 6e at 0° magnetic latitude and 90° magnetic longitude.

In Figure 6a for example at 0° elevation and below 1000 km height, the angle θ passes through 90° in a direction slightly north of west and of east. At 15° elevation in Figure 6b, θ crosses 90° in all directions between northeast and north at heights from 250 to 550 km, in all directions between northwest and north at heights from 400 to 550 km, and in directions slightly east of northeast and slightly west of northwest at heights somewhere below 250 and 400 km respectively. For the station at 60° magnetic latitude in Figure 3c, the angle θ remains larger than 90° in all directions and for all heights, permitting good Faraday rotation data to be reduced from all over the sky.

The following trend becomes apparent: Along the magnetic equator the angle θ passes through 90° below 1000 km height basically in eastern and western directions at all elevations. The further north the station is located, however, the more the directions at which θ crosses 90° shift from east and west toward north, and only in the lower elevation angles can the change of θ through 90° be observed. For stations south of the magnetic equator θ crosses 90° in southern, southeastern and southwestern directions. In Figure 6e for a station on the magnetic equator observing at 0° elevation it can be seen, however, that θ passes through 90° not in the eastern and western direction, but in the southern direction and slightly east and west of south. This occurs because the station coordinates are chosen for the dipole magnetic field and actually fall south of the true earth's magnetic equator.

The relationship between the geographic and the <u>true</u> magnetic coordinates is rather complex and the azimuth angle measured clockwise from geographic north does not easily fit into the irregular true field pattern; thus there exists no short and simple tabulation relating the geographic latitude and longitude

of the station and the elevation and azimuth angle of the observation to the occurrence of the angle θ passing through 90 degrees below 1000 km height. However, the general trend of occurrence can be considered as a first estimate, and will in many cases, eliminate the necessity for accurate determination of the angular conditions. For example, all stations that are located outside the equatorial region extending from about 12° north to 18° south, which is the range of the earth's magnetic equator, and are observing a geostationary satellite, remaining within a few degrees of the geographic equator, will not encounter the situation where θ passes through 90° below 1000 km height. The Faraday observations will be useful for ionospheric content reduction all over the visible sky. For stations within the equatorial band the relative locations of the station and satellite with respect to the magnetic equator might yield enough information for the decision whether careful examination and detailed computations for the particular case are necessary or not.

2.5 Effects of Additional Topside Model Layers

The latest improvement to the Bent ionospheric program was the modeling of 2 additional topside exponential layers, reaching from 1000 to 2000 and from 2000 to 3000 km height, above the existing 3 topside exponential layers. The complete model with 5 exponential topside layers was used in all prior tests for this investigation. To check out the influence of the high altitude topside extension of the ionospheric model on the computation of the Faraday factors, the data cases presented for the complete model in Table 1 and Tables 3a-c were recomputed using the 3 topside layer version of the model. Comparisons were performed for the cases where integration was carried out to 2000 km height, and it was found that the difference between the corresponding Faraday factors is very small. The use of the 5 layer versus the 3 layer model caused an increase in the vertical electron content on the average of 1.8% and in the extreme case of 2.9%; the Faraday factor only incrased by 0.7% on the average and by 1.9% in the maximum case. The influence on the Faraday factor is even smaller than the influence on the electron content because of the effect

of the magnetic field that decreases in strength with increasing altitude. The added model layers can, in some instances, enlarge the vertical electron content considerably more, as is apparent from the results of the following tests in Table 4. The effect on the Faraday factors though is quite a bit smaller.

2.6 Variation of the Integration Limit

Important for the correct determination of the Faraday factor converting the polarization data to vertical electron content is the proper height selection for the integration limit in the Faraday equation in Section 1.0. Detailed studies have already been performed on this subject in the past by Klobuchar and Mendillo, (Reference 4.). The argument brought forward was that the Faraday factor is in error if the integration is carried out to the satellite altitude. Instead the integration should only be carried out to heights above which the remaining amount of polarization is less than the absolute experimental error. At most observation sites, the equipment induces errors of ± 10° and this portion of rotation can occur at heights above 1000 to 3000 km. The recommended approach was to compute Faraday factors for porfiles up to 1000 km for converting the measured rotation angles to vertical electron content and to add to that amount a high altitude contribution of electron content in order to come up with the total electron content.

This concept seems to be substantiated by several tests computing the vertical electron content and the Faraday factors and integrating to heights of 1000 km as well as to 2000 and 3000 km. Table 4 lists the results for a station at 15° latitude and 0° longitude observing along the vertical path at 2 hour intervals, presenting the various integrated values and in addition the percentages by which the vertical content values and Faraday factors increase when stepping from the 1000 km to the 2000 km integration limit and from the 1000 to the 3000 km limit. Tables 1 and 3a-c include similar test results. Keeping in mind that the Faraday factor is proportional to the

vertical content $N_T = F\Omega$, we find that raising the integration limit from 1000 to 3000 km yields on average electron content values that are 10.8% larger and Faraday factors that are 2.9% larger than their respective values for the 1000 km integration limit. It is apparent that a sizable portion of the total electron content can be accumulated above 1000 km, while the corresponding increase in the rotation angle is clearly below the size of the experimental error.

Upon closer examination, however, this argument of fixing the upper integration limit of the integrals computing the Faraday factors does not hold up. A number of tests were performed computing total electron content and Faraday rotation from ground up to 33000 km, for various combinations of high, medium, and low magnetic latitude and solar activity conditions and different seasons. Electron content and Faraday conversion factors were computed for each 100 km height interval. The rotation angles for the same intervals were formed from these values, and the total values were obtained by summing over the contributions of all the segments.

Figure 7 shows the integrated electron content and Faraday rotation from ground up to height h as a percentage of the total values integrated to a satellite height of 33000 km for two selected cases. Faraday rotation is accumulated more rapid at lower heights than electron content; in the given cases 88 and 95% of the rotation are accumulated at 1000 km compared with 78 and 91% of the total content. The same condition is illustrated in Figure 8, only this time considering the percent of the total integrated values in each 100 km interval, and plotting the difference between these electron content and Faraday rotation contributions as a function of the interval height. For all intervals below 500-600 km the contributions to the total rotation exceed the corresponding percentages of electron content, but at the higher altitudes the contributions to the total content are considerably larger. This seems to indicate that the low altitude as well as the high altitude portion have to be included in the integration process for

the Faraday conversion factor, even though the amounts we are talking about are only of the same order or less than the instrumental errors. Excluding contributions above 1000 km from the computation by integrating only to a height of 1000 km and not all the way to the satellite would introduce a one-sided bias, and the resultant total content values would be consistently too small. The typical measurement errors of say $\pm 10\%$ may become +2 to -18% if this one-sided bias is not taken into account.

3.0 Conclusions

The results from the Faraday factor investigation point out the importance for modeling the factors correctly with respect to the station position where the magnetic latitude is of most significance and with respect to the direction of observation, since the elevation and azimuth angles determine the direction at which the magnetic field lines are intersected as well as the location at which the wave passes through the densest part of the ionosphere. For low accuracy requirements it might be acceptable to neglect the specific seasonal and diurnal influences since they only produce variations of about 2 to 6% in the Faraday factors. High precision in the high altitude end of the ionospheric model is not necessary, just as the day to day prediction errors in f_oF2 do not effect the Faraday factors to a great extent. However, prediction errors in ionospheric height, which could easily be caused by sudden day to day changes can have a significant influence on the Faraday factors. The predicted values of the height of maximum electron density obtained from the Bent Model are on average within the accuracy of the measured values, which considering instrumental and reduction techniques, are about 15 km. However, the day to day variations are quite a bit larger, and on occasion, deviations in the predictions of 100 km from the height measurements have been noted particularly in the equatorial region. The resulting errors in the Faraday factor are typically 5% for paths at vertical incidence. But for angular paths errors of around 30% in the Faraday factor might occur resulting in proportionally large errors in N_T, whenever the condition occurs that the

propagation angle θ falls between about 80 and 100° along a low elevation path.

To avoid errors in the computation of the Faraday factor, the angle θ between and the direction of propagation and the earth's magnetic field lines has to be carefully monitored along the ray path. When the condition $89.5° \leqq \theta \leqq 90.5$ occurs, the equation relating the Faraday rotation angle and vertical electron content no long holds true. When θ passes through 90° at a certain height, the wave experiences rotation of the polarization vector in one direction from the satellite down to that height, and rotation in the opposite direction below that height. Contributions to the rotation of the polarization vector in reversed directions cancel out, thus the measurement is not representative of the ionosphere between the satellite and the station.

There has been some question as to what the upper integration limit of the integrals computing the Faraday factors should be. In order to avoid any one-sided biases that might result in total electron content values being consistently too small and creating in effect unbalanced measurement errors of maybe +2 to -18%, the integration process should not be terminated at some fixed height, but carried out from ground all the way to the height of the satellite. In this case typical errors would be about $\pm$10%.

The possibility of mapping the Faraday factors on a worldwide basis was examined as a simple method of representing the conversion factors for any possible user. After the preceding investigations, however, it does not seem feasible. The complex relationship between the true magnetic coordinates and the geographic latitude, longitude, and azimuth angles eliminates the possibility of setting up some simple tables that would yield worldwide result of sufficient accuracy. If tabular results for specific stations are desired, however, such tables could be easily produced or could be represented in graphic form.

Table 1. Diurnal Variation of the Faraday Factor for 3 Stations with Integration Carried out to 1000, 2000, and 3000km Height

								VEC(1.E15 E/M**2)			FAR.FAC.(1.E11/(DEG*M**2))		
LAT.	LON.	DATE	UT	ELEV	AZIM	FOF2	INTEGRATED TO:	1000	2000	3000	1000	2000	3000 KM HEIGHT
-1.2	279.4	67 3 16	.0	90.0	0.	12.3		508.0	529.9	538.6	15100	15293	15422
-1.2	279.4	67 3 16	4.0	90.0	0.	11.3		378.0	389.2	393.7	14771	14909	14998
-1.2	279.4	67 3 16	8.0	90.0	0.	6.5		118.5	124.6	127.4	14704	14942	15117
-1.2	279.4	67 3 16	12.0	90.0	0.	6.7		147.4	156.6	160.8	14780	15067	15276
-1.2	279.4	67 3 16	16.0	90.0	0.	11.4		531.4	567.5	581.9	15289	15582	15780
-1.2	279.4	67 3 16	20.0	90.0	0.	12.7		678.0	718.9	735.2	15220	15484	15661
28.6	279.4	67 3 16	.0	90.0	0.	8.5		208.2	216.6	218.9	3678	3731	3753
28.6	279.4	67 3 16	4.0	90.0	0.	5.4		83.5	90.9	93.2	3817	3926	3978
28.6	279.4	67 3 16	8.0	90.0	0.	4.8		66.9	73.0	74.9	3796	3909	3964
28.6	279.4	67 3 16	12.0	90.0	0.	6.2		121.3	129.6	132.0	3705	3792	3831
28.6	279.4	67 3 16	16.0	90.0	0.	10.4		365.4	381.6	385.9	3685	3742	3766
28.6	279.4	67 3 16	20.0	90.0	0.	10.5		359.2	376.5	381.2	3716	3777	3804
68.6	279.4	67 3 16	.0	90.0	0.	5.8		123.7	137.5	139.8	2906	2994	3019
68.6	279.4	67 3 16	4.0	90.0	0.	4.8		85.1	95.8	97.7	2923	3020	3049
68.6	279.4	67 3 16	8.0	90.0	0.	4.2		67.4	76.9	78.6	2927	3035	3068
68.6	279.4	67 3 16	12.0	90.0	0.	4.5		84.4	95.6	97.6	2897	3000	3030
68.6	279.4	67 3 16	16.0	90.0	0.	6.0		155.1	173.6	176.7	2889	2983	3010
68.6	279.4	67 3 16	20.0	90.0	0.	6.8		200.1	223.8	227.7	2903	2996	3022

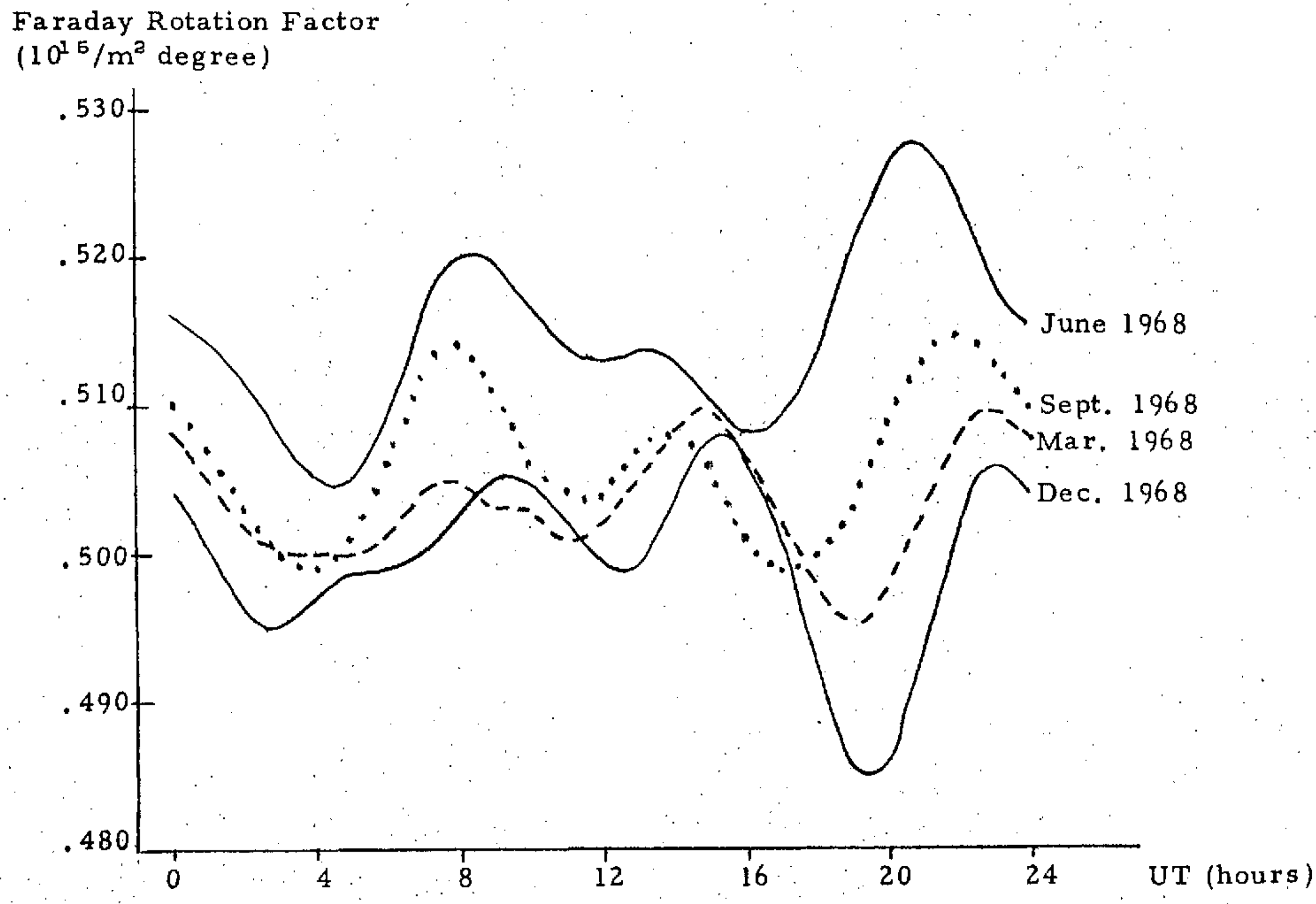

Figure 1. Seasonal and Diurnal Variation of the Faraday Factor F (equation (6)) for Honolulu Looking at an Elevation and Azimuth of 63.6° and 159.3°.

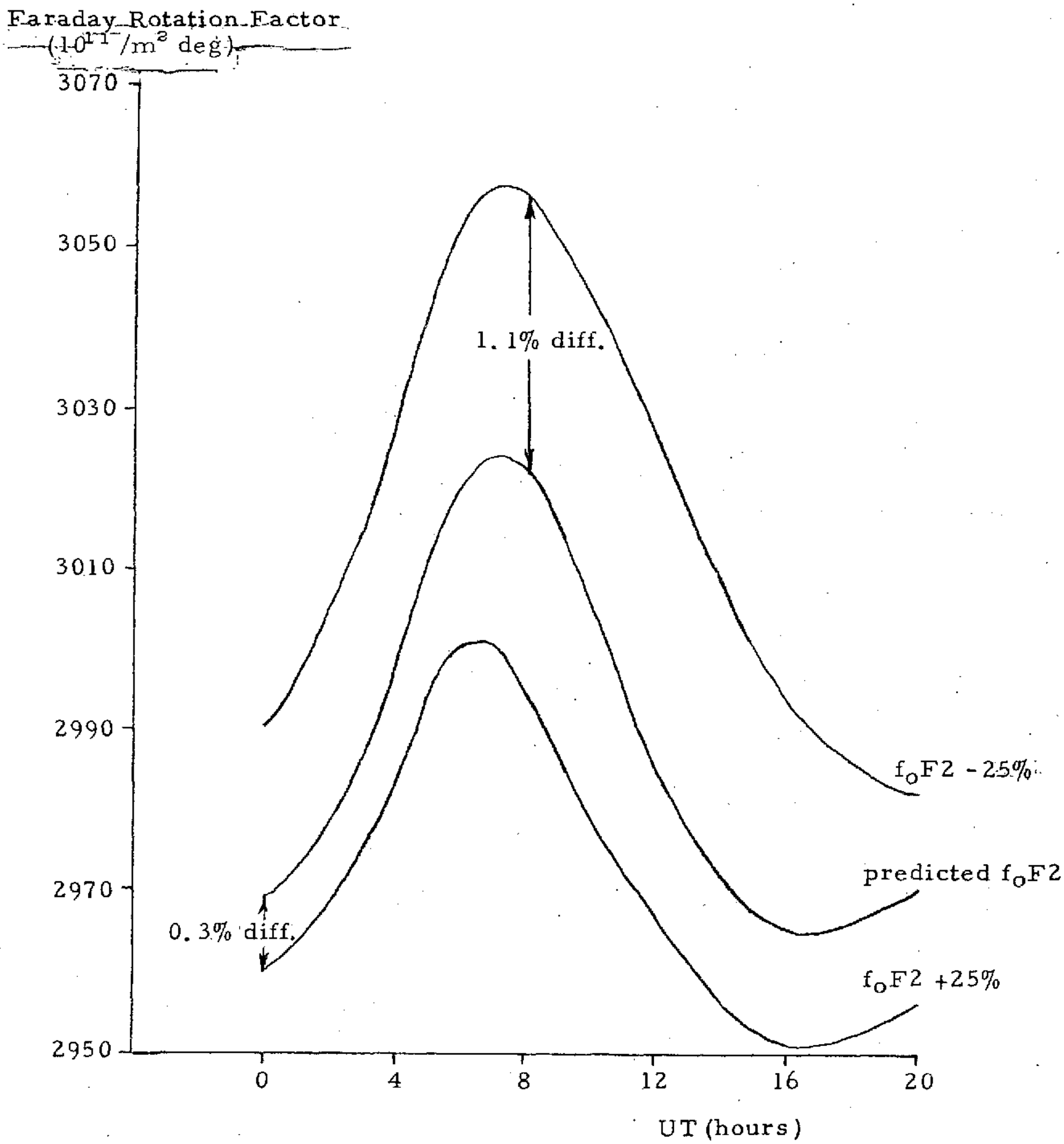

Figure 2. Effect of Increase and Decrease in f_oF2 on the Faraday Factor for a Vertical Path. Station Position = 68.6°, 279.4°, Date = 16 March 1967.

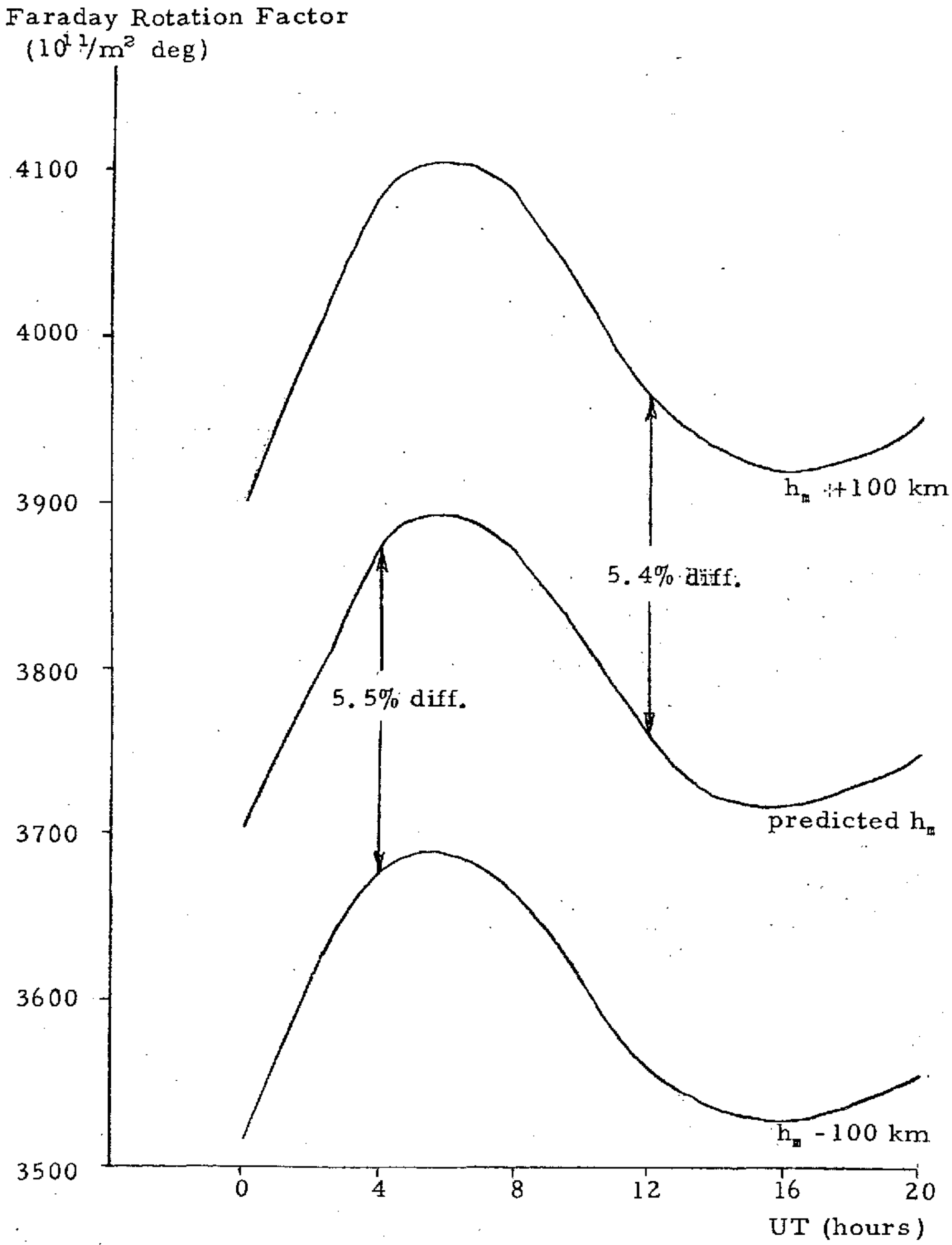

Figure 3a. Effect of Increase and Decrease in the Ionospheric Height on the Faraday Factor for a Vertical Path.
Station Position = 28.6°, 279.4°, Date=16 March 1967.

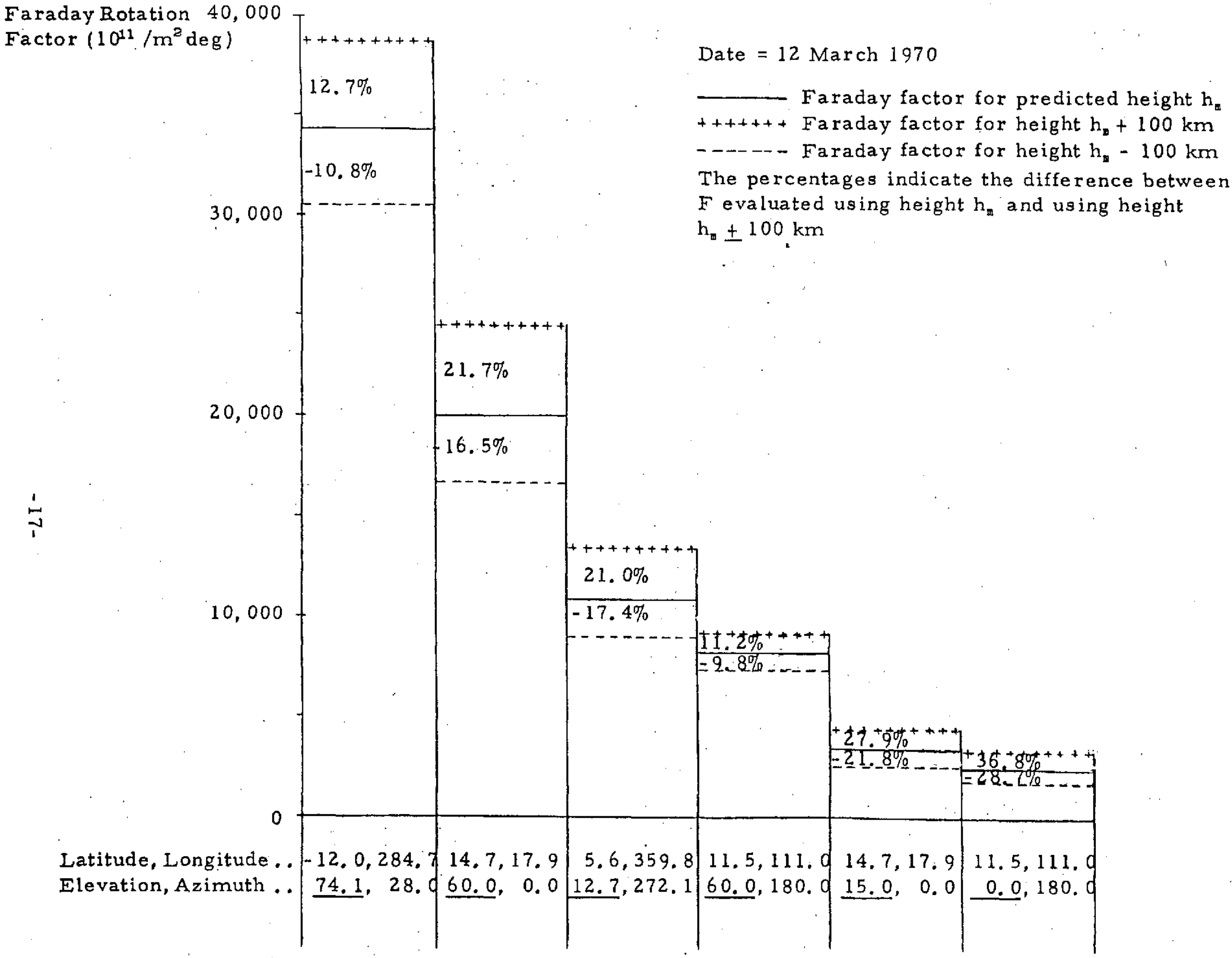

FIGURE 3b. Effect of Variation in Ionospheric Height on the Faraday Factor F for an Angular Path

TABLE 2a. EFFECT OF INCREASE AND DECREASE IN FOF2 AND HM ON THE FARADAY FACTOR FOR AN ANGULAR PATH

VERTICAL ELECTRON CONTENT (1.E15 E/M**2), FARADAY FACTOR (1.E11/(DEG*M**2))

DATE	UNIV TIME	GEOGRAPHIC LAT.	GEOGRAPHIC LON.	ELEV	AZIM	THETA AT HEIGHT 100 KM	THETA AT HEIGHT 1000 KM	FOF2	HM	VEC	%DIFF	FAR.FAC.	%DIFF
70 3 12	6.6	11.5	111.0	.0	180.0	153.6	98.2	14.4	366.	895.4		2425.	
								+25%		1611.5	80.0	2578.	6.3
								-25%		439.5	-50.9	2312.	-4.7
									+100 KM	905.9	1.2	3316.	36.8
									-100 KM	890.7	-.5	1729.	-28.7
70 3 12	12.8	14.7	17.9	15.0	.0	33.9	79.1	14.8	347.	805.9		3393.	
								+25%		1437.9	78.4	3531.	4.1
								-25%		400.3	-50.3	3297.	-2.8
									+100 KM	816.4	1.3	4340.	27.9
									-100 KM	800.7	-.6	2654.	-21.8
70 3 12	18.6	33.5	291.0	.0	270.0	101.6	130.1	11.9	332.	481.0		2467.	
								+25%		840.6	74.8	2484.	.7
								-25%		282.3	-41.3	2470.	.1
									+100 KM	488.5	1.6	2607.	5.7
									-100 KM	476.9	-.9	2368.	-4.0
70 3 12	23.8	43.9	212.3	.0	90.0	94.6	122.7	10.9	314.	379.9		3475.	
								+25%		643.2	69.3	3468.	-.2
								-25%		234.1	-38.4	3484.	.3
									+100 KM	385.7	1.5	3414.	-1.7
									-100 KM	376.5	-.9	3738.	7.6
70 3 12	6.6	11.5	111.0	60.0	180.0	125.0	111.7	10.6	455.	456.7		8260.	
								+25%		792.7	73.6	8380.	1.5
								-25%		285.6	-37.5	8282.	.3
									+100 KM	463.8	1.6	9182.	11.2
									-100 KM	453.8	-.6	7453.	-9.8
70 3 12	12.8	14.7	17.9	60.0	.0	70.4	85.5	13.1	393.	608.7		20064.	
								+25%		1075.9	76.8	20637.	2.9
								-25%		325.0	-46.6	19978.	-.4
									+100 KM	617.7	1.5	24419.	21.7
									-100 KM	604.4	-.7	16762.	-16.5

ORIGINAL PAGE IS OF POOR QUALITY

TABLE 26. EFFECT OF INCREASE AND DECREASE IN FOF2 AND HM ON THE FARADAY FACTOR FOR AN ANGULAR PATH

VERTICAL ELECTRON CONTENT (1.E15 E/M**2), FARADAY FACTOR (1.E11/(DEG*M**2))

DATE	UNIV TIME	GEOGRAPHIC LAT.	LON.	ELEV	AZIM	THETA AT HEIGHT 100 KM	1000 KM	FOF2	HM	VEC	%DIFF	FAR.FAC.	%DIFF
69 1 30	22.1	37.4	237.8	37.9	221.0	153.6	163.5	9.9	307.	292.2		2442.	
		Stanford-ATS1						+25%		472.9	61.8	2442.	-.0
								-25%		178.6	-38.9	2459.	.7
									+100 KM	297.1	1.7	2620.	7.3
									-100 KM	289.2	-1.0	2276.	-6.8
69 1 30	22.1	37.4	237.8	27.8	123.0	124.1	137.5	10.0	305.	293.5		2839.	
		Stanford-ATS3						+25%		478.1	62.9	2839.	-.0
								-25%		180.5	-38.5	2854.	.5
									+100 KM	298.5	1.7	2994.	5.4
									-100 KM	290.5	-1.0	2698.	-5.0
70 3 12	19.0	-12.0	284.7	74.1	28.0	77.1	83.3	10.9	444.	492.6		34356.	
		Huancayo-ATS3						+25%		861.5	74.9	34993.	1.9
								-25%		304.6	-38.2	34422.	.2
									+100 KM	499.9	1.5	38710.	12.7
									-100 KM	489.8	-.6	30634.	-10.8
70 3 12	18.7	42.6	289.2	40.9	177.3	149.3	163.0	11.0	330.	423.9		2400.	
		Sagamore Hill-ATS3						+25%		717.7	69.3	2409.	.4
								-25%		257.7	-39.2	2403.	.1
									+100 KM	430.1	1.5	2543.	6.0
									-100 KM	420.3	-.9	2267.	-5.6
70 3 12	14.0	5.6	359.8	12.7	272.1	74.2	81.9	11.0	449.	451.7		11067.	
		Accra-ATS3						+25%		784.0	73.6	11323.	2.3
								-25%		282.8	-37.4	11086.	.2
									+100 KM	459.1	1.6	13392.	21.0
									-100 KM	448.4	-.7	9141.	-17.4

TABLE 2a. EFFECT OF INCREASE AND DECREASE IN FOF2 AND HM ON THE FARADAY FACTOR FOR AN ANGULAR PATH

VERTICAL ELECTRON CONTENT (1.E15 E/M**2), FARADAY FACTOR (1.E11/(DEG*M**2))

DATE	UNIV TIME	GEOGRAPHIC LAT.	LON.	ELEV	AZIM	THETA AT HEIGHT 100 KM	1000 KM	FOF2	HM	VEC	%DIFF	FAR.FAC.	%DIFF
69 1 30	8.5	18.4	293.1	67.0	198.8	159.1	154.1	3.4	330.	31.8		4006.	
		Arecibo-ATS3						+25%		51.7	62.9	3994.	-.3
								-25%		17.3	-45.6	4019.	.3
									+100 KM	32.7	3.0	4269.	6.6
									-100 KM	31.2	-1.8	3763.	-6.1
69 1 30	10.5	18.4	293.1	67.0	198.8	159.1	154.1	4.4	305.	56.4		3925.	
		Arecibo-ATS3						+25%		87.2	54.5	3921.	-.1
								-25%		29.0	-48.6	3949.	.6
									+100 KM	57.7	2.3	4180.	6.5
									-100 KM	55.6	-1.4	3687.	-6.1
69 1 30	12.5	18.4	293.1	67.0	198.8	159.1	154.1	9.1	258.	230.2		3774.	
		Arecibo-ATS3						+25%		365.0	58.5	3753.	-.6
								-25%		135.4	-41.2	3797.	.6
									+100 KM	233.7	1.5	4017.	6.4
									-100 KM	228.2	-.9	3546.	-6.0
69 1 30	14.5	18.4	293.1	67.0	198.8	159.1	154.1	10.4	273.	324.5		3789.	
		Arecibo-ATS3						+25%		547.3	68.7	3800.	.3
								-25%		196.9	-39.3	3811.	.6
									+100 KM	328.9	1.4	4031.	6.4
									-100 KM	321.9	-.8	3561.	-6.0
69 1 30	16.5	18.4	293.1	67.0	198.8	159.1	154.1	10.0	318.	294.4		3910.	
		Arecibo-ATS3						+25%		477.3	62.2	3908.	-.1
								-25%		180.8	-38.6	3929.	.5
									+100 KM	299.2	1.6	4159.	6.4
									-100 KM	291.6	-1.0	3676.	-6.0

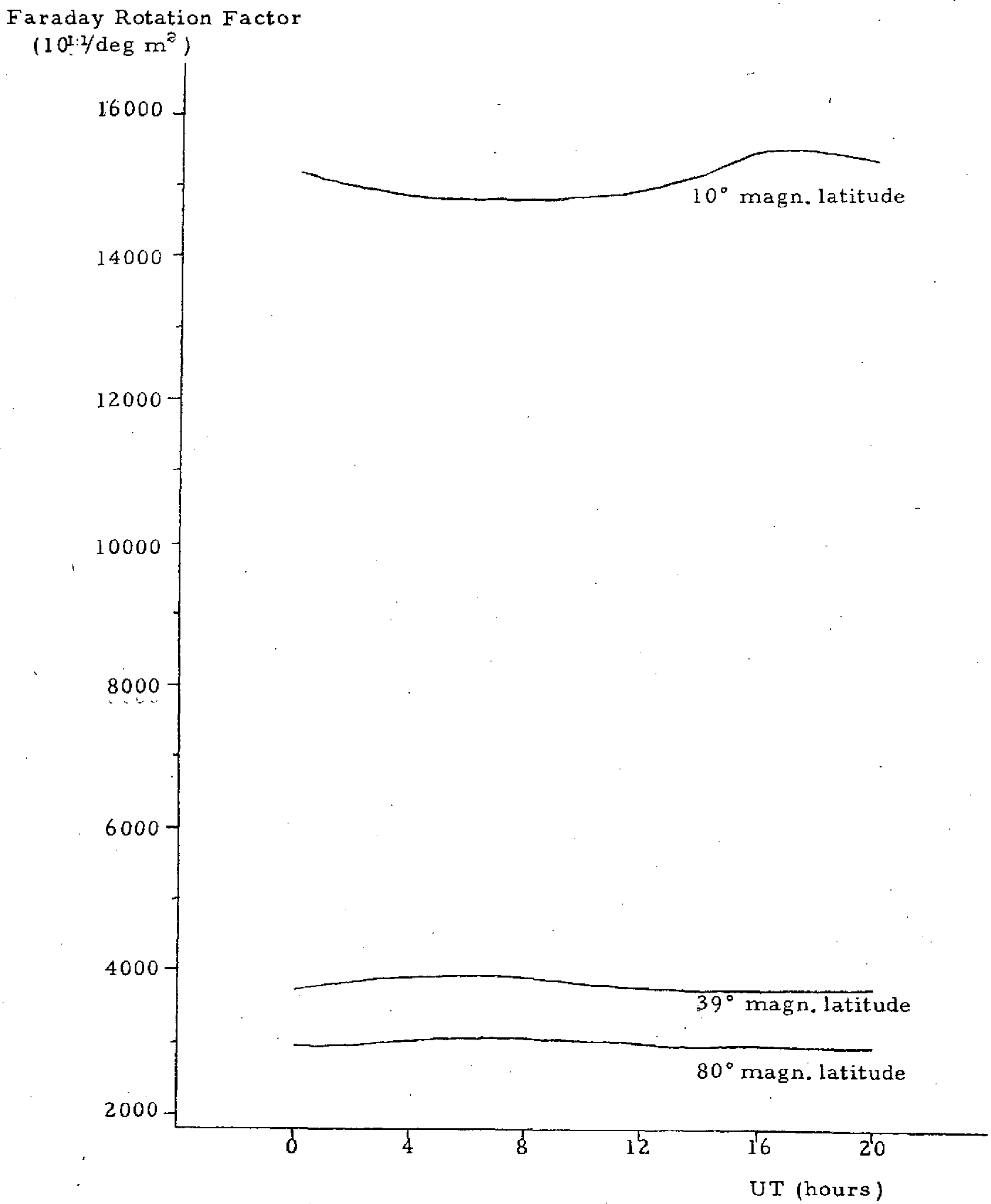

Figure 4. Variation of the Faraday Factor with Magnetic Latitude for a Vertical Path and with the Diurnal Changes on 16 March 1967.

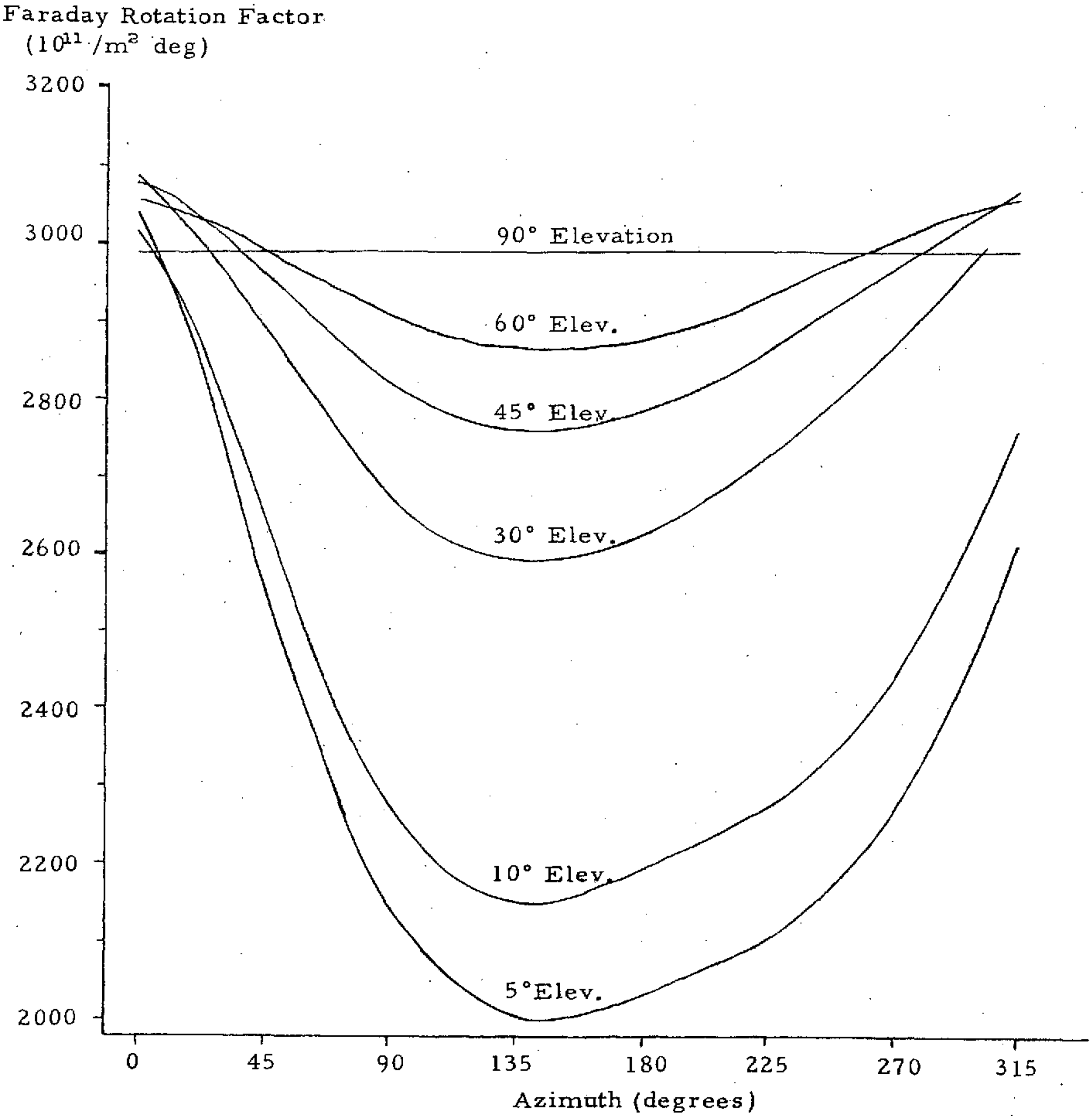

Figure 5a. Variation of the Faraday Factor with Changes in Elevation and Azimuth Angles at 80° Magnetic Latitude. Station Position = 68.6°, 279.4°, Date = 16 March 1967, UT=12 hours.

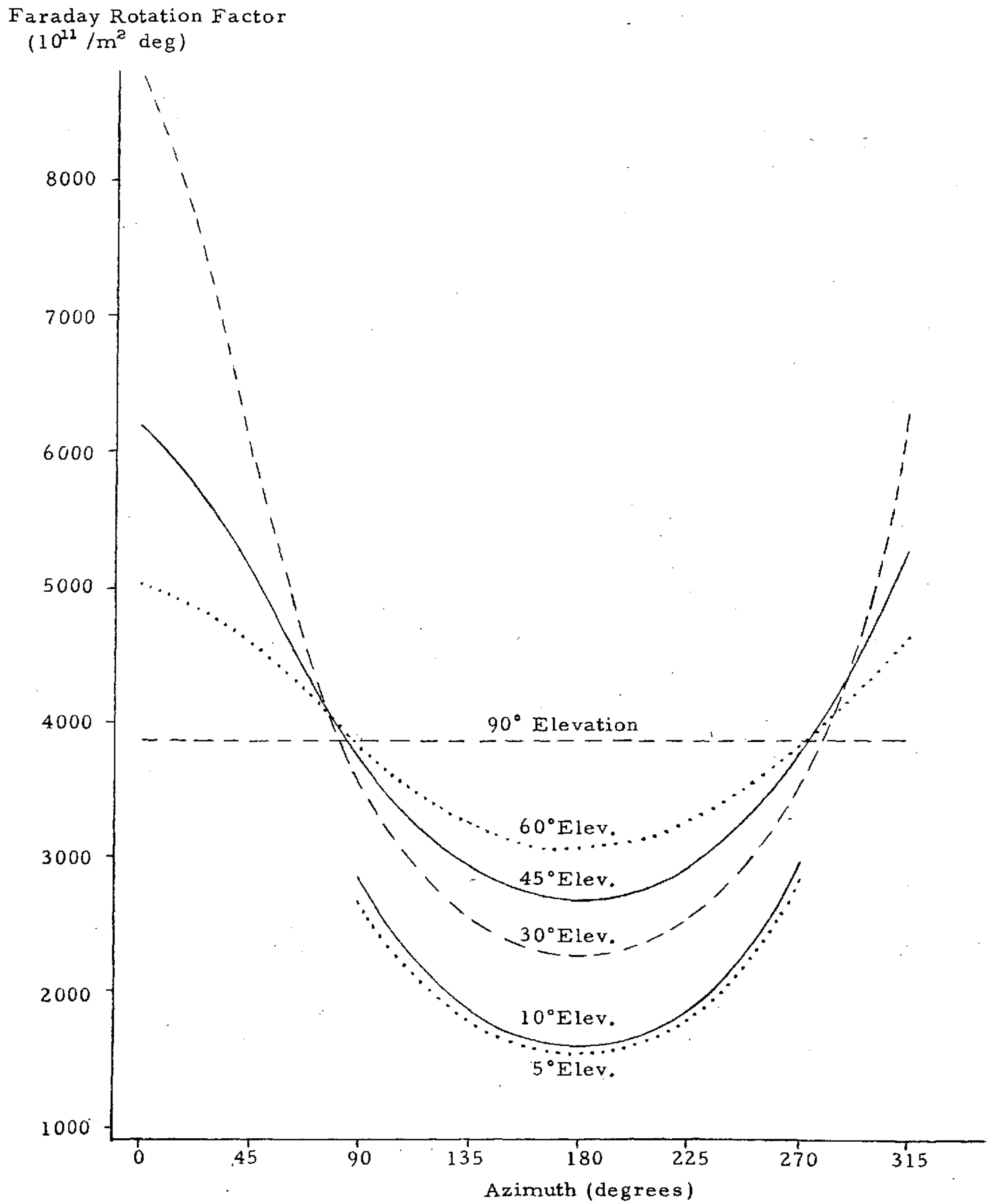

Figure 5b. Variation of the Faraday Factor with Changes in Elevation and Azimuth Angles at 39° Magnetic Latitude.
Station Position=28.6°, 279.4°, Date=16 March 1967, UT=11 hours.

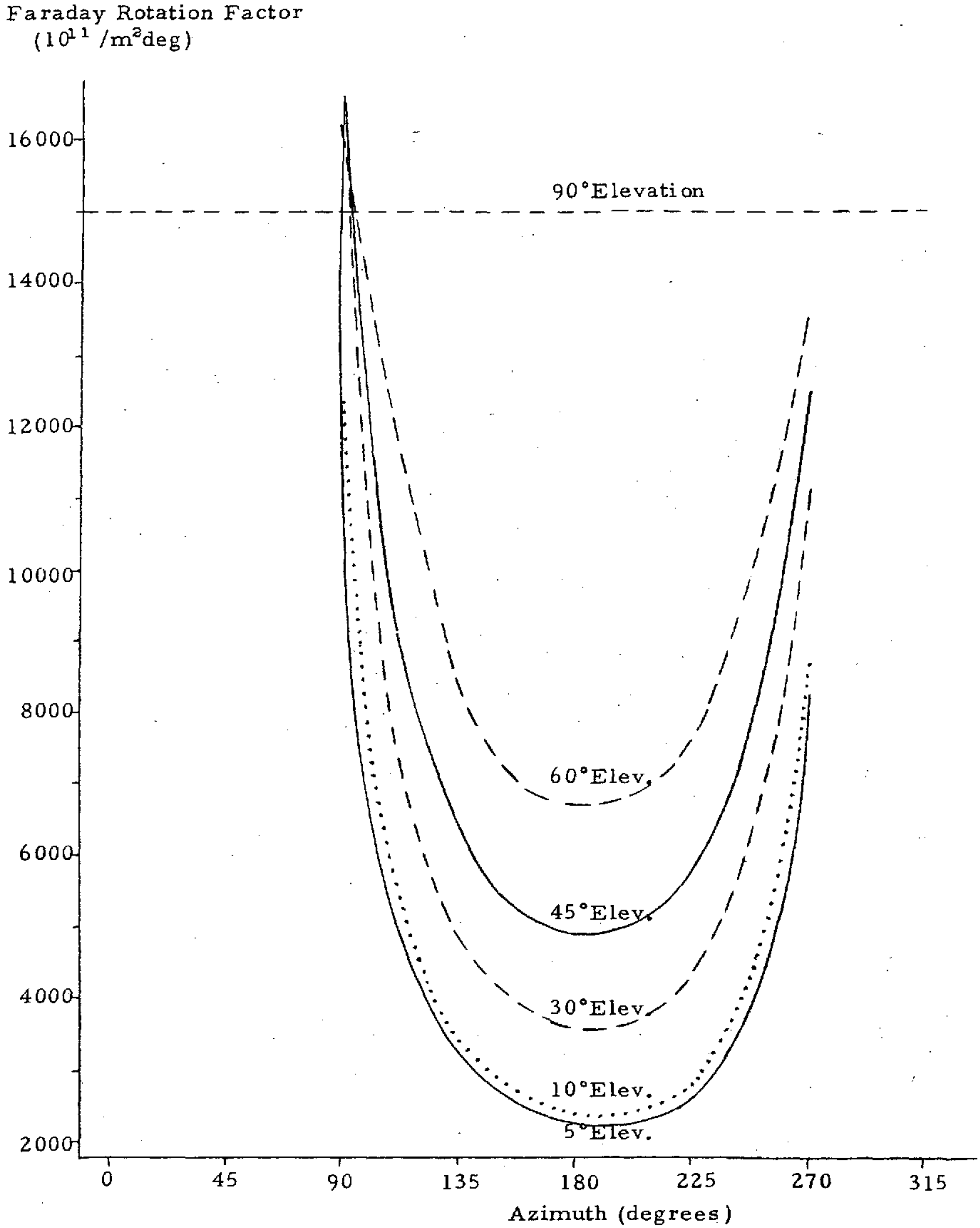

Figure 5c. Variation of the Faraday Factor with Changes in Elevation and Azimuth Angles at 10° Magnetic Latitude.
Station Position = -1.2°, 279.4°, Date = 16 Mar 1967, UT=14 hours.

Table 3a. Variation of the Faraday Factor with Changes in Elevation and Azimuth for 3 Stations with Integration Carried out to 1000, 2000 and 3000 km Height

LAT.	LON.	DATE	UT	ELEV	AZIM	FOF2	INTEGRATED TO:	VEC(1.E15 E/M**2)			FAR.FAC.(1.E11/(DEG*M**2))			
								1000	2000	3000	1000	2000	3000 KM HEIGH	
-1.2	279.4	67 3 16	14.0	90.0	0.	10.7		419.7	440.3	448.6	14901	15124	15270	
-1.2	279.4	67 3 16	14.0	45.0	0.	10.6		400.1	418.5	425.8	12874	13390	13539	* 1250 km
-1.2	279.4	67 3 16	14.0	45.0	45.	10.8		420.9	440.4	448.1	25336	25977	26074	* 825
-1.2	279.4	67 3 16	14.0	45.0	90.	10.9		440.6	462.0	470.5	16611	16753	16881	
-1.2	279.4	67 3 16	14.0	45.0	135.	10.9		437.8	459.9	468.7	6273	6432	6525	
-1.2	279.4	67 3 16	14.0	45.0	180.	10.8		422.6	444.3	453.0	4844	4980	5058	
-1.2	279.4	67 3 16	14.0	45.0	225.	10.6		407.0	427.8	436.2	5674	5828	5916	
-1.2	279.4	67 3 16	14.0	45.0	270.	10.5		397.7	417.6	425.6	12408	12637	12778	
-1.2	279.4	67 3 16	14.0	45.0	315.	10.5		392.1	410.7	418.1	37272	37958	37922	* 750
-1.2	279.4	67 3 16	14.0	10.0	0.	10.1		349.9	364.4	369.7	2867	2976	3012	* 1200
-1.2	279.4	67 3 16	14.0	10.0	45.	10.8		415.0	431.7	438.1	4730	4889	4942	* 925
-1.2	279.4	67 3 16	14.0	10.0	90.	11.3		494.7	518.4	527.8	12292	12402	12521	
-1.2	279.4	67 3 16	14.0	10.0	135.	11.0		461.9	487.8	498.2	3323	3456	3523	
-1.2	279.4	67 3 16	14.0	10.0	180.	10.8		428.3	450.3	459.0	2371	2464	2510	* 2825
-1.2	279.4	67 3 16	14.0	10.0	225.	10.2		367.8	387.0	394.7	2715	2820	2873	* 3000
-1.2	279.4	67 3 16	14.0	10.0	270.	9.8		337.5	355.7	363.0	8536	8777	8907	
-1.2	279.4	67 3 16	14.0	10.0	315.	9.7		314.7	329.6	335.3	5130	5344	5411	* 1050

* Resultant Faraday factors are not useable since the angle θ between the direction of propagation and the magnetic field crossed 90°, indicating a change in the direction of the polarization twist along the path.

Table 3b. Variation of the Faraday Factor with Changes in Elevation and Azimuth for 3 Stations with Integration Carried out to 1000, 2000 and 3000 km Height

							INTEGRATED TO:	VEC(1.E15 E/M**2)			FAR.FAC.(1.E11/(DEG*M**2))			
.AT.	LON.	DATE	UT	ELEV	AZIM	FOF2		1000	2000	3000	1000	2000	3000 KM HEIGH	
28.6	279.4	67 3 16	11.0	90.0	0.	4.6		68.7	74.9	76.9	3761	3874	3929	
28.6	279.4	67 3 16	11.0	45.0	0.	4.5		67.5	73.7	75.5	6153	6209	6252	
28.6	279.4	67 3 16	11.0	45.0	45.	4.7		73.1	79.6	81.5	5069	5155	5205	
28.6	279.4	67 3 16	11.0	45.0	90.	4.8		76.3	82.9	85.0	3630	3731	3781	
28.6	279.4	67 3 16	11.0	45.0	135.	4.8		73.9	80.4	82.5	2839	2938	2986	
28.6	279.4	67 3 16	11.0	45.0	180.	4.6		68.4	74.6	76.6	2600	2698	2745	
28.6	279.4	67 3 16	11.0	45.0	225.	4.5		64.3	70.2	72.2	2832	2935	2986	
28.6	279.4	67 3 16	11.0	45.0	270.	4.4		62.9	68.9	70.7	3655	3764	3819	
28.6	279.4	67 3 16	11.0	45.0	315.	4.4		63.8	69.8	71.6	5163	5253	5304	
28.6	279.4	67 3 16	11.0	10.0	0.	4.2		59.4	65.5	67.0	14619	12854	12612	* 300 km
28.6	279.4	67 3 16	11.0	10.0	45.	5.1		87.9	95.6	97.6	6791	6665	6679	* 150
28.6	279.4	67 3 16	11.0	10.0	90.	5.8		105.1	113.0	115.3	2829	2911	2950	
28.6	279.4	67 3 16	11.0	10.0	135.	5.3		89.6	96.6	39.0	1828	1909	1946	
28.6	279.4	67 3 16	11.0	10.0	180.	4.3		58.3	63.5	65.5	1588	1675	1719	
28.6	279.4	67 3 16	11.0	10.0	225.	4.0		49.6	54.5	56.3	1814	1915	1965	
28.6	279.4	67 3 16	11.0	10.0	270.	4.2		56.1	61.7	63.5	2929	3039	3093	
28.6	279.4	67 3 16	11.0	10.0	315.	4.0		52.4	57.9	59.3	7597	7332	7327	* 175

* Resultant Faraday factors are not useable since the angle θ between the direction of propagation and the magnetic field crossed 90°, indicating a change in the direction of the polarization twist along the path.

Table 3c. Variation of the Faraday Factor with Changes in Elevation and Azimuth for 3 Stations with Integration Carried out to 1000, 2000 and 3000 km Height.

								VEC(1•E15 E/M**2)			FAR•FAC•(1•E11/(DEG*M**2))		
LAT•	LON•	DATE	UT	ELEV	AZIM	FOF2	INTEGRATED TO:	1000	2000	3000	1000	2000	3000 KM HEIGH
68•6	279•4	67 3 16	12•0	90•0	0•	4•5		84•4	95•6	97•6	2897	3000	3030
68•6	279•4	67 3 16	12•0	45•0	0•	4•7		89•6	101•3	103•3	2993	3094	3124
68•6	279•4	67 3 16	12•0	45•0	45•	4•8		94•9	106•9	109•0	2876	2976	3005
68•6	279•4	67 3 16	12•0	45•0	90•	4•8		94•7	106•6	108•7	2741	2837	2865
68•6	279•4	67 3 16	12•0	45•0	135•	4•6		88•9	100•3	102•3	2682	2776	2804
68•6	279•4	67 3 16	12•0	45•0	180•	4•4		80•5	91•2	93•1	2706	2799	2828
68•6	279•4	67 3 16	12•0	45•0	225•	4•2		74•5	84•7	86•5	2782	2875	2905
68•6	279•4	67 3 16	12•0	45•0	270•	4•2		74•8	85•2	87•0	2889	2984	3013
68•6	279•4	67 3 16	12•0	45•0	315•	4•4		81•3	92•3	94•2	2989	3086	3116
68•6	279•4	67 3 16	12•0	10•0	0•	5•2		107•5	120•8	123•1	2902	3037	3082
68•6	279•4	67 3 16	12•0	10•0	45•	5•5		125•1	139•8	142•3	2572	2660	2687
68•6	279•4	67 3 16	12•0	10•0	90•	5•6		130•3	145•1	147•7	2208	2292	2315
68•6	279•4	67 3 16	12•0	10•0	135•	5•2		109•1	121•3	123•5	2089	2168	2191
68•6	279•4	67 3 16	12•0	10•0	180•	4•3		73•5	82•8	84•5	2131	2212	2239
68•6	279•4	67 3 16	12•0	10•0	225•	3•5		47•9	55•0	56•4	2201	2290	2322
68•6	279•4	67 3 16	12•0	10•0	270•	3•4		47•6	55•2	56•6	2360	2455	2488
68•6	279•4	67 3 16	12•0	10•0	315•	4•3		72•8	83•2	85•1	2688	2772	2805

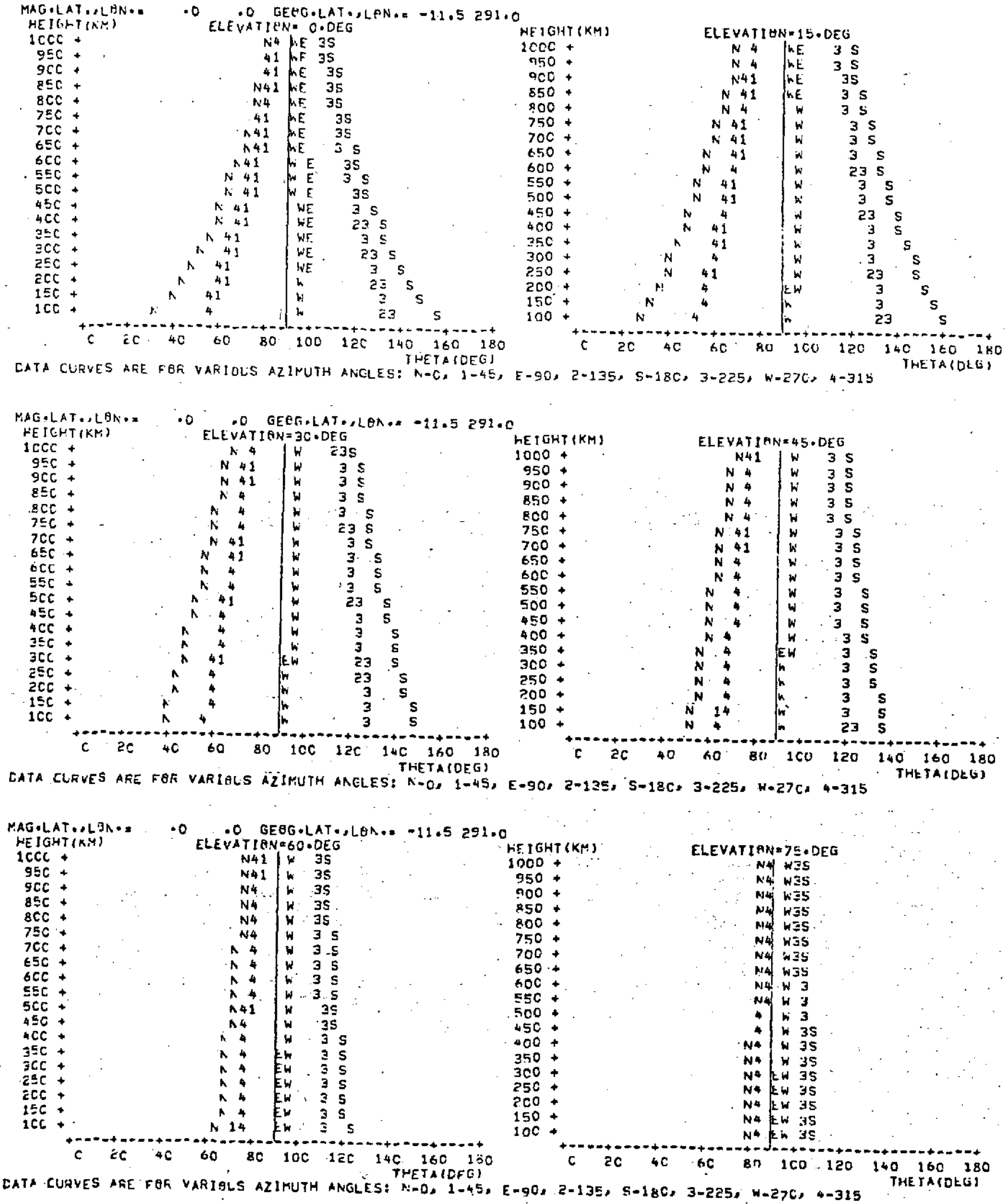

Figure 6a. Variation of the Angle θ Between the Direction of Propagation and the Magnetic Field

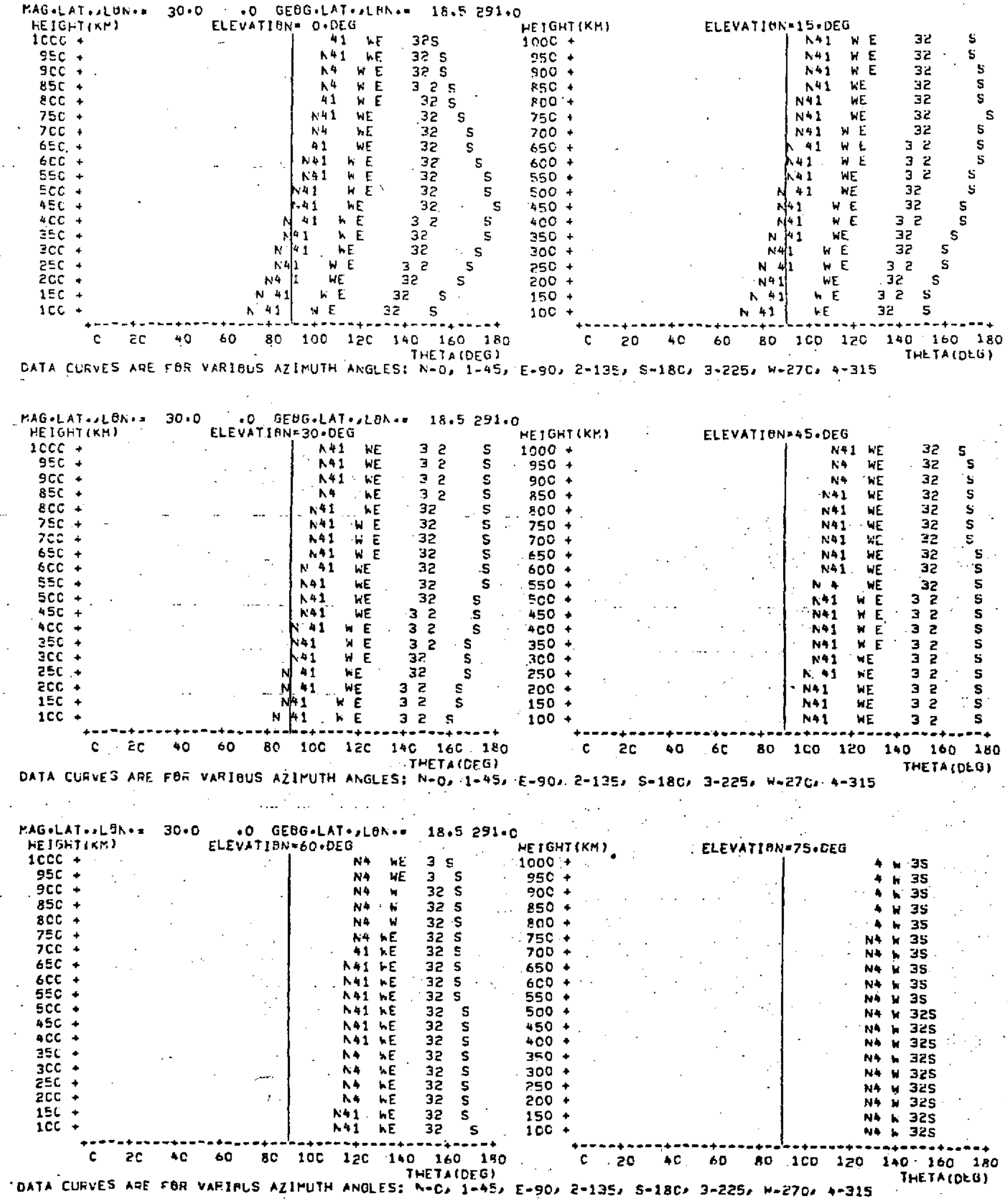

Figure 6b. Variation of the Angle θ Between the Direction of Propagation and the Magnetic Field

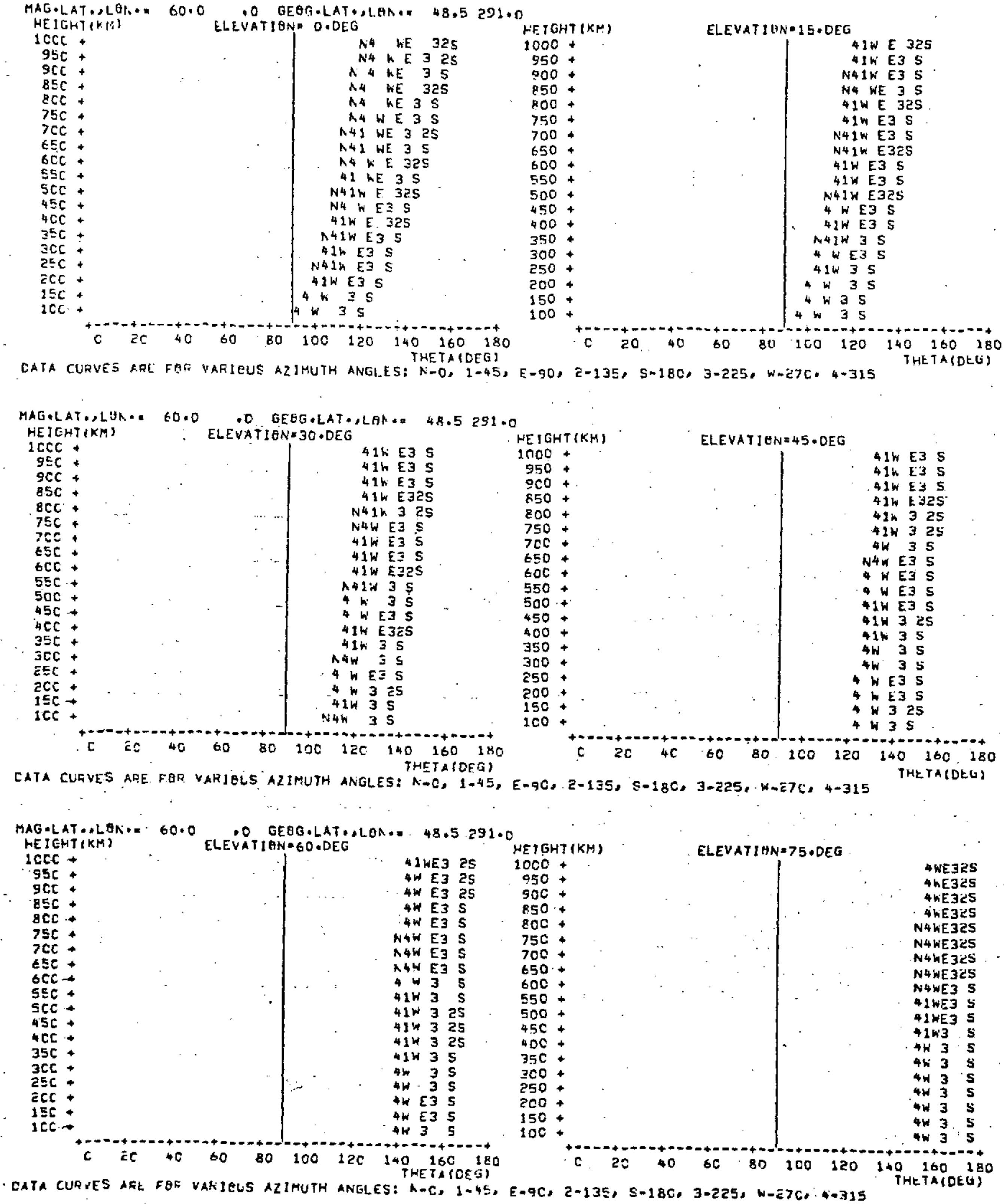

Figure 6c. Variation of the Angle θ Between the Direction of Propagation and the Magnetic Field

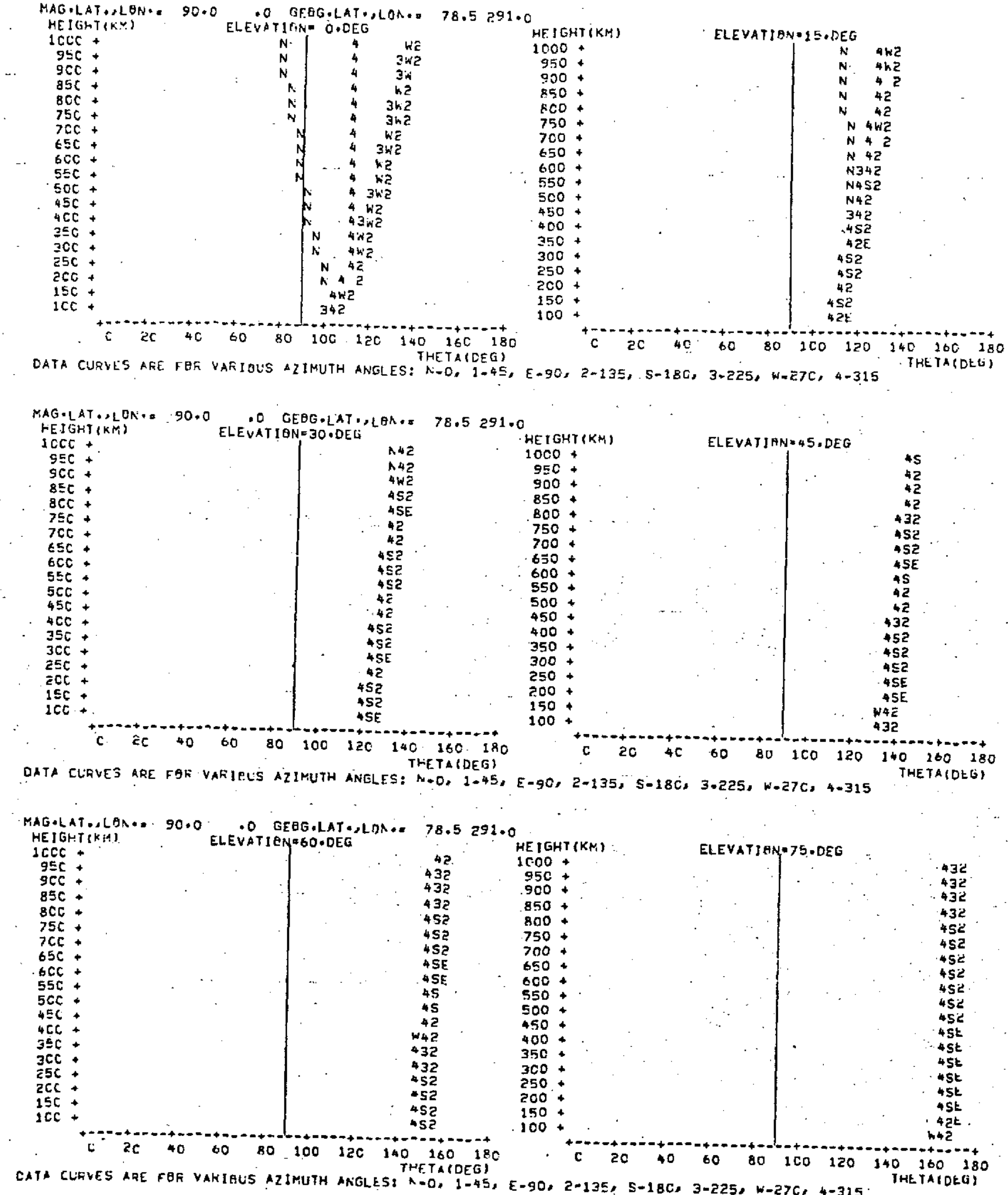

Figure 6d. Variation of the Angle θ Between the Direction of Propagation and the Magnetic Field

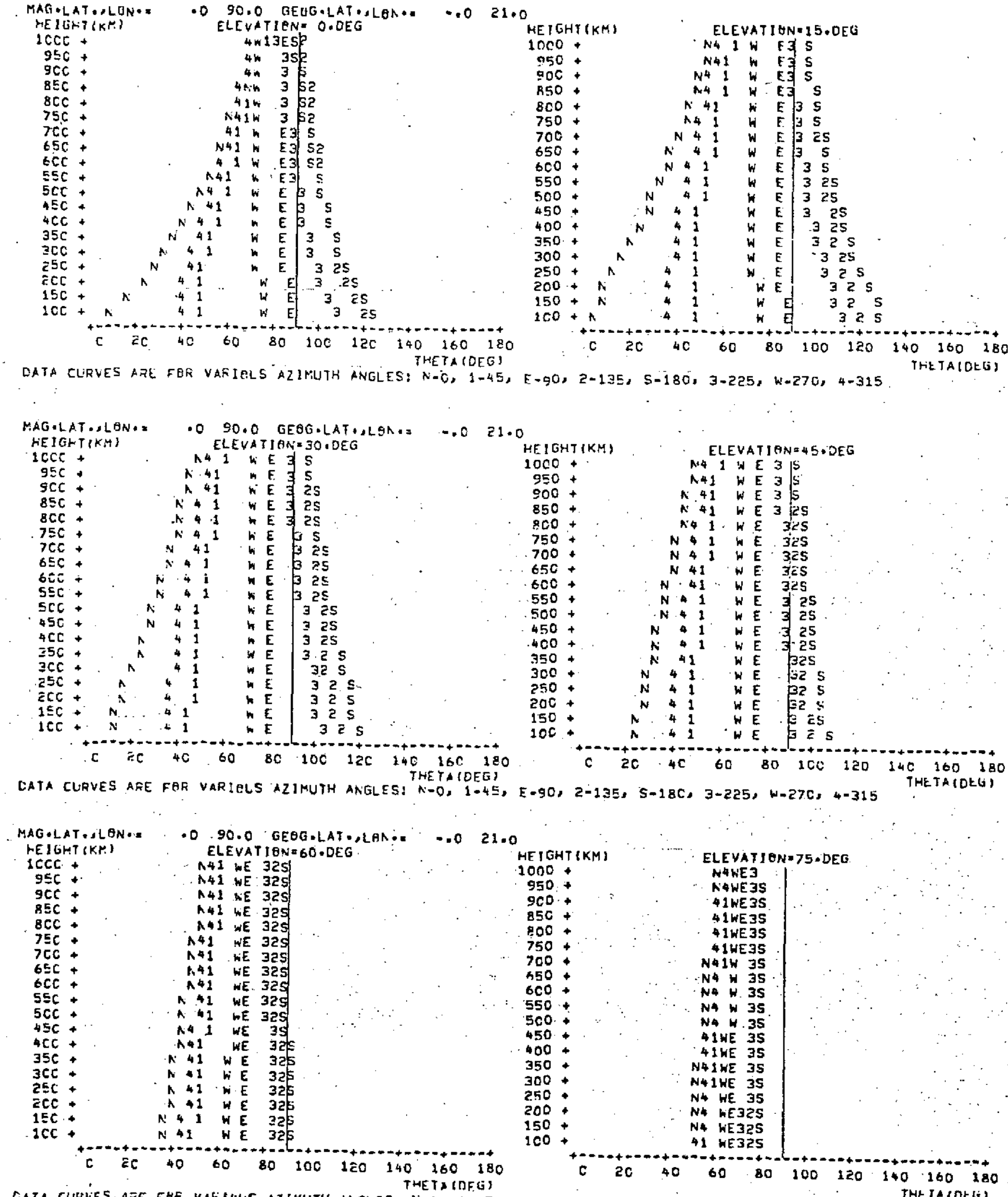

Figure 6e. Variation of the Angle θ Between the Direction of Propagation and the Magnetic Field

Table 4. Comparison of Changes in Vertical Electron Content and Faraday Factor due to Integration Carried to 1000, 2000 and 3000 km Height

LAT.	LON.	DATE	UT	ELEV	AZIM	FOF2	INTEGRATED TO:	VEC(1.E15 E/M**2) 1000	2000	3000	FAR.FAC.(1.E11/(DEG*M**2)) 1000	2000	3000 KM HEIGHT
15.0	.0	65 10 10	.0	90.0	0.	6.6		105.7	111.5	114.5	19537	19787	20002
							% DIFF.1-2K &1-3K:		5.5	8.3		1.3	2.4
15.0	.0	65 10 10	2.0	90.0	0.	5.0		64.0	68.4	70.9	19526	19840	20125
							% DIFF.1-2K &1-3K:		6.9	10.7		1.6	3.1
15.0	.0	65 10 10	4.0	90.0	0.	2.8		21.5	25.3	27.6	19773	20506	21181
							% DIFF.1-2K &1-3K:		17.7	28.2		3.7	7.1
15.0	.0	65 10 10	6.0	90.0	0.	4.4		57.5	62.9	66.0	19577	19997	20383
							% DIFF.1-2K &1-3K:		9.4	14.8		2.1	4.1
15.0	.0	65 10 10	8.0	90.0	0.	7.8		179.0	191.1	197.0	19639	19939	20184
							% DIFF.1-2K &1-3K:		6.7	10.0		1.5	2.8
15.0	.0	65 10 10	10.0	90.0	0.	8.2		224.0	240.2	247.9	19817	20128	20382
							% DIFF.1-2K &1-3K:		7.2	10.6		1.6	2.9
15.0	.0	65 10 10	12.0	90.0	0.	9.3		285.9	306.0	315.1	19876	20176	20410
							% DIFF.1-2K &1-3K:		7.0	10.2		1.5	2.7
15.0	.0	65 10 10	14.0	90.0	0.	10.1		314.6	334.3	343.2	19779	20052	20264
							% DIFF.1-2K &1-3K:		6.3	9.1		1.4	2.5
15.0	.0	65 10 10	16.0	90.0	0.	10.9		339.4	355.5	362.7	19690	19902	20065
							% DIFF.1-2K &1-3K:		4.7	6.9		1.1	1.9
15.0	.0	65 10 10	18.0	90.0	0.	10.4		279.2	291.5	297.0	19657	19854	20006
							% DIFF.1-2K &1-3K:		4.4	6.4		1.0	1.8
15.0	.0	65 10 10	20.0	90.0	0.	9.1		209.4	218.7	223.0	19645	19845	19999
							% DIFF.1-2K &1-3K:		4.5	6.5		1.0	1.8
15.0	.0	65 10 10	22.0	90.0	0.	8.2		162.7	170.7	174.5	19610	19832	20012
							% DIFF.1-2K &1-3K:		4.9	7.3		1.1	2.0

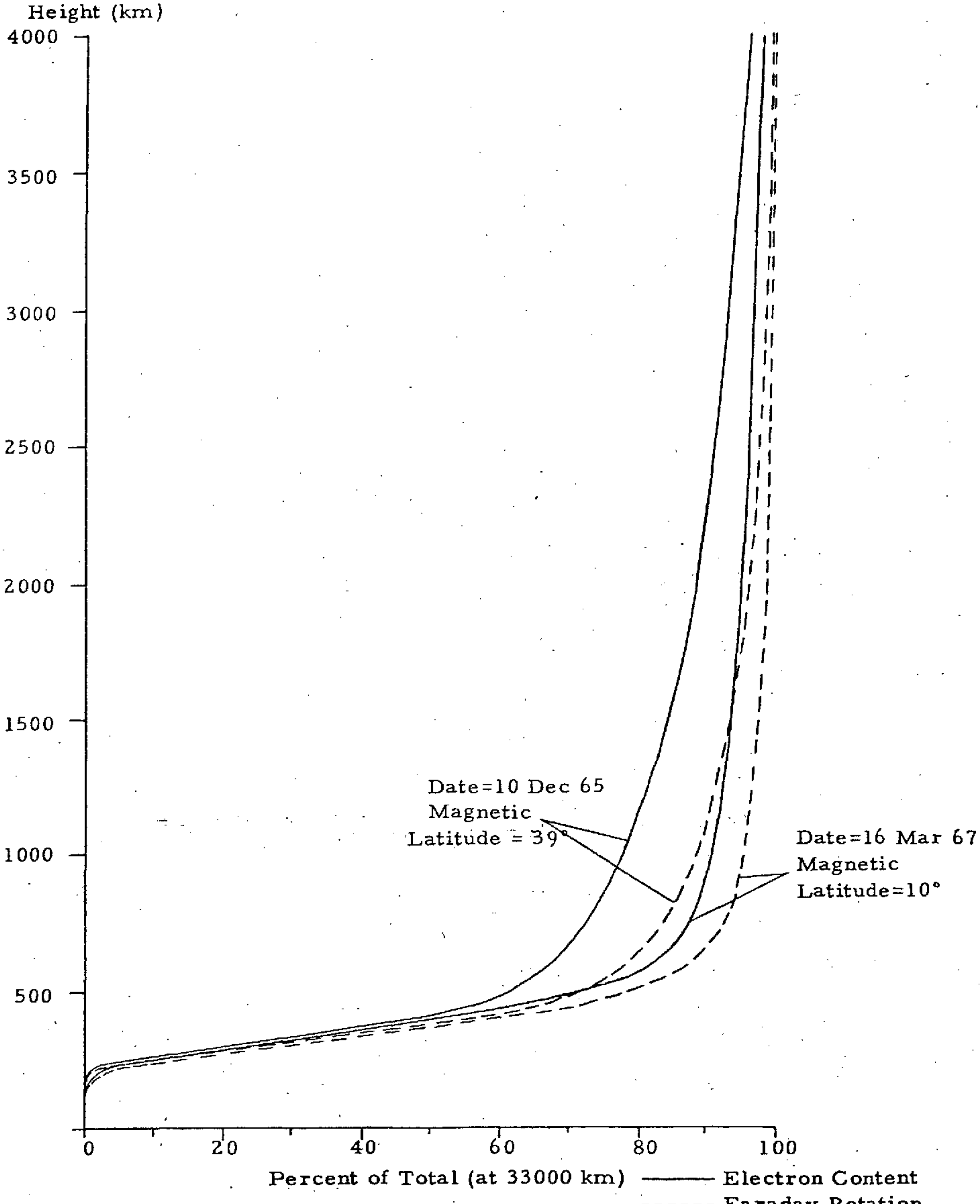

Figure 7. Comparison of the Amount of EC and Far. Rotation Accummulated from Ground up to a Varying Height

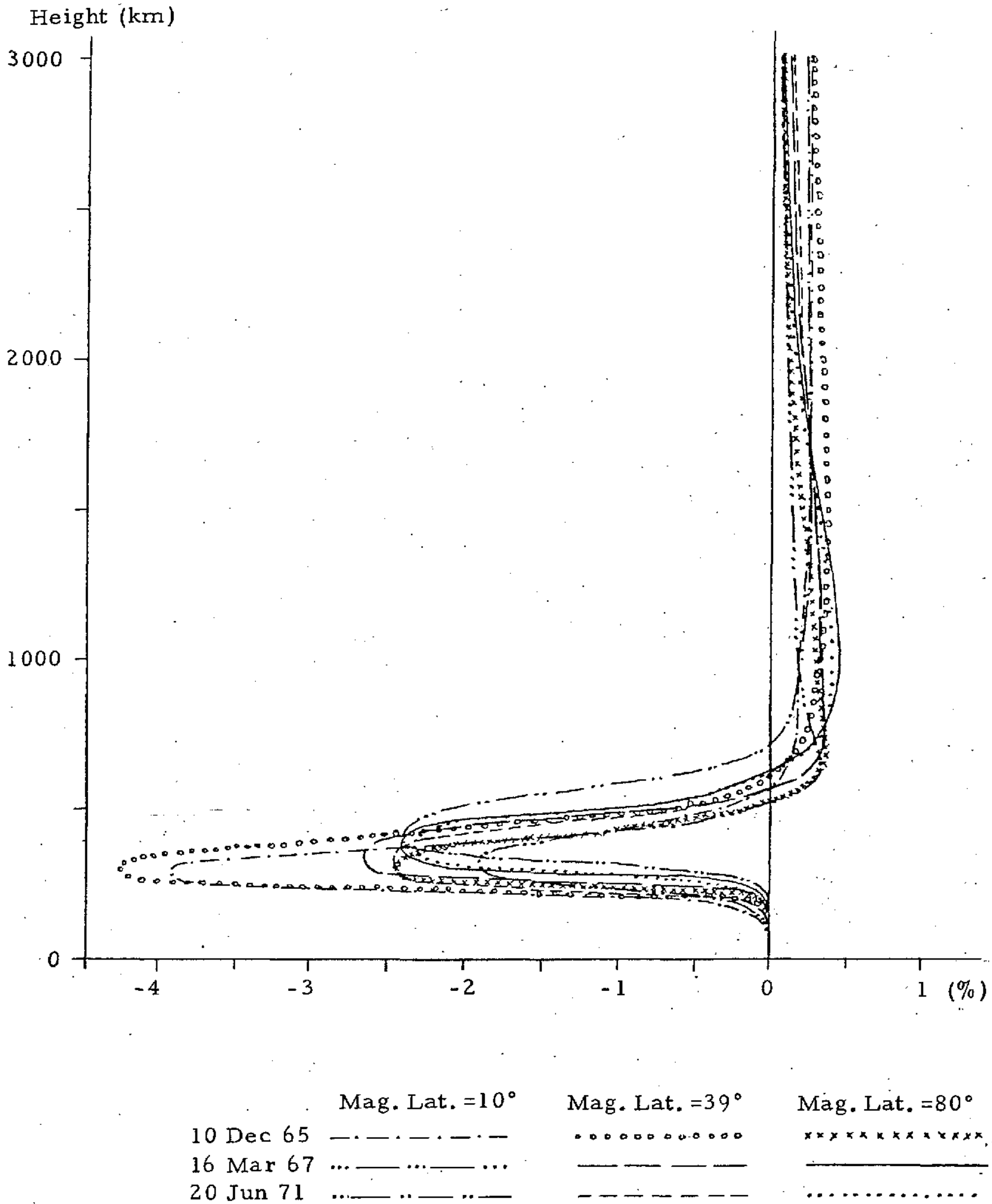

Figure 8. Difference between Percent Contributions of Electron Content and Faraday Rotation in each 100 km Height Interval. Percentages are taken of the total values integrated from 0 to a satellite height of 33000 km.

APPENDIX A

Observations at Cape Kennedy

At the Cape Kennedy location, latitude = 28.4°, longitude = 279.4°, 2 types of experiments were set up, a digisonde measuring critical frequency f_oF2 and height of the F layer h'F, and a polarimeter measuring Faraday rotation angles Ω that were converted to total electron content N_T. Approximately a 6 month span of data was reduced, f_oF2 and height data for two time periods 19 October 73 to 24 Nov 73 and from 20 Dec 73 to 7 Mar 74, and total content data from 20 Dec 73 to 7 March 74.

The height of the F layer was converted to an approximate height at f_oF2 by a rough conversion process relating the mean h'F observation to the mean h_m prediction on an hourly basis for the total reduction period. Figure 9 shows the mean height curves along with the resultant scale constants. The Faraday rotation angles were converted to total electron content by the relation $N_T = F\Omega$ using a fixed conversion factor of $F = 0.293 \times 10^{15}$ el/m² degrees. Considering the results from the preceding report, the error introduced by the use of a fixed rather than a variable factor was thought acceptable for the following reasons. For this particular case, both station position and direction of observation were fixed. The specific seasonal and diurnal variations will introduce at most, errors of about 6%, and the day to day variations in f_oF2 and height may contribute up to a 5% error in the Faraday factor. The large possible errors due to height changes do not apply to this case, since the angular observation path has a relatively high elevation of 54° and azimuth of 156° for which the propagation angle θ does not come close to 90°. Thus the use of a fixed factor will at most introduce an error of 7.8%, and combining this in RSS fashion with the inherent instrumental errors of about 10%, the overall error in the total electron content values should not exceed 12.7%.

On a daily and monthly mean basis comparisons were performed between the measured values of f_oF2, height and total electron content and the

corresponding predictions and updated values obtained from the Bent Ionospheric Model. The diurnal plots are given day by day showing the height variations in Figures 12a-l and the changes in f_oF2 in Figures 11a-l. Figures 10a-l show the curves for the total electron content predictions and the measurements as reduced from the Faraday rotation observations as well as the total content values updated with the f_oF2 measurements. The diurnal curves giving the monthly means of the measurements as well as the RMS residuals, measured minus predicted or updated values, are plotted in Figures 13 a-f and 14, 15a-g for electron content, f_oF2 and height respectively. The monthly mean statistics are listed in more detail in Tables 5a-g, where the daytime percent errors and the number of data points are included.

The overall results are summarized in Table 6 as the RMS percent errors for the daytime period from 8 to 18 hours local time. Over the total reduction period the Bent model f_oF2 predictions deviate by 14% from the measurements and for the height by 8%; the error in the total electron content predictions of 31.5% is reduced to 24.0% when updating with f_oF2 observations. These percentages fit in with the results from previous extensive investigations at many different sites quoted in Reference 1. The update with realtime data, however, shows a much greater improvement for the time span from Jan-Mar 74 than for the total period; here the daytime RMS error is reduced from 30.9% for the predictions to 20.6% for the updated values of total content.

It requires closer examination to find out why the f_oF2 update is not as effective for the Dec 73 and April-May 74 results of total content as for the data during the remaining months. As seen on Figure 13a, the RMS error in electron content for Dec 73 is greater for the update than for the predictions at 15 and 16 hours UT. On the daily curves in Figure 10c for Dec 24 at 16 UT for example, we find the measured content value to be smaller than the basic prediction while the update is considerably larger due to a larger than predicted f_oF2 measurement as seen in Figure 11c.

Here we have an ionospheric irregularity where a sudden sharp increase in f_oF2 is not accompanied by a corresponding increase in total content; the increased electron density must be limited to a very narrow interval close to $h_m F2$. A few such points effect the monthly averages significantly, and replacing for example the update by the predictions at 13, 15, and 16 hours UT when the update does not give an overall improvement, would result in an RMS error for the Dec 73 update statistics of 17.2%. This is an improvement over the 21.8% error for the predictions alone that fits in with the Jan-Mar 74 results.

The update in April and May 74 shows a less than average improvement for the same reason as in Dec 73. The Bent Model fits extremely good to an average relationship for the variation between the quantities of f_oF2 and total content. On Jan 25 for example, the much higher than normal f_oF2 observations between about 16 and 20 hours UT as seen in Figure 11e, are used to update the total content predictions resulting in a near perfect match for the much higher than average electron content measurements in Figure 10e. On several occasions in April and May 74, however, the higher than predicted f_oF2 observations are not accompanied by a typical increase in the total electron content, and large discrepancies between the predicted and measured values can be noted, as on April 12 and 13 in Figure 10k.

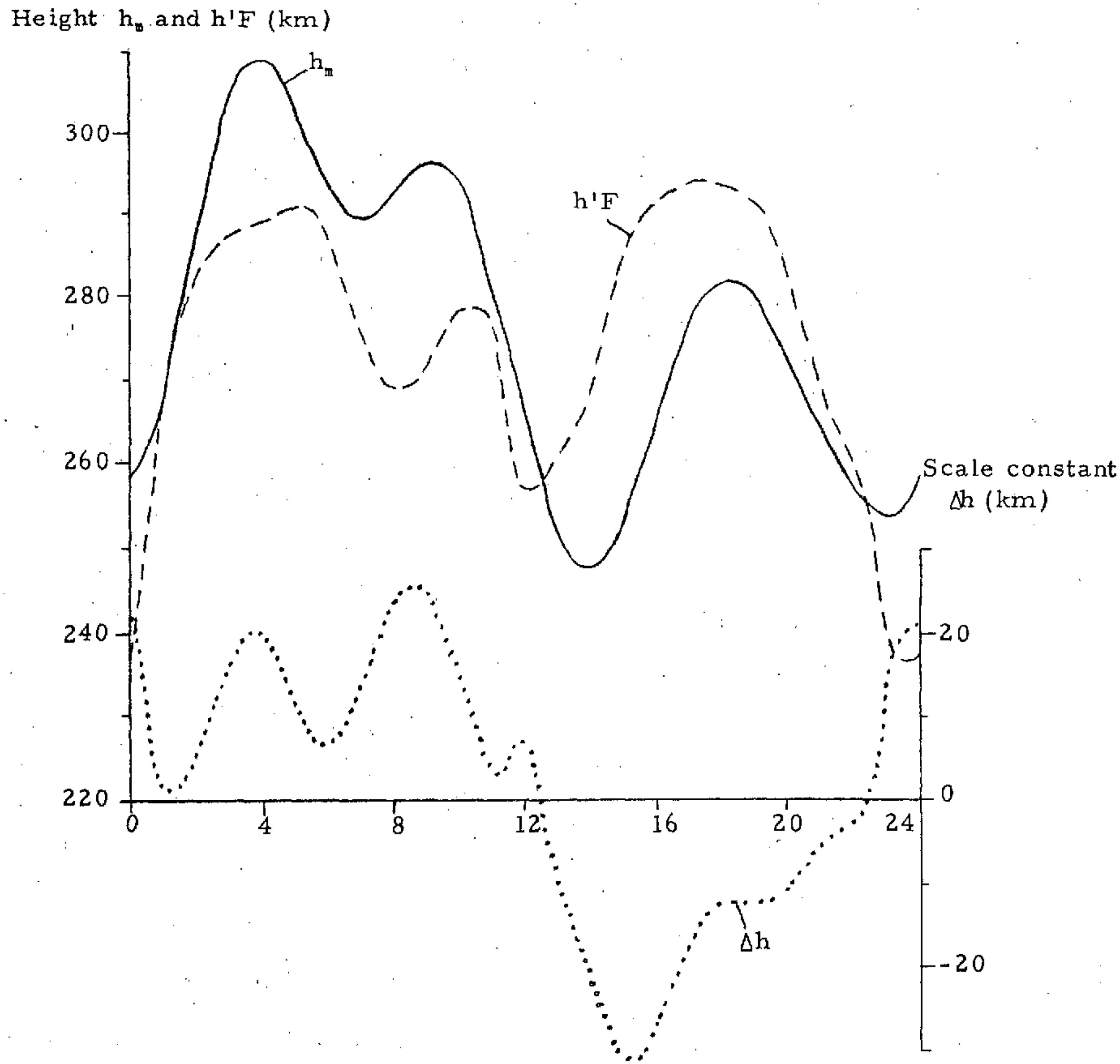

Figure 9. Diurnal Mean Curves for Oct 73-May 74 of Predicted h_m, Observed h'F, and the Difference Δh.

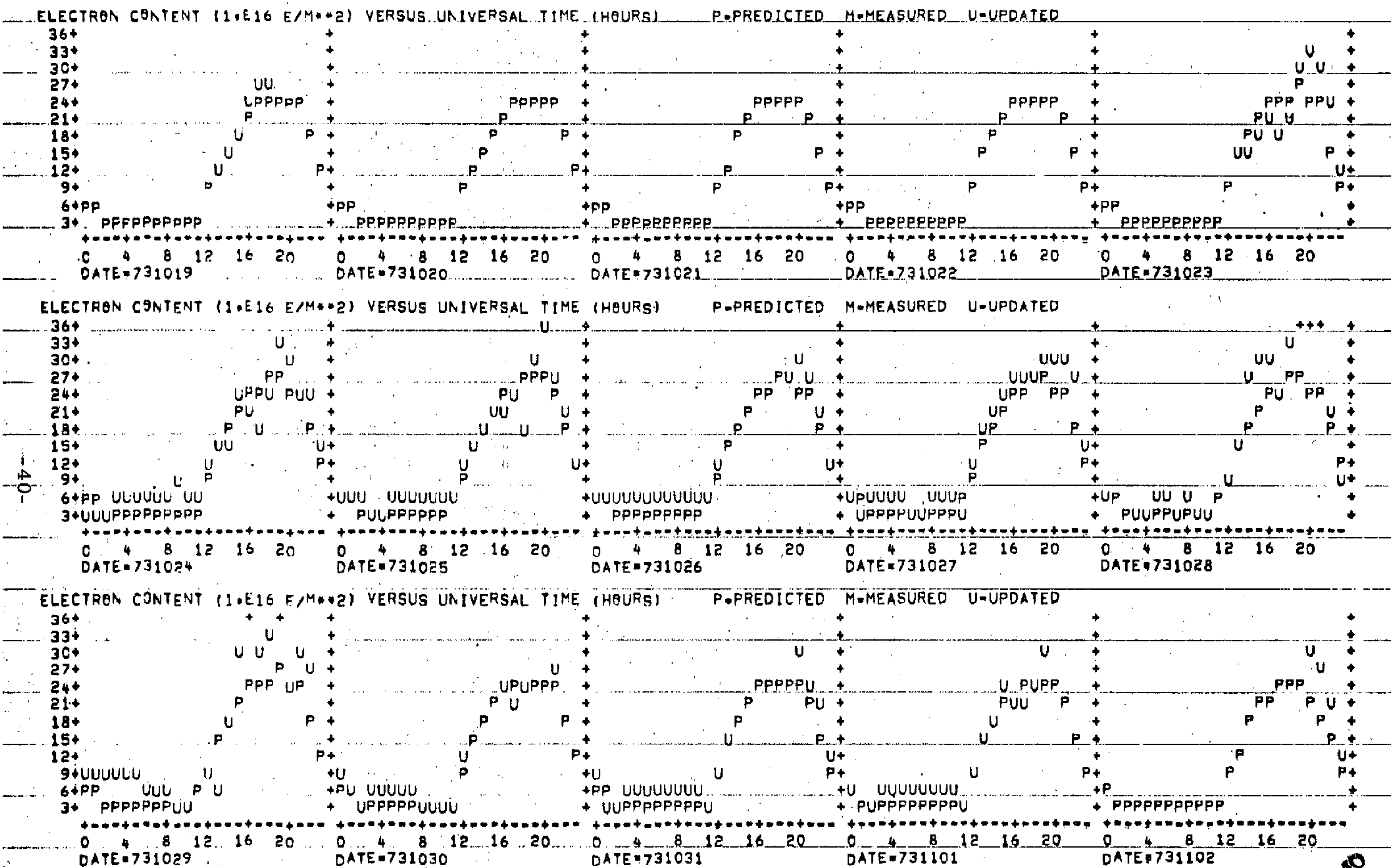
ELECTRON CONTENT (1.E16 E/M**2) VERSUS UNIVERSAL TIME (HOURS) P=PREDICTED M=MEASURED U=UPDATED
DATE=731019
DATE=731020
DATE=731021
DATE=731022
DATE=731023
ELECTRON CONTENT (1.E16 E/M**2) VERSUS UNIVERSAL TIME (HOURS) P=PREDICTED M=MEASURED U=UPDATED
DATE=731024
DATE=731025
DATE=731026
DATE=731027
DATE=731028
ELECTRON CONTENT (1.E16 E/M**2) VERSUS UNIVERSAL TIME (HOURS) P=PREDICTED M=MEASURED U=UPDATED
DATE=731029
DATE=731030
DATE=731031
DATE=731101
DATE=731102

Figure 10a.

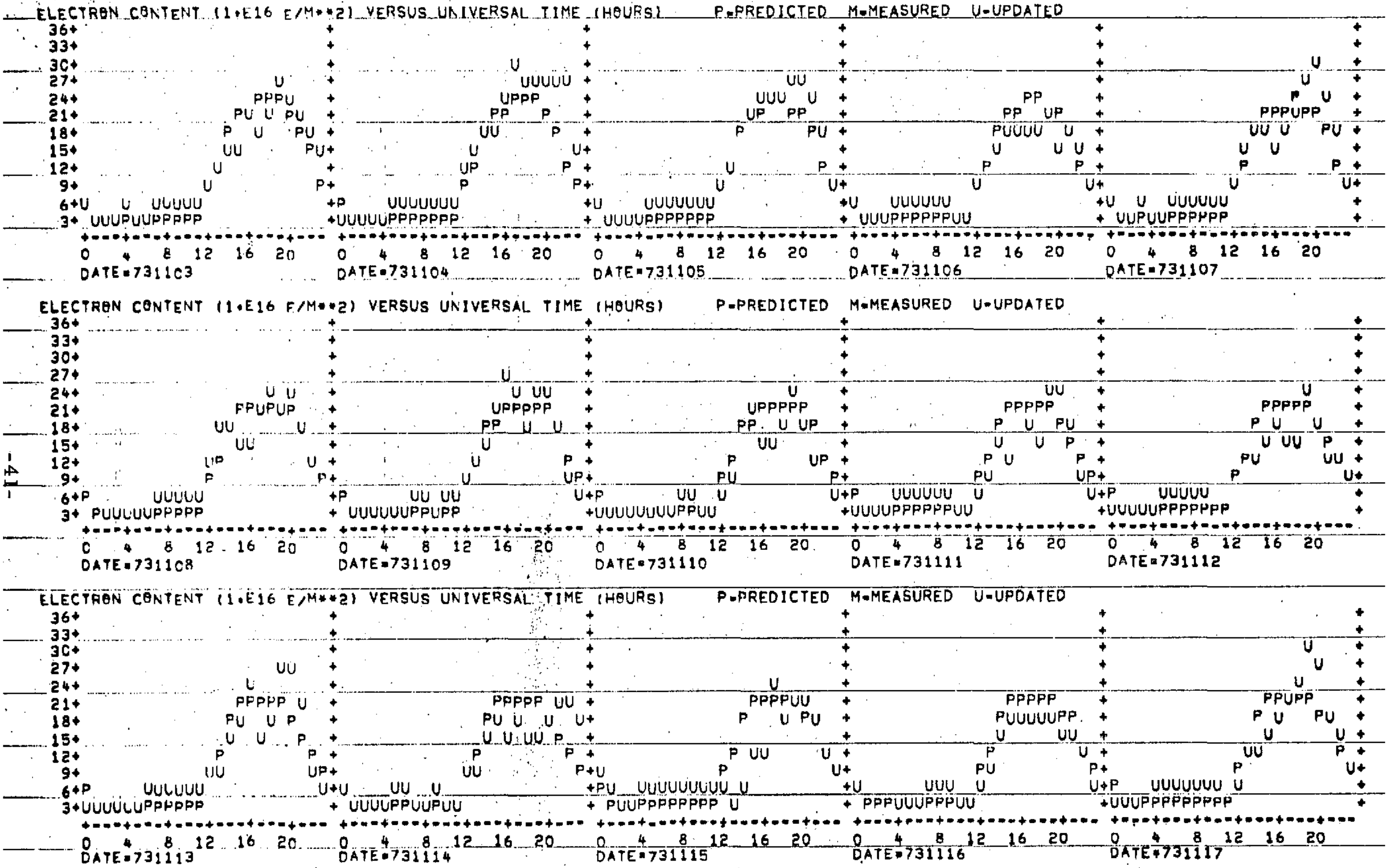
ELECTRON CONTENT (1*E16 E/M**2) VERSUS UNIVERSAL TIME (HOURS)
P=PREDICTED M=MEASURED U=UPDATED
36 33 30 27 24 21 18 15 12 9 6 3
0 4 8 12 16 20
DATE=731103
DATE=731104
DATE=731105
DATE=731106
DATE=731107
ELECTRON CONTENT (1*E16 E/M**2) VERSUS UNIVERSAL TIME (HOURS)
P=PREDICTED M=MEASURED U=UPDATED
DATE=731108
DATE=731109
DATE=731110
DATE=731111
DATE=731112
ELECTRON CONTENT (1*E16 E/M**2) VERSUS UNIVERSAL TIME (HOURS)
P=PREDICTED M=MEASURED U=UPDATED
DATE=731113
DATE=731114
DATE=731115
DATE=731116
DATE=731117

Figure 10b.

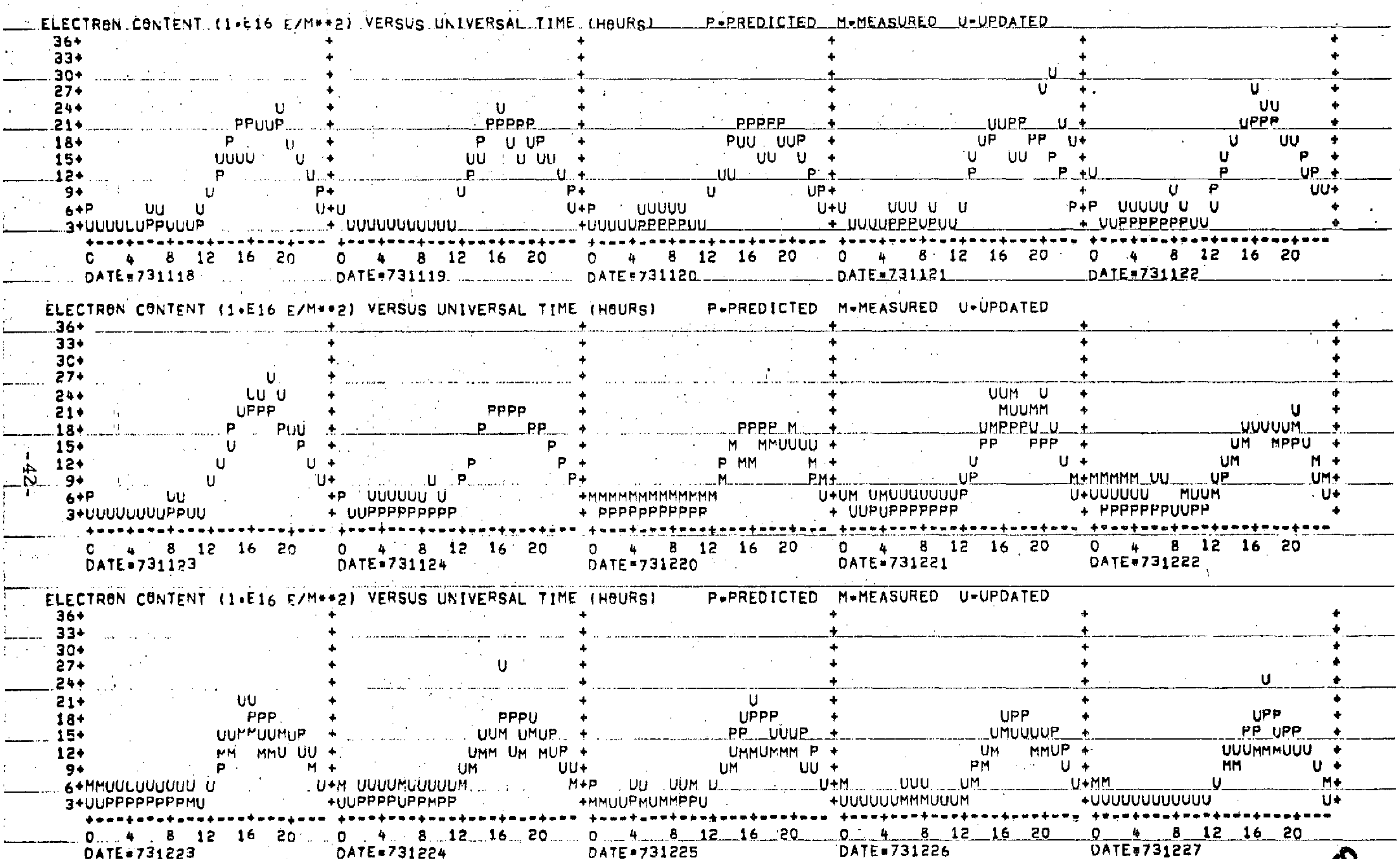
ELECTRON CONTENT (1*E16 E/M**2) VERSUS UNIVERSAL TIME (HOURS) P=PREDICTED M=MEASURED U=UPDATED
DATE=731118 DATE=731119 DATE=731120 DATE=731121 DATE=731122
ELECTRON CONTENT (1*E16 E/M**2) VERSUS UNIVERSAL TIME (HOURS) P=PREDICTED M=MEASURED U=UPDATED
DATE=731123 DATE=731124 DATE=731220 DATE=731221 DATE=731222
ELECTRON CONTENT (1*E16 E/M**2) VERSUS UNIVERSAL TIME (HOURS) P=PREDICTED M=MEASURED U=UPDATED
DATE=731223 DATE=731224 DATE=731225 DATE=731226 DATE=731227

Figure 10c.

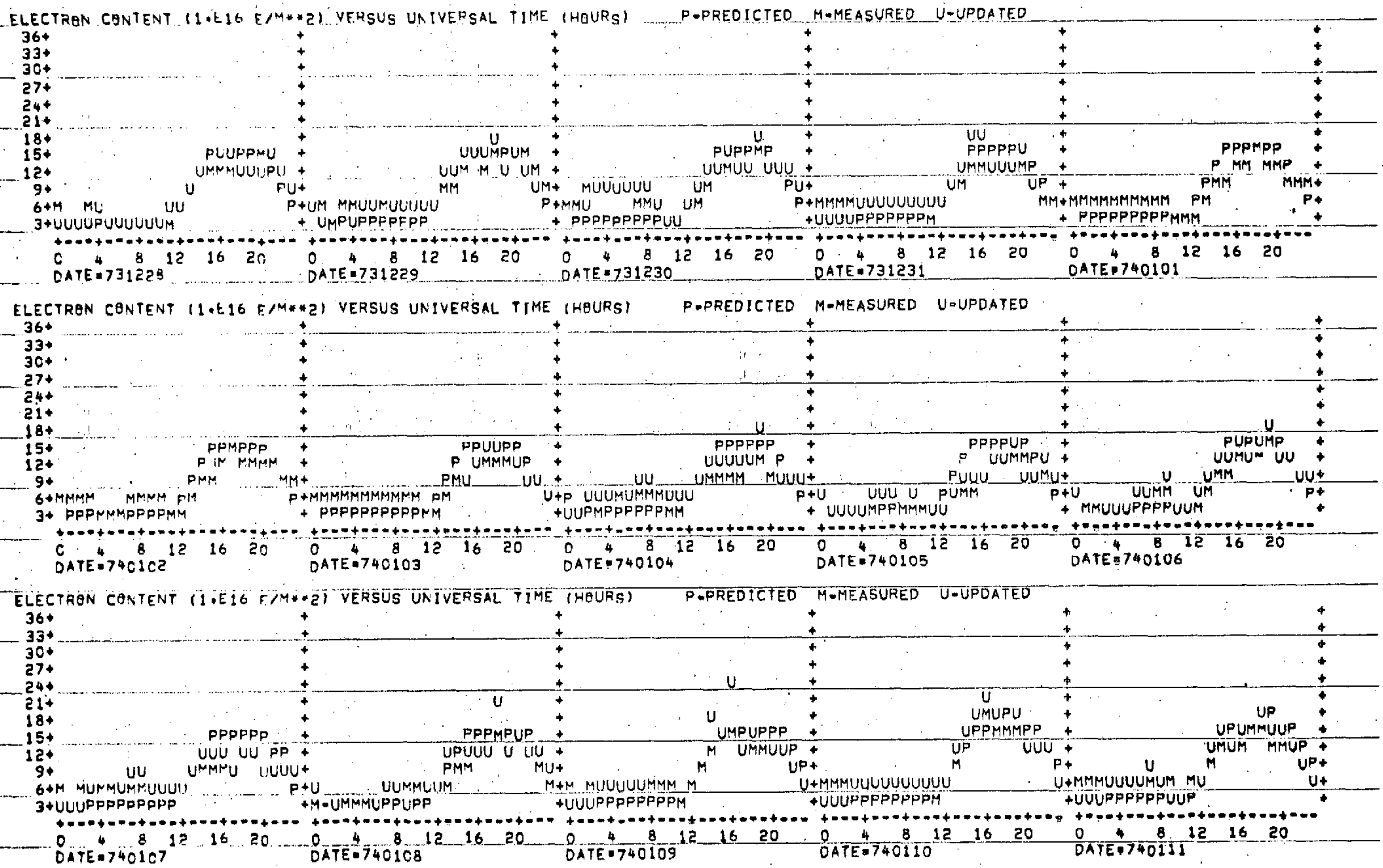
ELECTRON CONTENT (1.E16 E/M**2) VERSUS UNIVERSAL TIME (HOURS) P=PREDICTED M=MEASURED U=UPDATED
DATE=731228
DATE=731229
DATE=731230
DATE=731231
DATE=740101
ELECTRON CONTENT (1.E16 E/M**2) VERSUS UNIVERSAL TIME (HOURS) P=PREDICTED M=MEASURED U=UPDATED
DATE=740102
DATE=740103
DATE=740104
DATE=740105
DATE=740106
ELECTRON CONTENT (1.E16 E/M**2) VERSUS UNIVERSAL TIME (HOURS) P=PREDICTED M=MEASURED U=UPDATED
DATE=740107
DATE=740108
DATE=740109
DATE=740110
DATE=740111

Figure 10d.

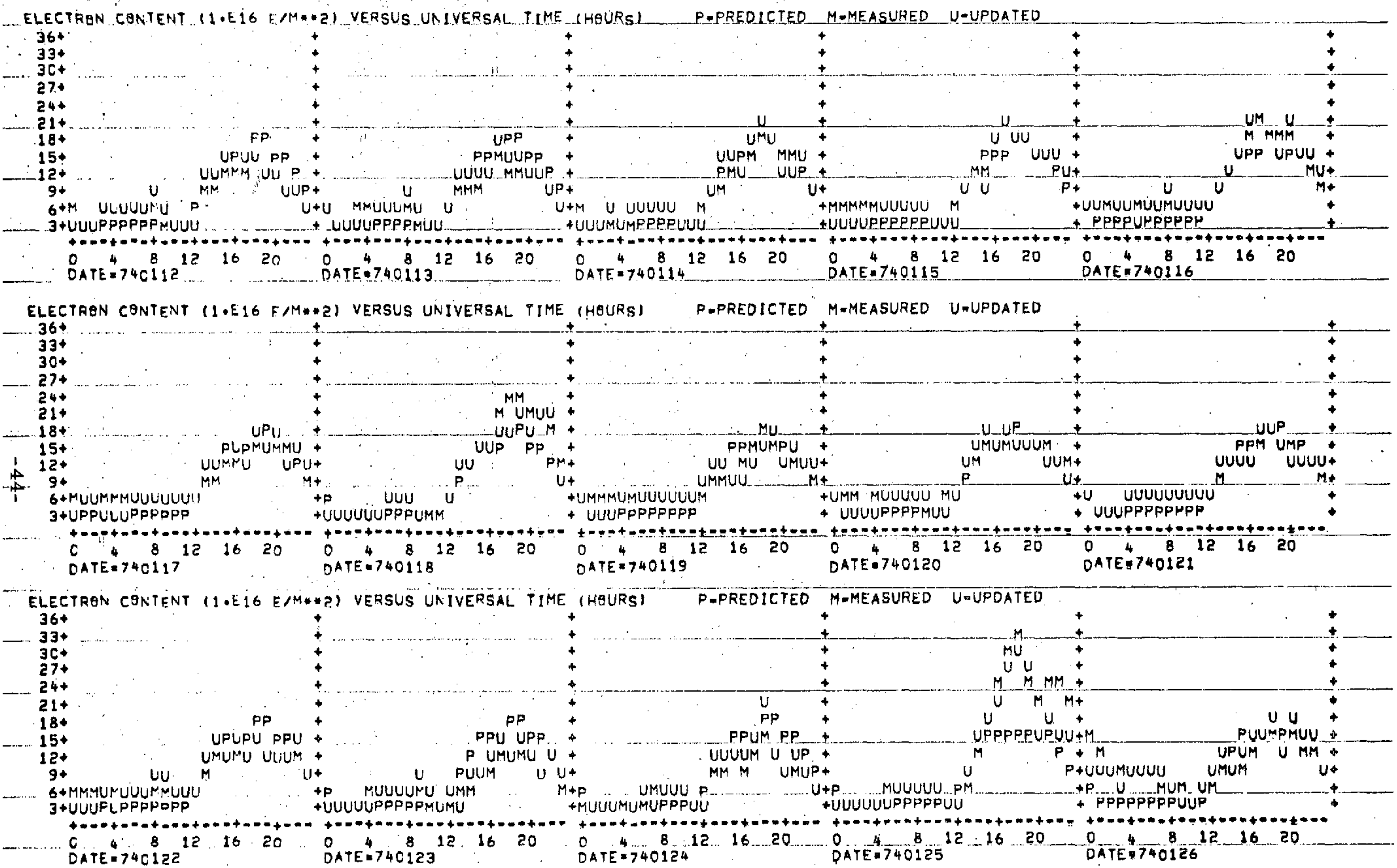
ELECTRON CONTENT (1.E16 E/M**2) VERSUS UNIVERSAL TIME (HOURS)
P=PREDICTED M=MEASURED U=UPDATED
DATE=740112
DATE=740113
DATE=740114
DATE=740115
DATE=740116
ELECTRON CONTENT (1.E16 E/M**2) VERSUS UNIVERSAL TIME (HOURS)
P=PREDICTED M=MEASURED U=UPDATED
DATE=740117
DATE=740118
DATE=740119
DATE=740120
DATE=740121
ELECTRON CONTENT (1.E16 E/M**2) VERSUS UNIVERSAL TIME (HOURS)
P=PREDICTED M=MEASURED U=UPDATED
DATE=740122
DATE=740123
DATE=740124
DATE=740125
DATE=740126

Figure 10e.

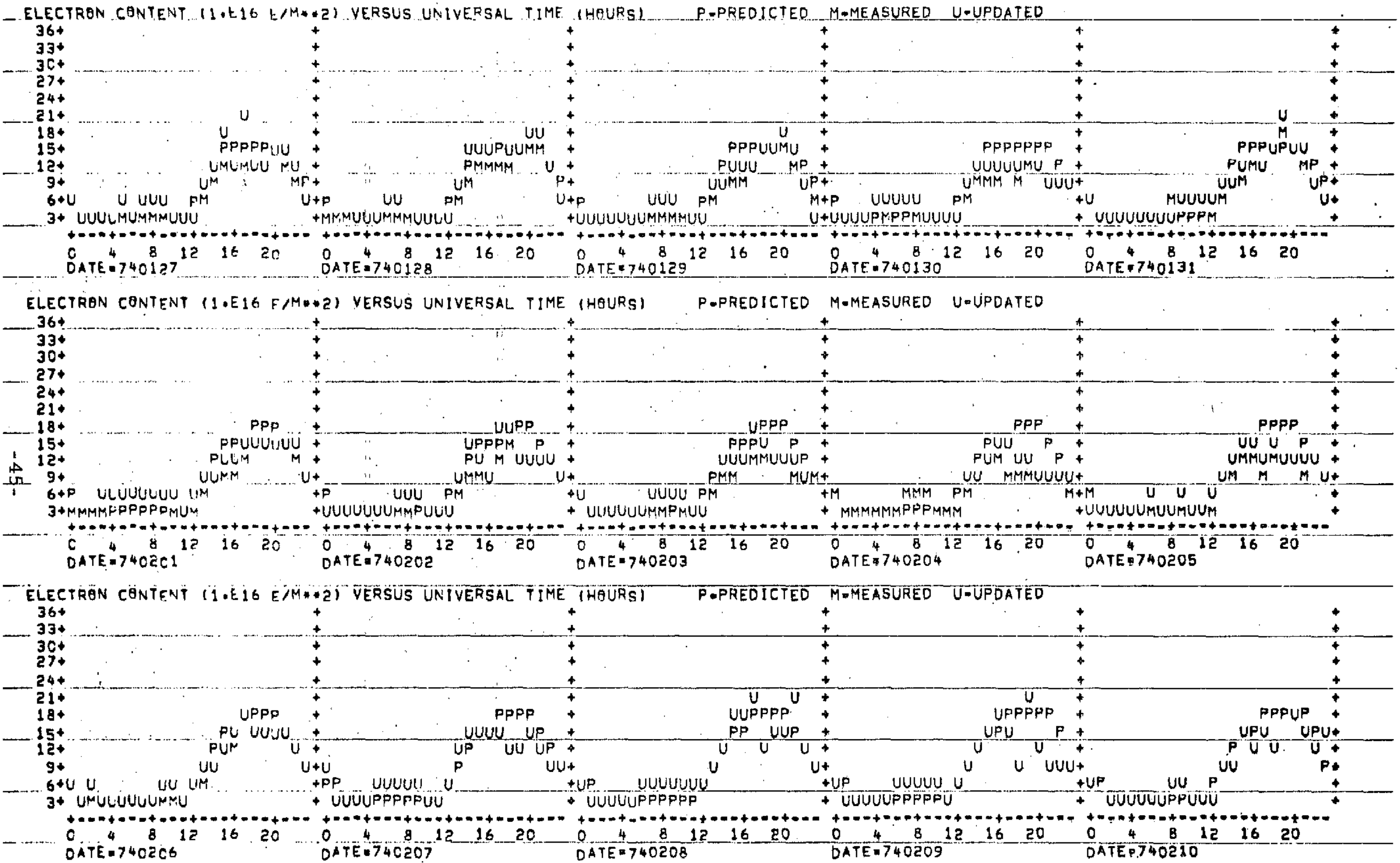

ELECTRON CONTENT (1.E16 E/M**2) VERSUS UNIVERSAL TIME (HOURS) P=PREDICTED M=MEASURED U=UPDATED
DATE=740127
DATE=740128
DATE=740129
DATE=740130
DATE=740131
ELECTRON CONTENT (1.E16 E/M**2) VERSUS UNIVERSAL TIME (HOURS) P=PREDICTED M=MEASURED U=UPDATED
DATE=740201
DATE=740202
DATE=740203
DATE=740204
DATE=740205
ELECTRON CONTENT (1.E16 E/M**2) VERSUS UNIVERSAL TIME (HOURS) P=PREDICTED M=MEASURED U=UPDATED
DATE=740206
DATE=740207
DATE=740208
DATE=740209
DATE=740210

Figure 10f.

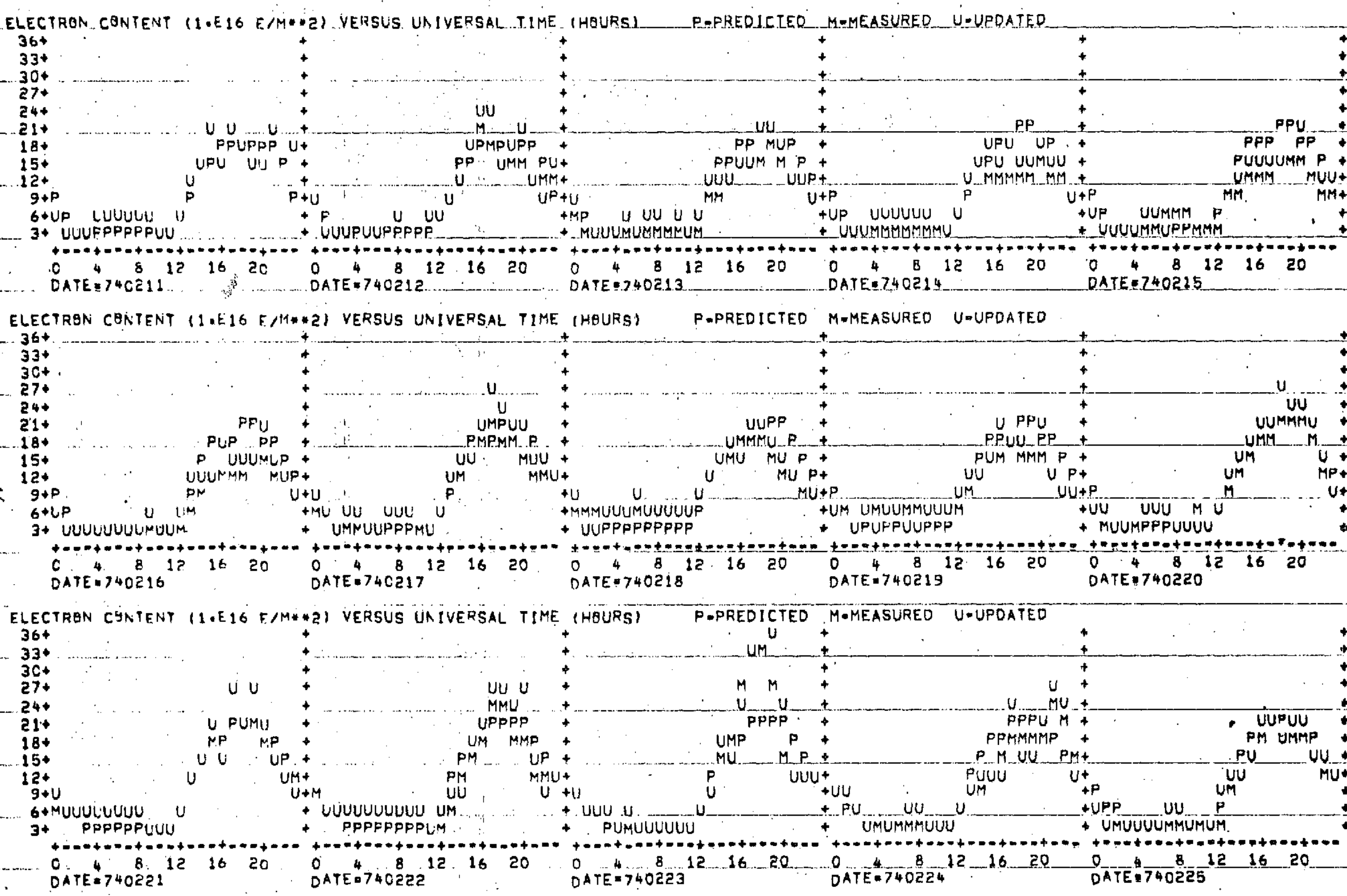

ELECTRON CONTENT (1.E16 E/M**2) VERSUS UNIVERSAL TIME (HOURS) P=PREDICTED M=MEASURED U=UPDATED
DATE=740211
DATE=740212
DATE=740213
DATE=740214
DATE=740215
ELECTRON CONTENT (1.E16 E/M**2) VERSUS UNIVERSAL TIME (HOURS) P=PREDICTED M=MEASURED U=UPDATED
DATE=740216
DATE=740217
DATE=740218
DATE=740219
DATE=740220
ELECTRON CONTENT (1.E16 E/M**2) VERSUS UNIVERSAL TIME (HOURS) P=PREDICTED M=MEASURED U=UPDATED
DATE=740221
DATE=740222
DATE=740223
DATE=740224
DATE=740225

Figure 10g.

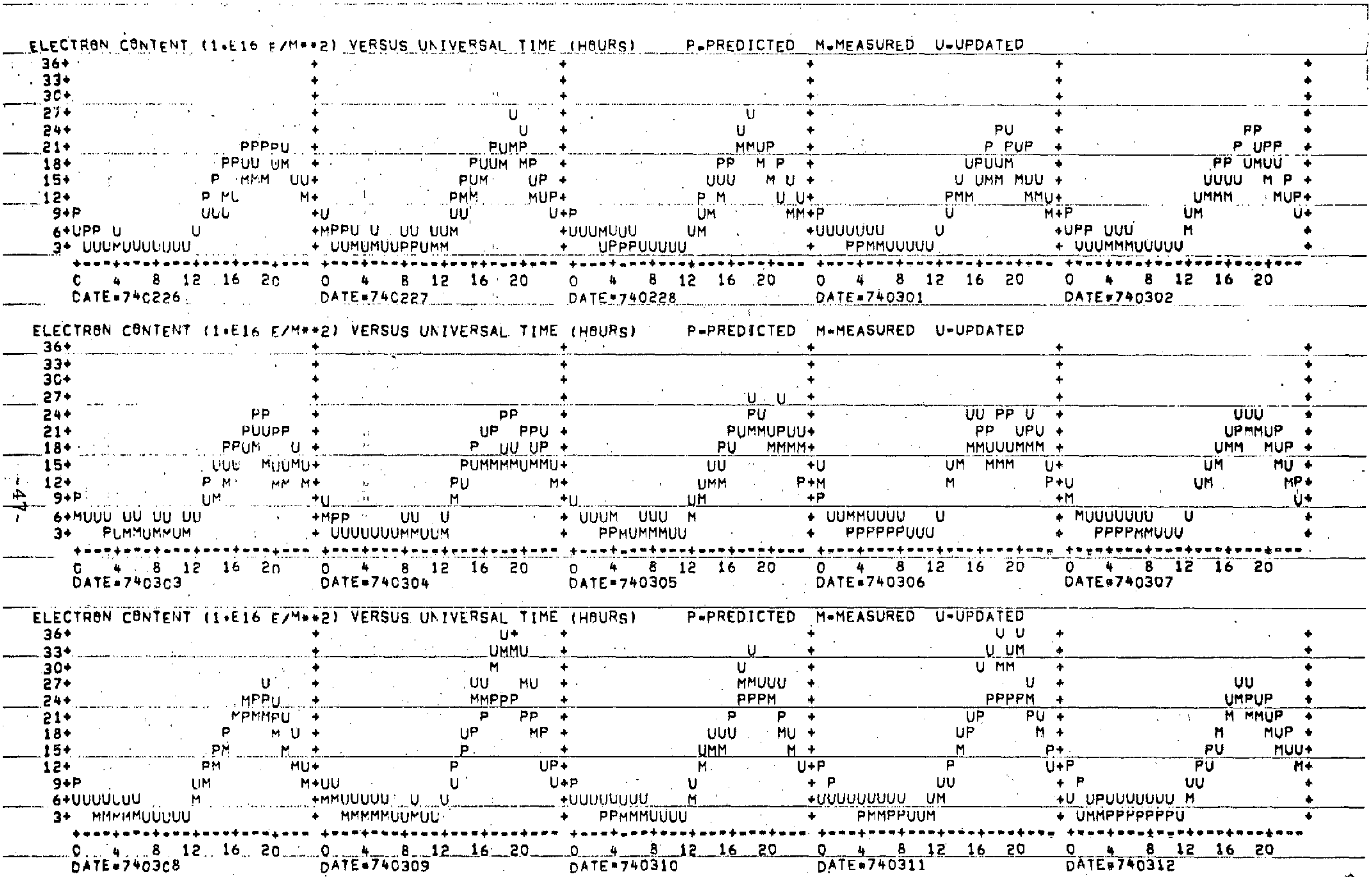
ELECTRON CONTENT (1.E16 E/M**2) VERSUS UNIVERSAL TIME (HOURS) P=PREDICTED M=MEASURED U=UPDATED
DATE=740226
DATE=740227
DATE=740228
DATE=740301
DATE=740302
ELECTRON CONTENT (1.E16 E/M**2) VERSUS UNIVERSAL TIME (HOURS) P=PREDICTED M=MEASURED U=UPDATED
DATE=740303
DATE=740304
DATE=740305
DATE=740306
DATE=740307
ELECTRON CONTENT (1.E16 E/M**2) VERSUS UNIVERSAL TIME (HOURS) P=PREDICTED M=MEASURED U=UPDATED
DATE=740308
DATE=740309
DATE=740310
DATE=740311
DATE=740312

Figure 10h.

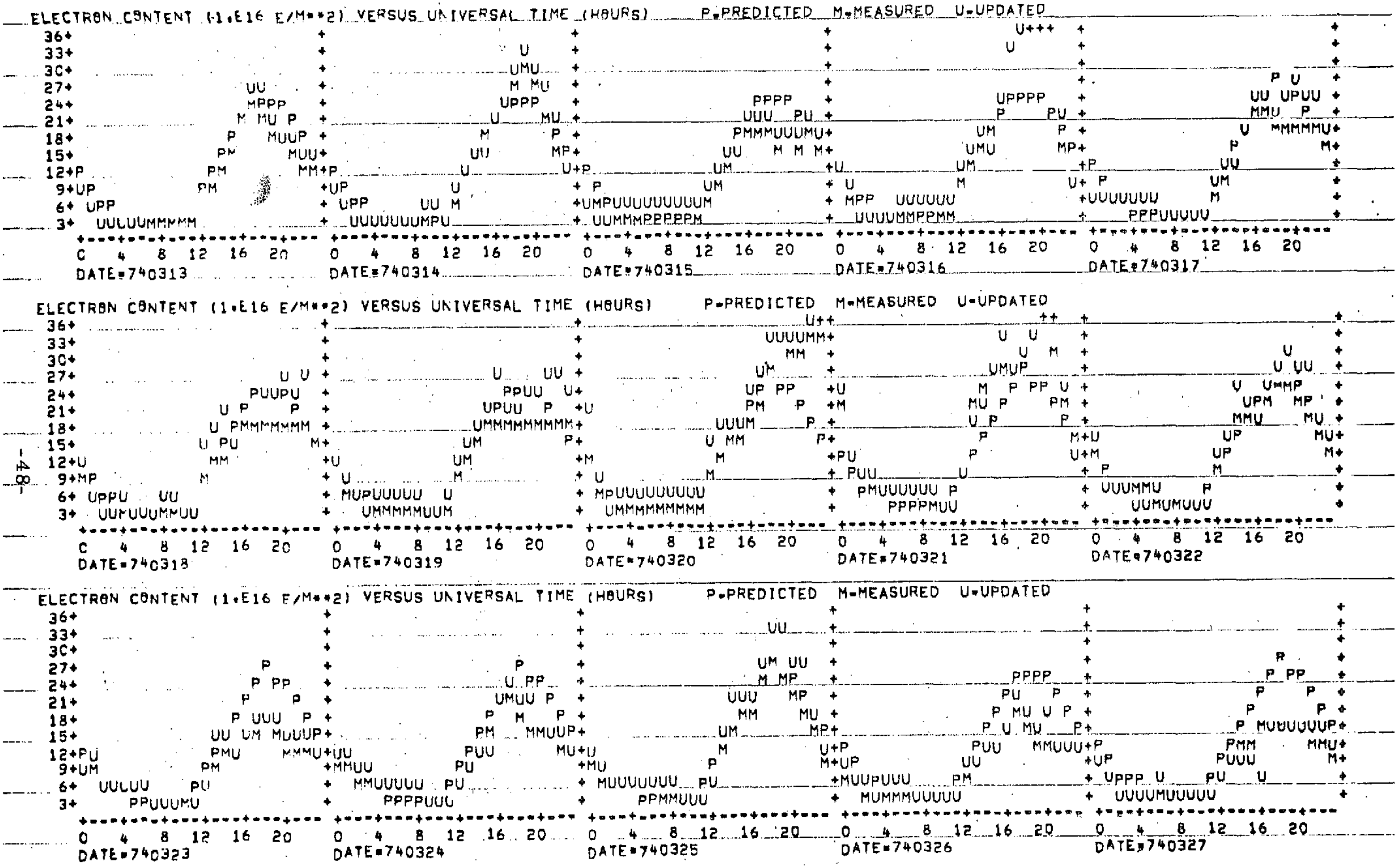
ELECTRON CONTENT (1.E16 E/M**2) VERSUS UNIVERSAL TIME (HOURS) P=PREDICTED M=MEASURED U=UPDATED
DATE=740313
DATE=740314
DATE=740315
DATE=740316
DATE=740317
ELECTRON CONTENT (1.E16 E/M**2) VERSUS UNIVERSAL TIME (HOURS) P=PREDICTED M=MEASURED U=UPDATED
DATE=740318
DATE=740319
DATE=740320
DATE=740321
DATE=740322
ELECTRON CONTENT (1.E16 E/M**2) VERSUS UNIVERSAL TIME (HOURS) P=PREDICTED M=MEASURED U=UPDATED
DATE=740323
DATE=740324
DATE=740325
DATE=740326
DATE=740327

Figure 10i.

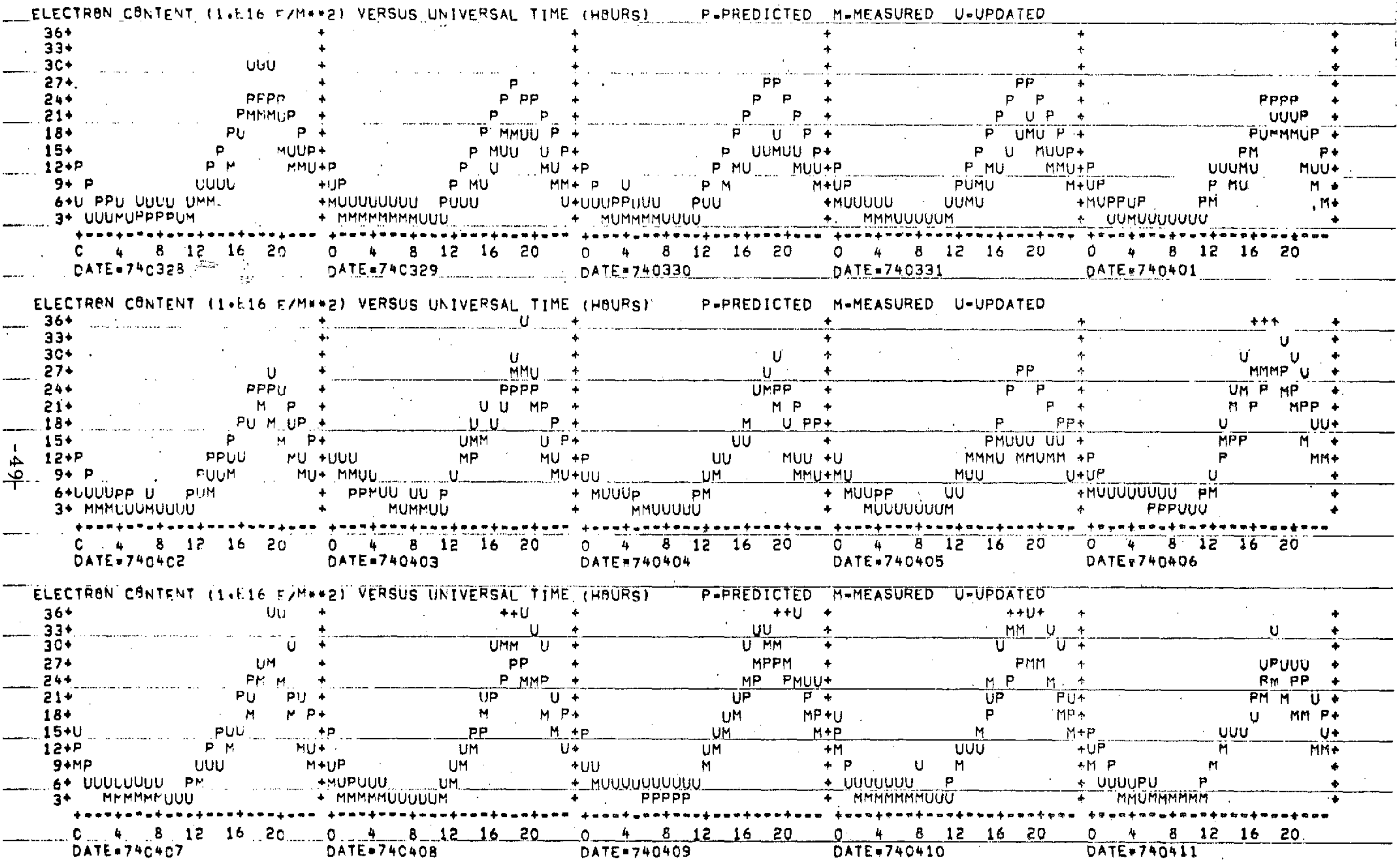
ELECTRON CONTENT (1.E16 E/M**2) VERSUS UNIVERSAL TIME (HOURS)   P=PREDICTED M=MEASURED U=UPDATED
DATE=740328
DATE=740329
DATE=740330
DATE=740331
DATE=740401
ELECTRON CONTENT (1.E16 E/M**2) VERSUS UNIVERSAL TIME (HOURS)   P=PREDICTED M=MEASURED U=UPDATED
DATE=740402
DATE=740403
DATE=740404
DATE=740405
DATE=740406
ELECTRON CONTENT (1.E16 E/M**2) VERSUS UNIVERSAL TIME (HOURS)   P=PREDICTED M=MEASURED U=UPDATED
DATE=740407
DATE=740408
DATE=740409
DATE=740410
DATE=740411

Figure 10j.

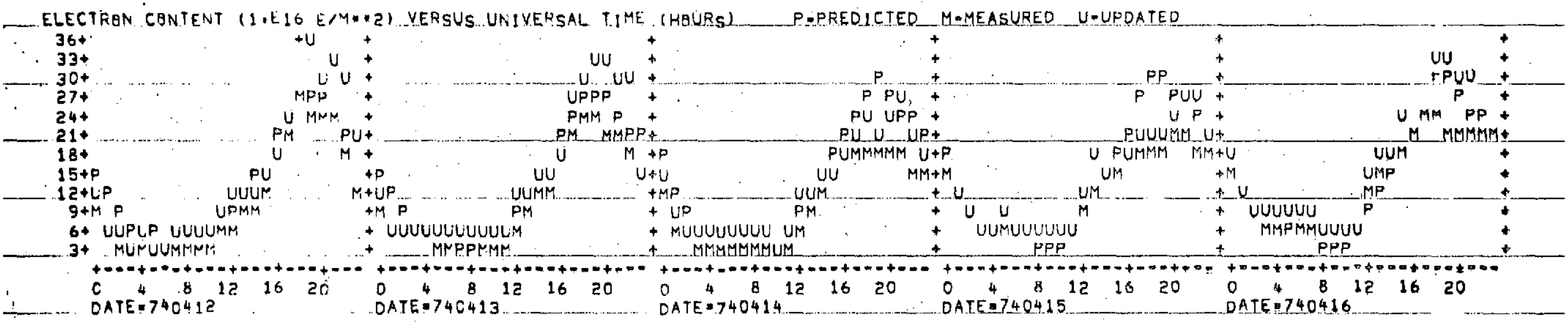
ELECTRON CONTENT (1.E16 E/M**2) VERSUS UNIVERSAL TIME (HOURS)
P=PREDICTED M=MEASURED U=UPDATED
DATE=740412
DATE=740413
DATE=740414
DATE=740415
DATE=740416

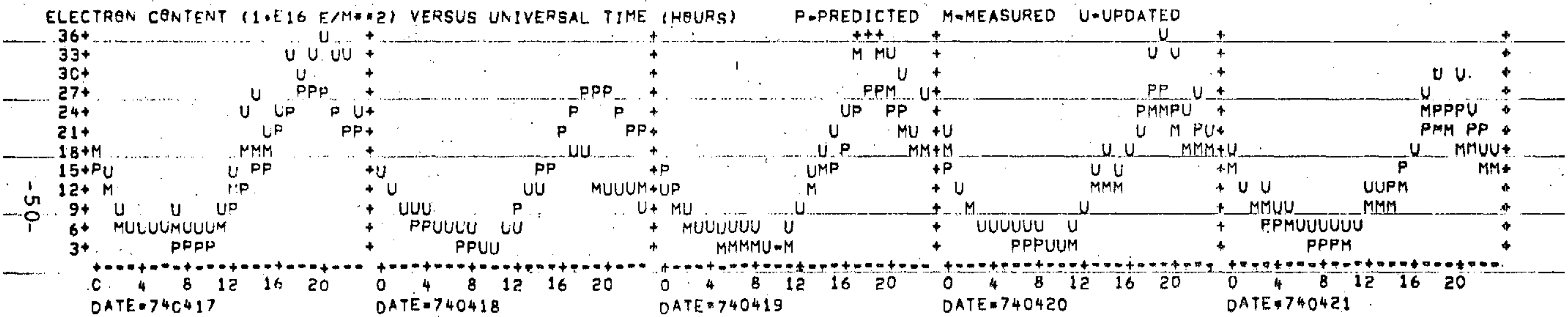
ELECTRON CONTENT (1.E16 E/M**2) VERSUS UNIVERSAL TIME (HOURS)
P=PREDICTED M=MEASURED U=UPDATED
DATE=740417
DATE=740418
DATE=740419
DATE=740420
DATE=740421

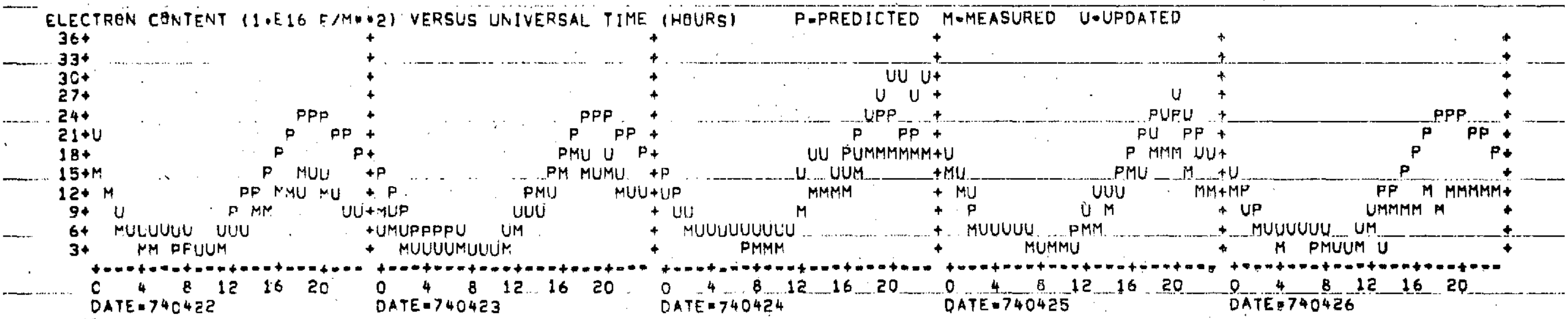
ELECTRON CONTENT (1.E16 E/M**2) VERSUS UNIVERSAL TIME (HOURS)
P=PREDICTED M=MEASURED U=UPDATED
DATE=740422
DATE=740423
DATE=740424
DATE=740425
DATE=740426

Figure 10k.

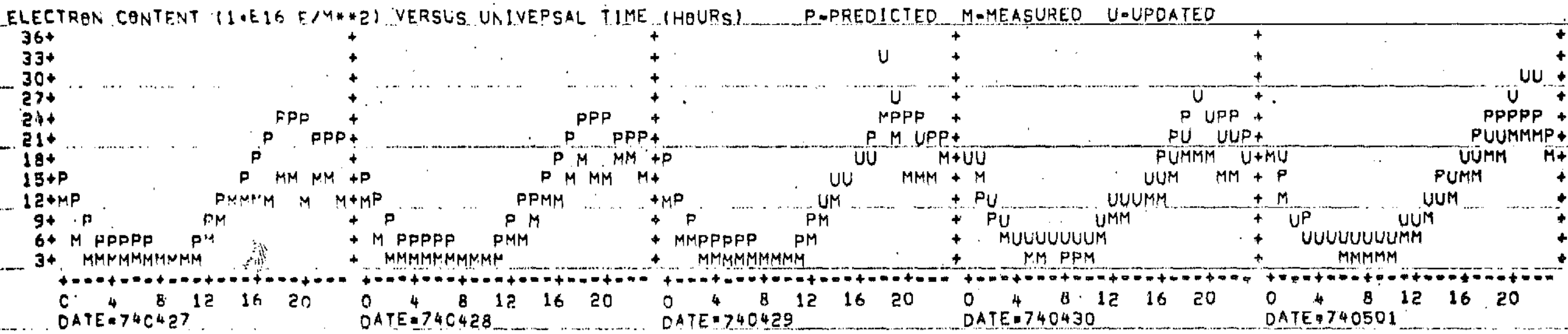
ELECTRON CONTENT (1.E16 E/M**2) VERSUS UNIVERSAL TIME (HOURS)
P=PREDICTED M=MEASURED U=UPDATED
DATE=740427
DATE=740428
DATE=740429
DATE=740430
DATE=740501

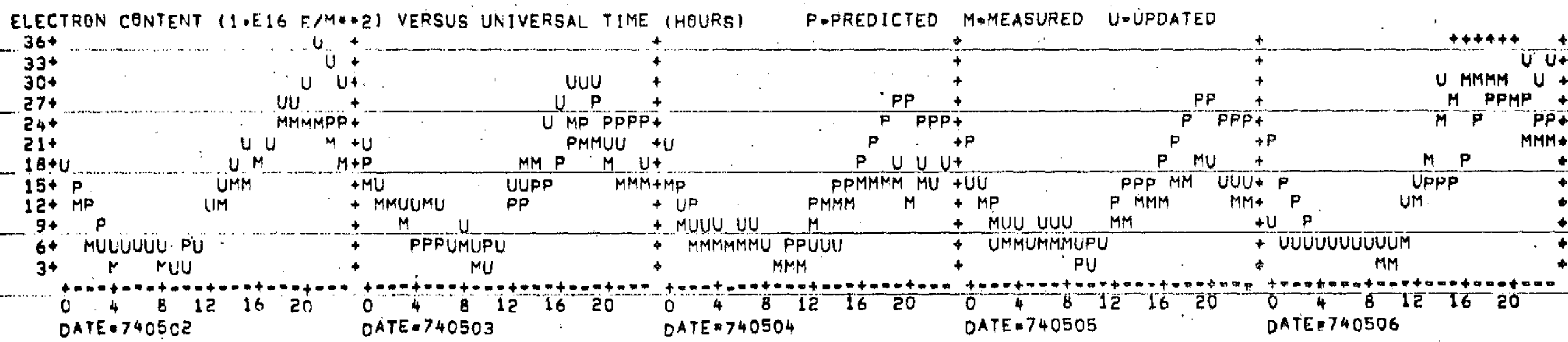
ELECTRON CONTENT (1.E16 E/M**2) VERSUS UNIVERSAL TIME (HOURS)
P=PREDICTED M=MEASURED U=UPDATED
DATE=740502
DATE=740503
DATE=740504
DATE=740505
DATE=740506

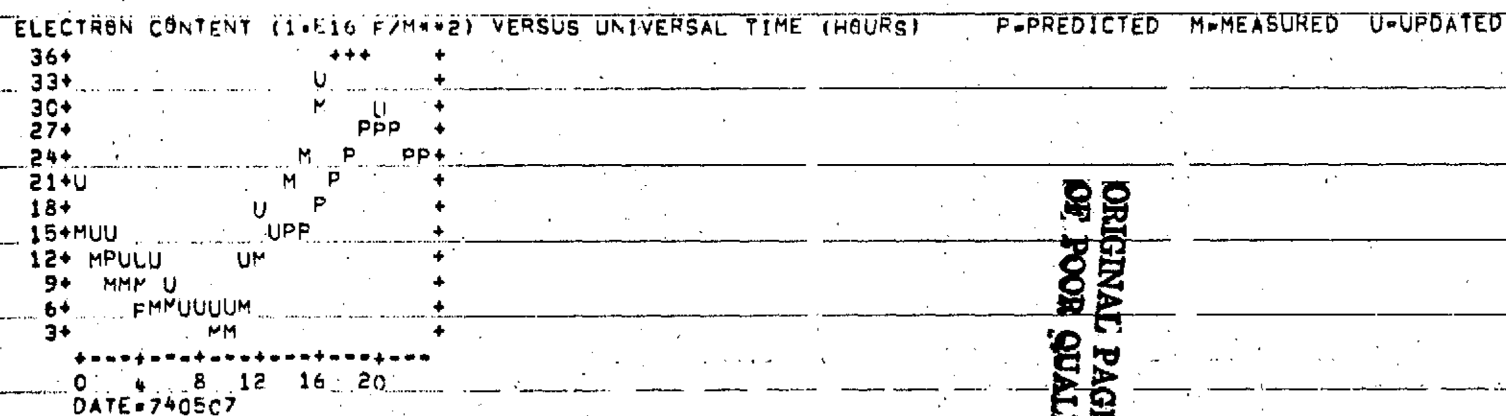
ELECTRON CONTENT (1.E16 E/M**2) VERSUS UNIVERSAL TIME (HOURS)
P=PREDICTED M=MEASURED U=UPDATED
DATE=740507

Figure 10-1.

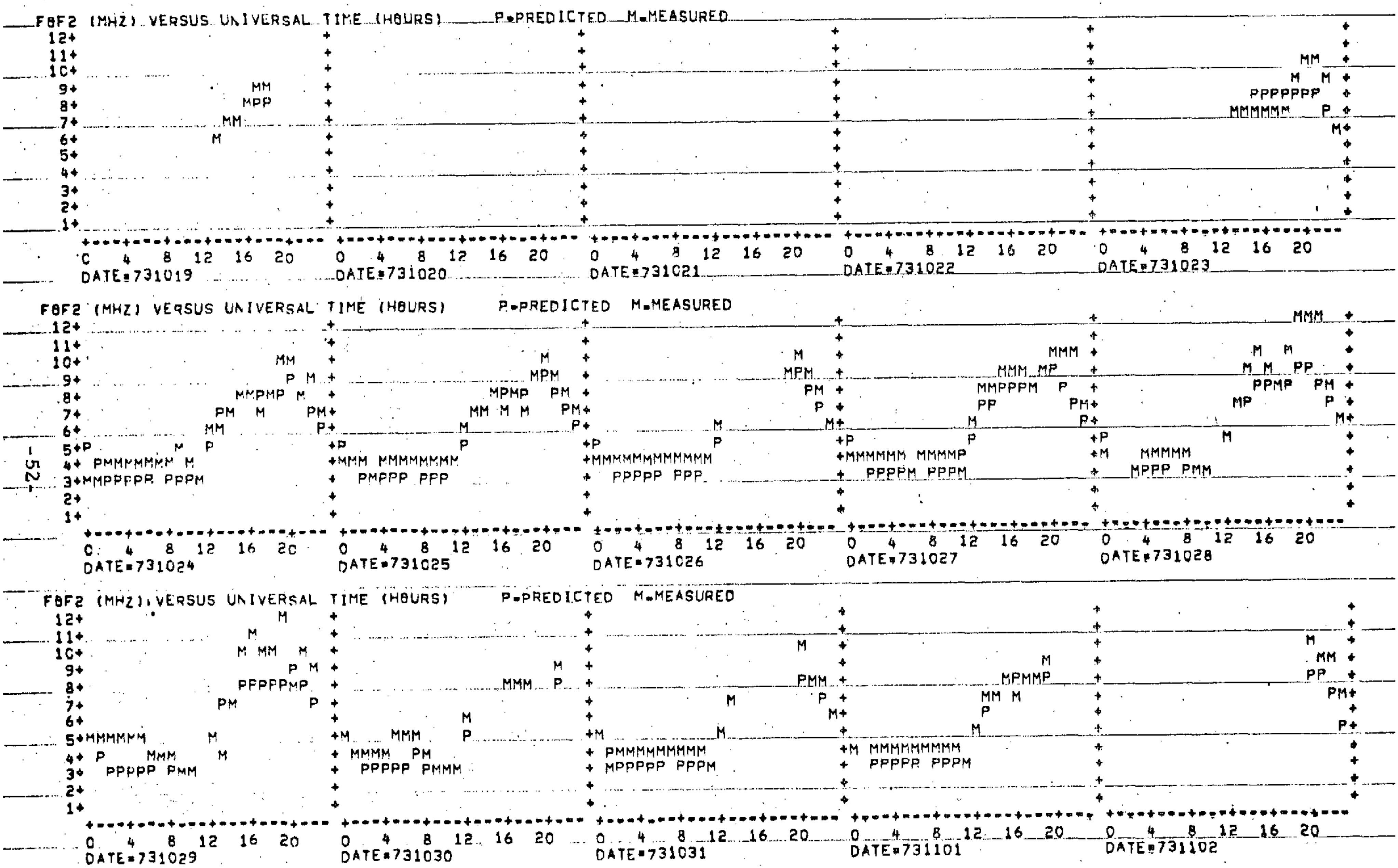
F0F2 (MHZ) VERSUS UNIVERSAL TIME (HOURS) P=PREDICTED M=MEASURED
DATE=731019
DATE=731020
DATE=731021
DATE=731022
DATE=731023
F0F2 (MHZ) VERSUS UNIVERSAL TIME (HOURS) P=PREDICTED M=MEASURED
DATE=731024
DATE=731025
DATE=731026
DATE=731027
DATE=731028
F0F2 (MHZ) VERSUS UNIVERSAL TIME (HOURS) P=PREDICTED M=MEASURED
DATE=731029
DATE=731030
DATE=731031
DATE=731101
DATE=731102

Figure 11a.

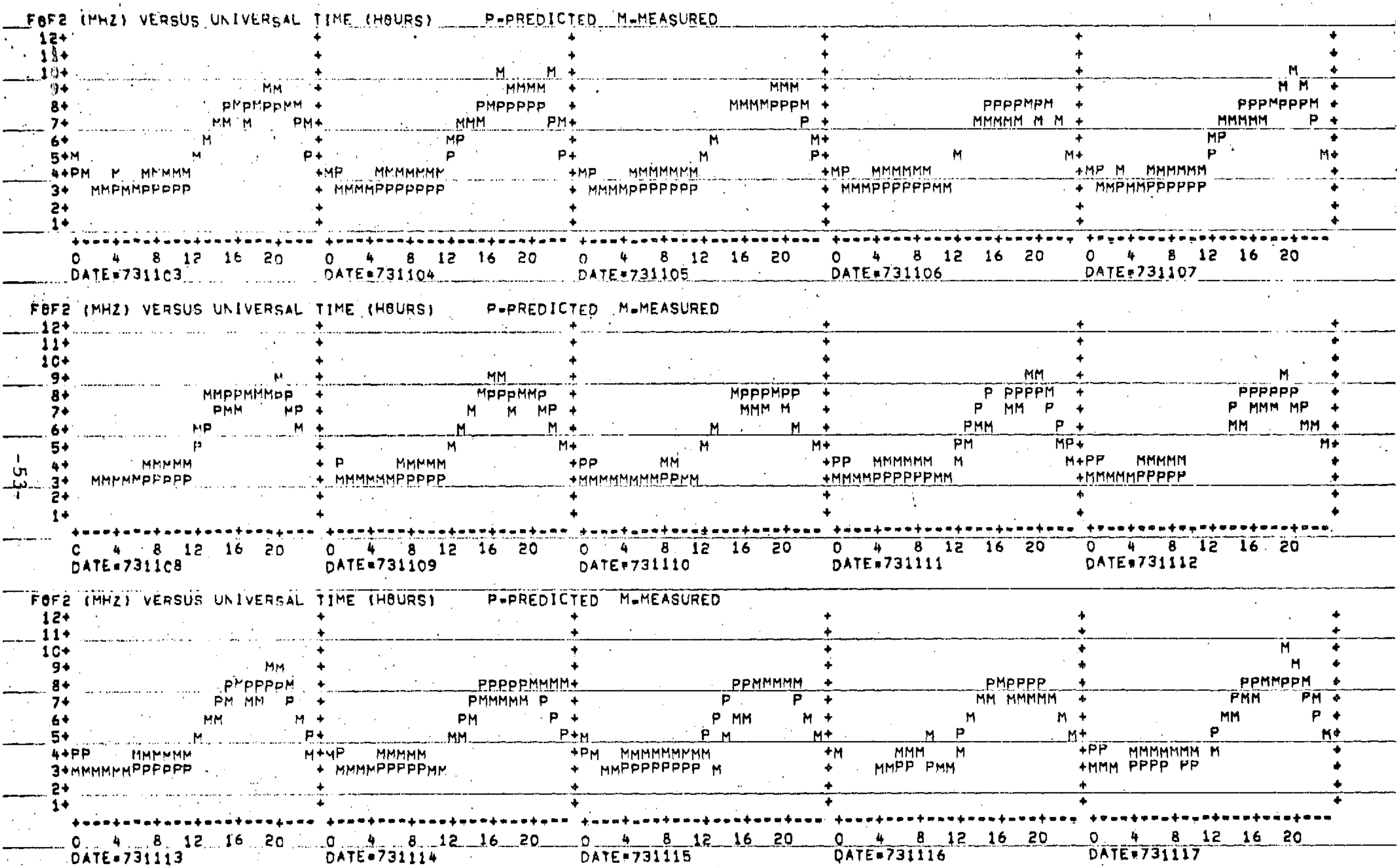
FOF2 (MHZ) VERSUS UNIVERSAL TIME (HOURS) P=PREDICTED M=MEASURED
DATE=731103
DATE=731104
DATE=731105
DATE=731106
DATE=731107
FOF2 (MHZ) VERSUS UNIVERSAL TIME (HOURS) P=PREDICTED M=MEASURED
DATE=731108
DATE=731109
DATE=731110
DATE=731111
DATE=731112
FOF2 (MHZ) VERSUS UNIVERSAL TIME (HOURS) P=PREDICTED M=MEASURED
DATE=731113
DATE=731114
DATE=731115
DATE=731116
DATE=731117

Figure 11b.

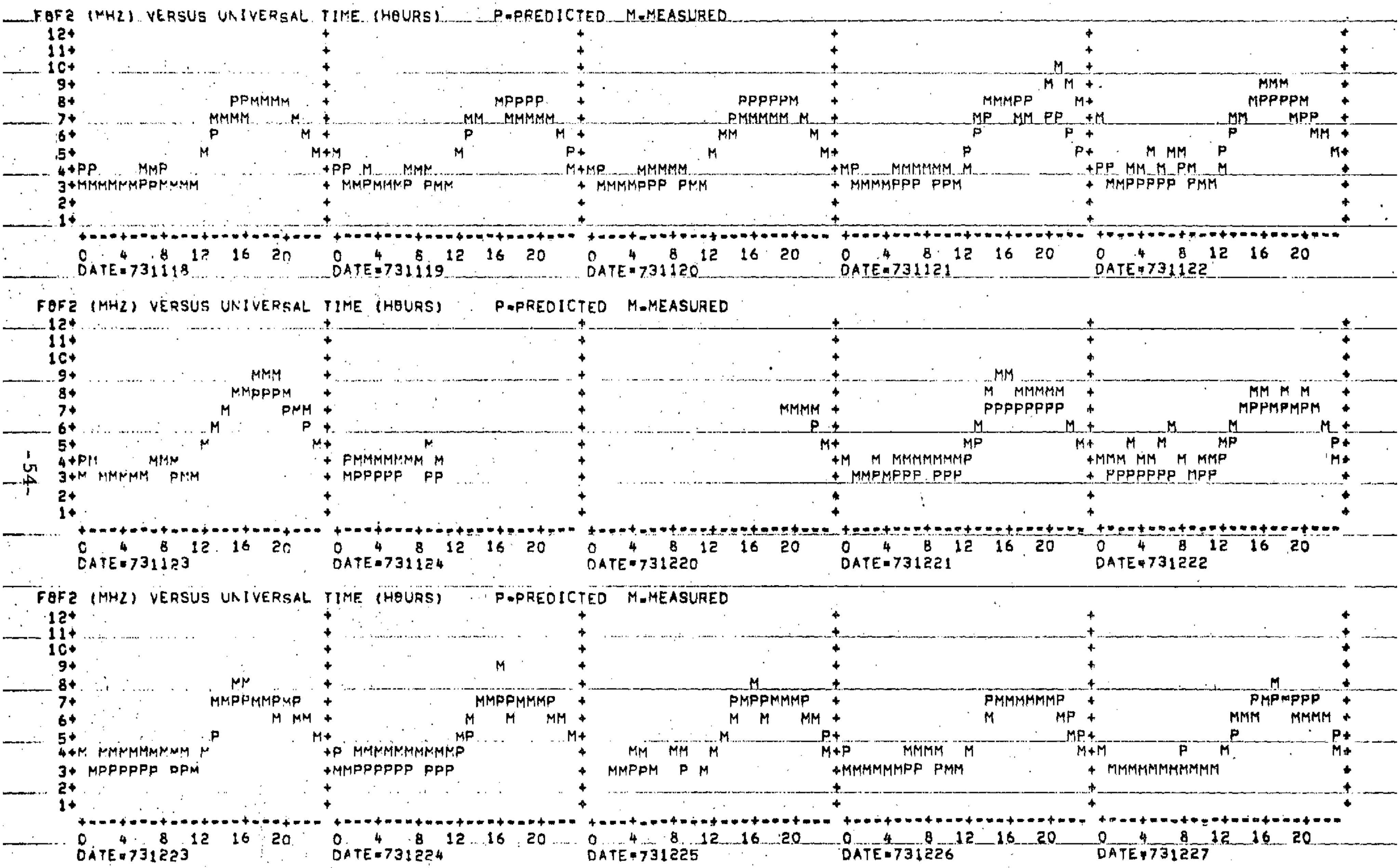
F0F2 (MHZ) VERSUS UNIVERSAL TIME (HOURS) P=PREDICTED M=MEASURED
0 4 8 12 16 20
DATE=731118
DATE=731119
DATE=731120
DATE=731121
DATE=731122
F0F2 (MHZ) VERSUS UNIVERSAL TIME (HOURS) P=PREDICTED M=MEASURED
DATE=731123
DATE=731124
DATE=731220
DATE=731221
DATE=731222
F0F2 (MHZ) VERSUS UNIVERSAL TIME (HOURS) P=PREDICTED M=MEASURED
DATE=731223
DATE=731224
DATE=731225
DATE=731226
DATE=731227

Figure 11c.

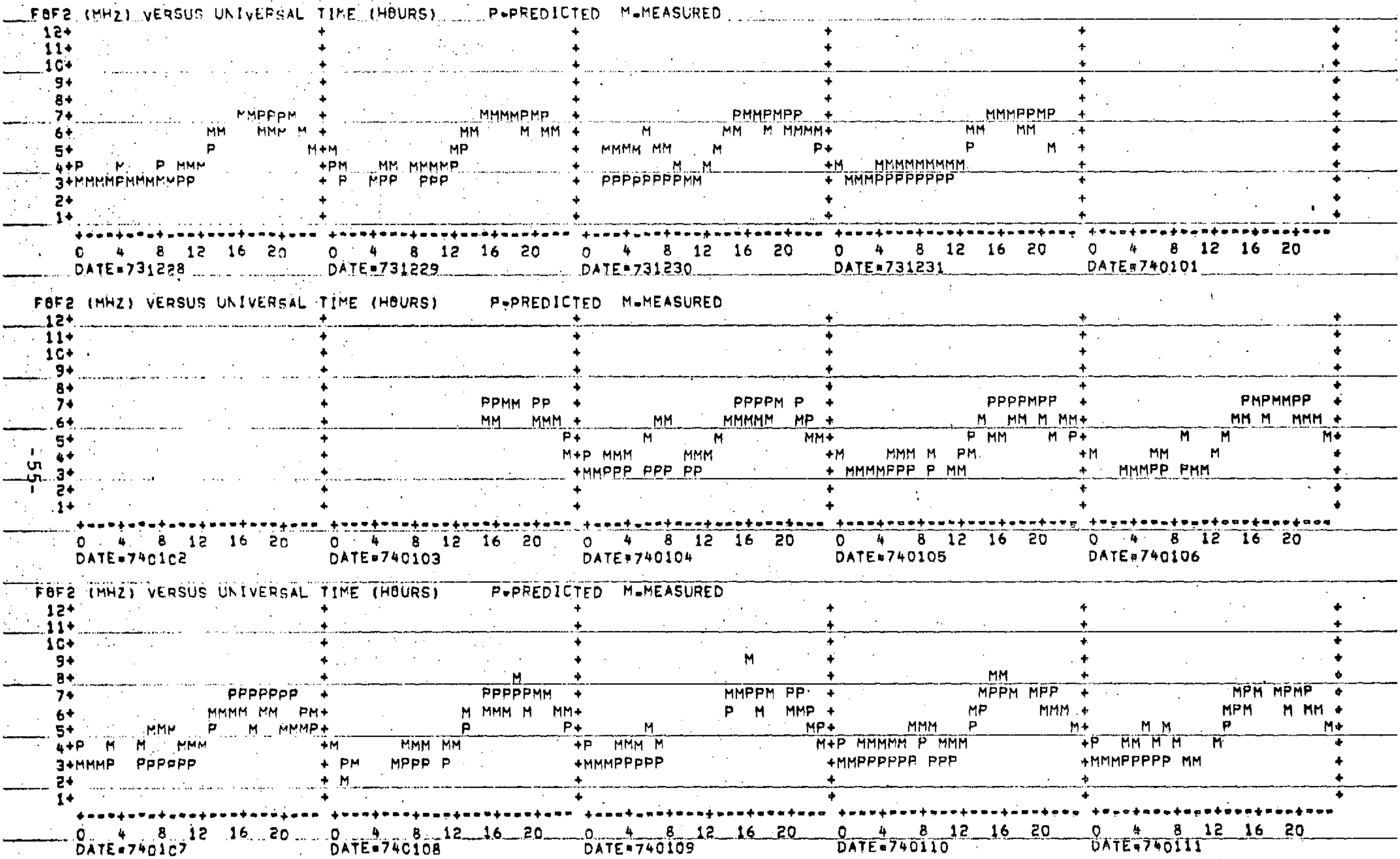
F0F2 (MHZ) VERSUS UNIVERSAL TIME (HOURS) P=PREDICTED M=MEASURED
DATE=731228
DATE=731229
DATE=731230
DATE=731231
DATE=740101
F0F2 (MHZ) VERSUS UNIVERSAL TIME (HOURS) P=PREDICTED M=MEASURED
DATE=740102
DATE=740103
DATE=740104
DATE=740105
DATE=740106
F0F2 (MHZ) VERSUS UNIVERSAL TIME (HOURS) P=PREDICTED M=MEASURED
DATE=740107
DATE=740108
DATE=740109
DATE=740110
DATE=740111

Figure 11d.

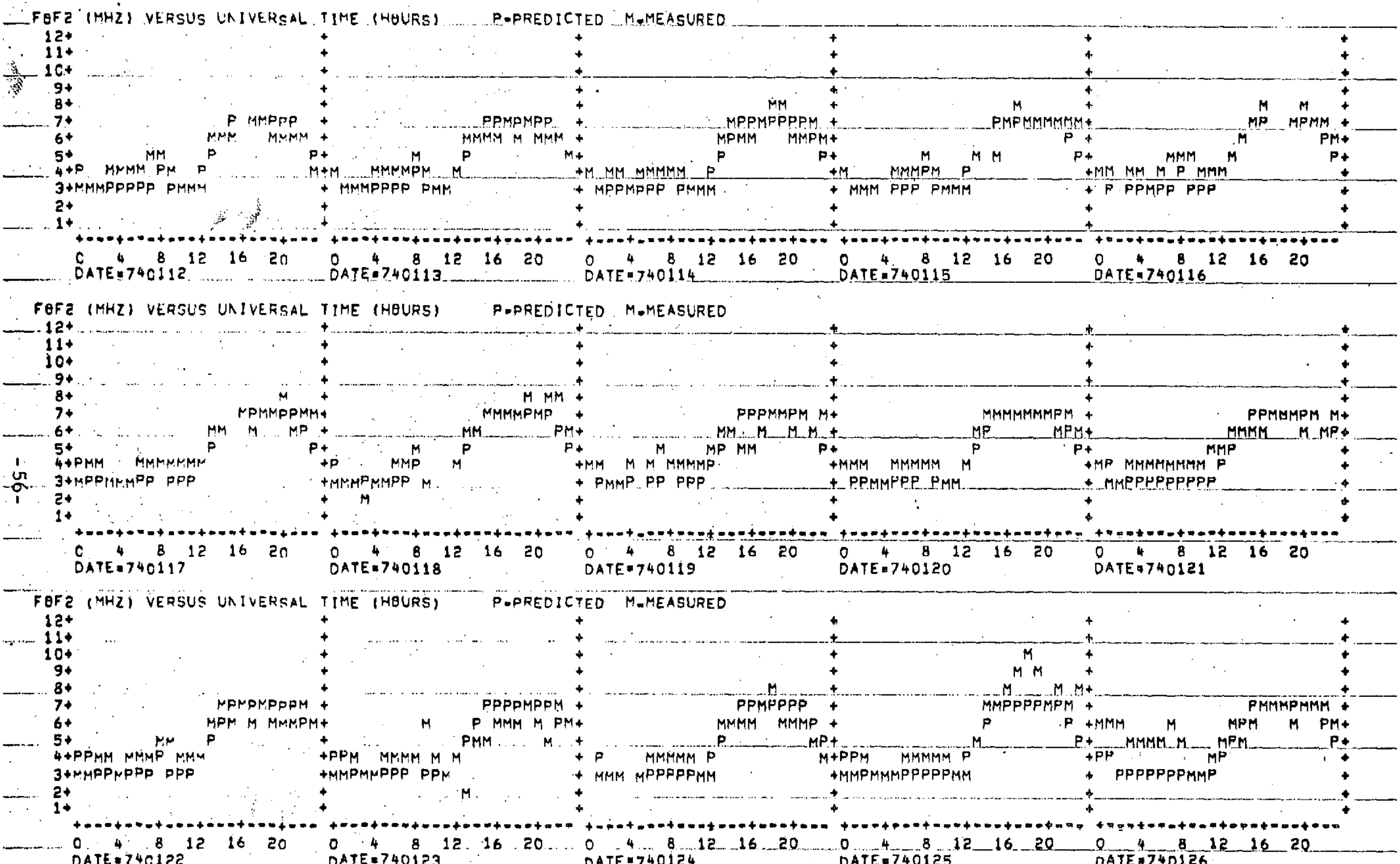
FOF2 (MHZ) VERSUS UNIVERSAL TIME (HOURS) P=PREDICTED M=MEASURED
DATE=740112
DATE=740113
DATE=740114
DATE=740115
DATE=740116
FOF2 (MHZ) VERSUS UNIVERSAL TIME (HOURS) P=PREDICTED M=MEASURED
DATE=740117
DATE=740118
DATE=740119
DATE=740120
DATE=740121
FOF2 (MHZ) VERSUS UNIVERSAL TIME (HOURS) P=PREDICTED M=MEASURED
DATE=740122
DATE=740123
DATE=740124
DATE=740125
DATE=740126

Figure 11e.

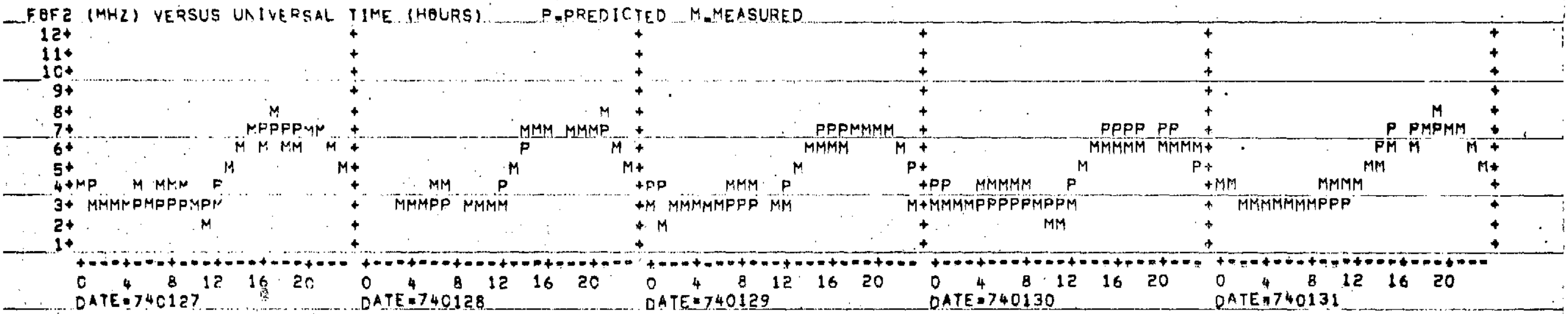
FOF2 (MHZ) VERSUS UNIVERSAL TIME (HOURS) P=PREDICTED M=MEASURED
DATE=740127
DATE=740128
DATE=740129
DATE=740130
DATE=740131

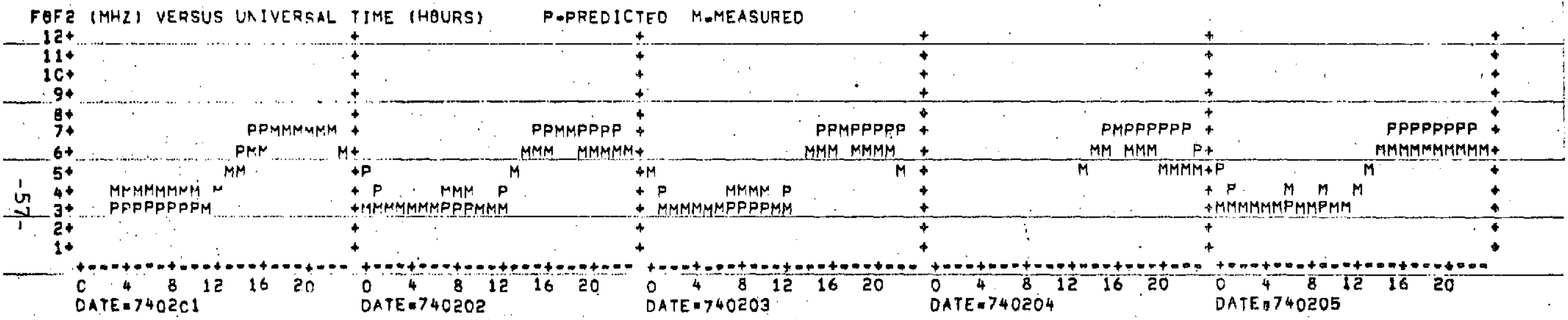
FOF2 (MHZ) VERSUS UNIVERSAL TIME (HOURS) P=PREDICTED M=MEASURED
DATE=740201
DATE=740202
DATE=740203
DATE=740204
DATE=740205

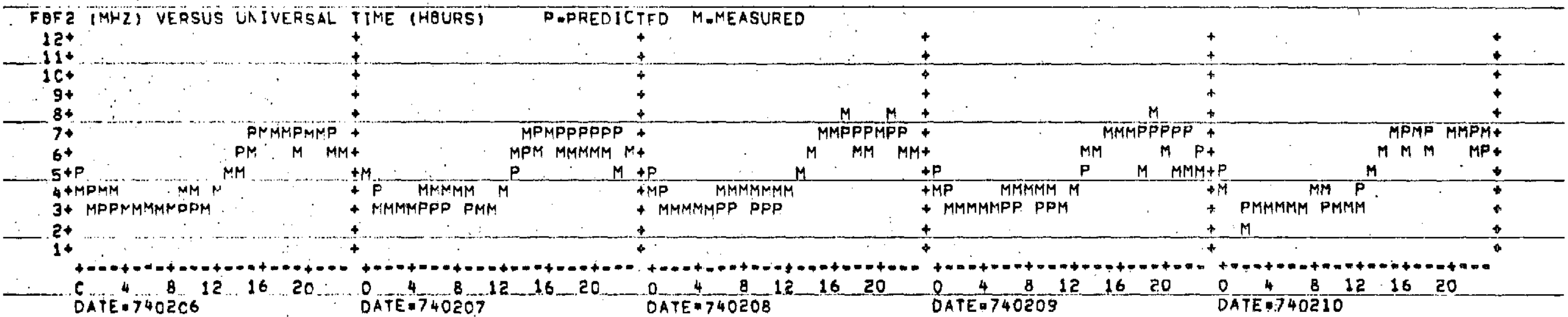
FOF2 (MHZ) VERSUS UNIVERSAL TIME (HOURS) P=PREDICTED M=MEASURED
DATE=740206
DATE=740207
DATE=740208
DATE=740209
DATE=740210

Figure 11f.

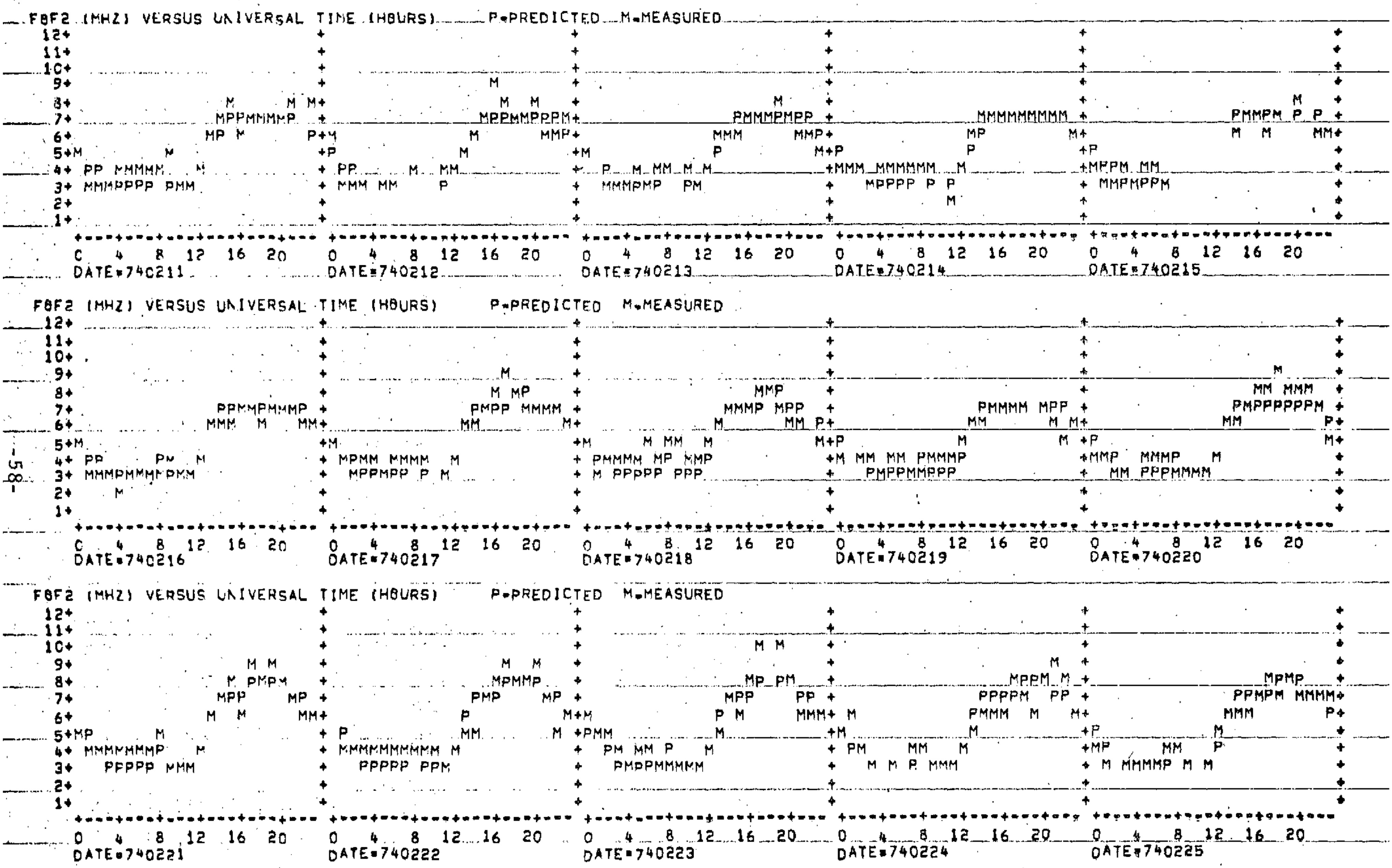
FBF2 (MHZ) VERSUS UNIVERSAL TIME (HOURS) P=PREDICTED M=MEASURED
DATE=740211
DATE=740212
DATE=740213
DATE=740214
DATE=740215
FBF2 (MHZ) VERSUS UNIVERSAL TIME (HOURS) P=PREDICTED M=MEASURED
DATE=740216
DATE=740217
DATE=740218
DATE=740219
DATE=740220
FBF2 (MHZ) VERSUS UNIVERSAL TIME (HOURS) P=PREDICTED M=MEASURED
DATE=740221
DATE=740222
DATE=740223
DATE=740224
DATE=740225

Figure 11g.

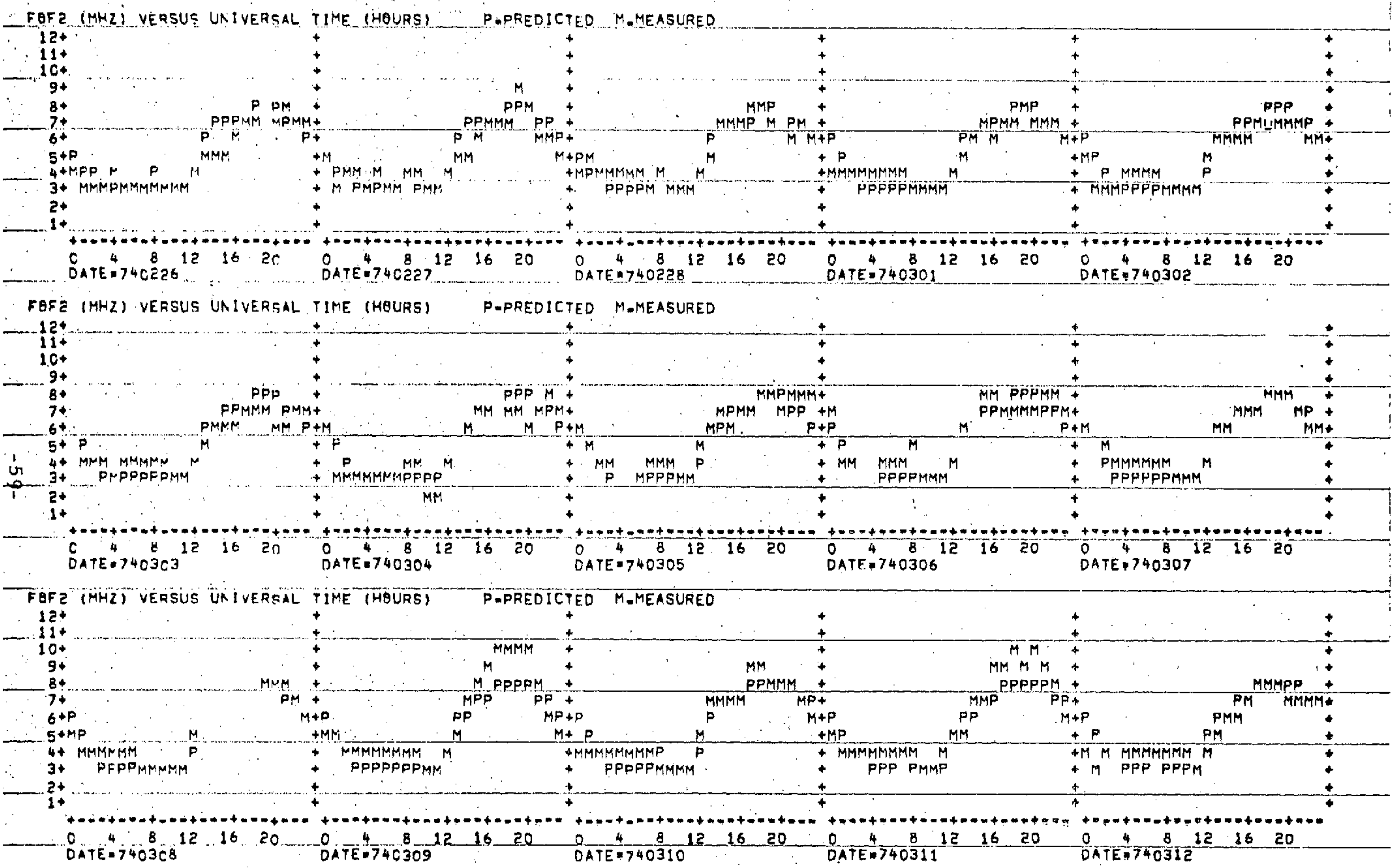
FBF2 (MHZ) VERSUS UNIVERSAL TIME (HOURS) P=PREDICTED M=MEASURED
DATE=740226
DATE=740227
DATE=740228
DATE=740301
DATE=740302
FBF2 (MHZ) VERSUS UNIVERSAL TIME (HOURS) P=PREDICTED M=MEASURED
DATE=740303
DATE=740304
DATE=740305
DATE=740306
DATE=740307
FBF2 (MHZ) VERSUS UNIVERSAL TIME (HOURS) P=PREDICTED M=MEASURED
DATE=740308
DATE=740309
DATE=740310
DATE=740311
DATE=740312

Figure 11h.

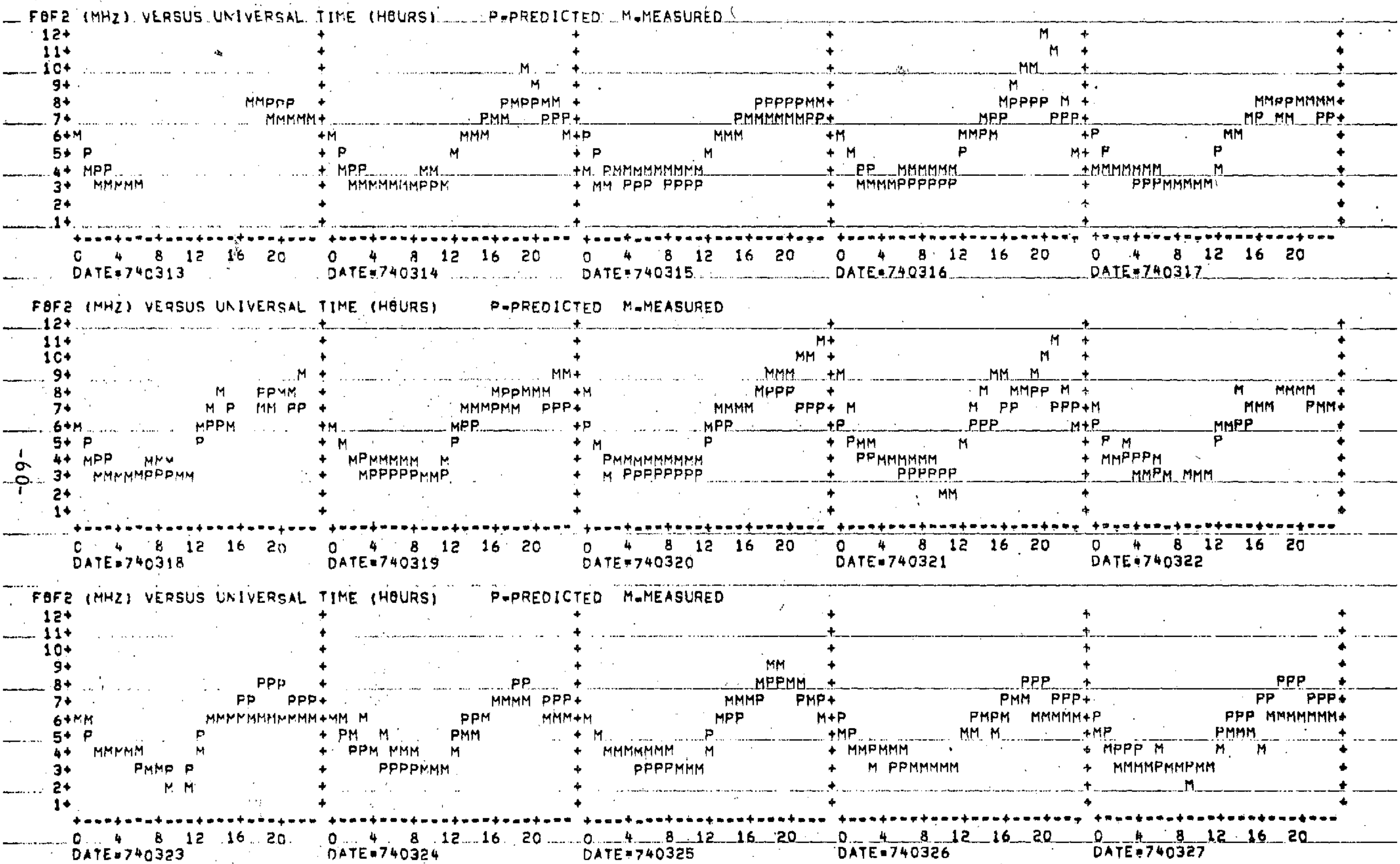
F0F2 (MHZ) VERSUS UNIVERSAL TIME (H0URS) P=PREDICTED M=MEASURED
DATE=740313
DATE=740314
DATE=740315
DATE=740316
DATE=740317
F0F2 (MHZ) VERSUS UNIVERSAL TIME (H0URS) P=PREDICTED M=MEASURED
DATE=740318
DATE=740319
DATE=740320
DATE=740321
DATE=740322
F0F2 (MHZ) VERSUS UNIVERSAL TIME (H0URS) P=PREDICTED M=MEASURED
DATE=740323
DATE=740324
DATE=740325
DATE=740326
DATE=740327

Figure 11-i.

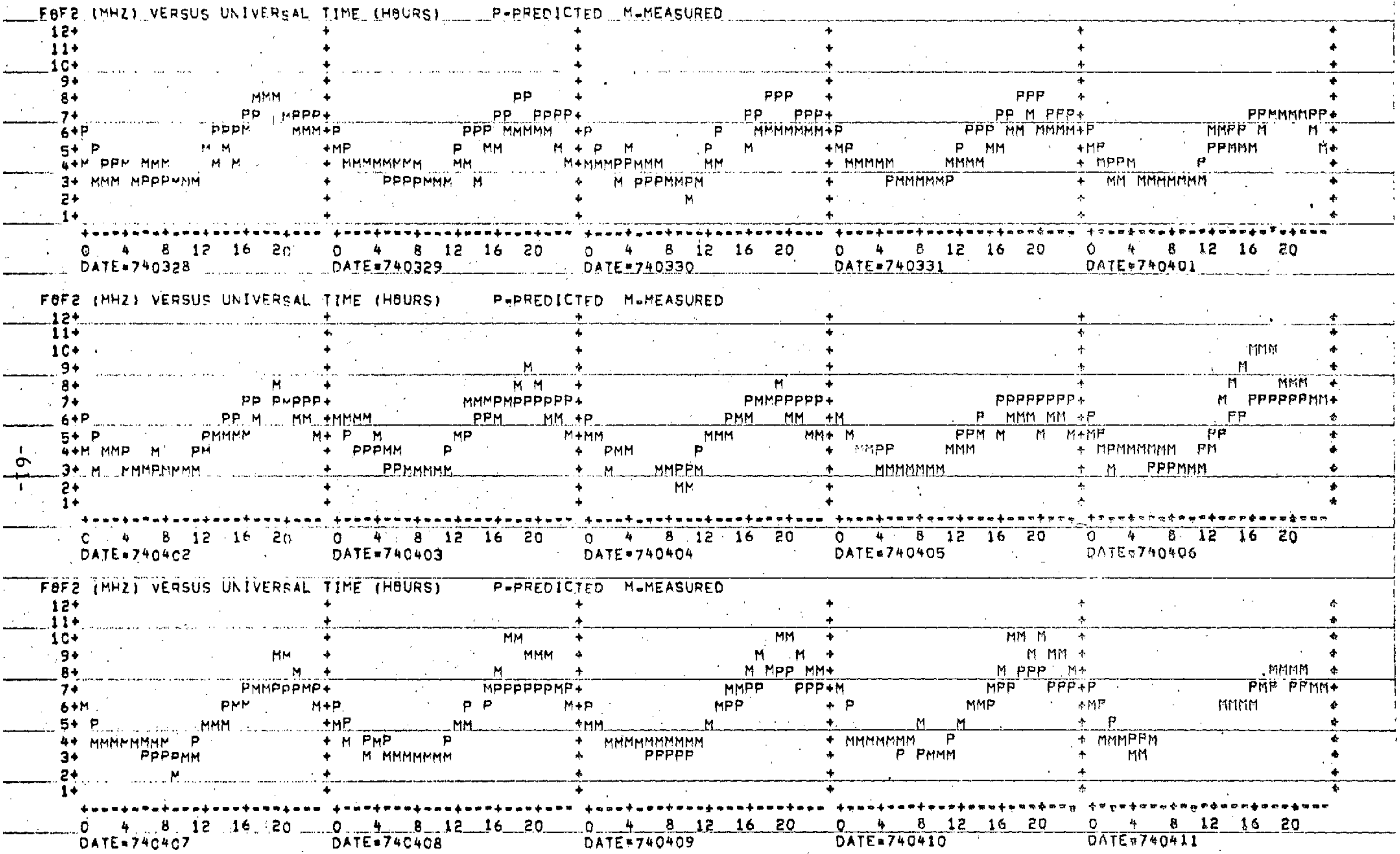
F0F2 (MHZ) VERSUS UNIVERSAL TIME (HOURS) P=PREDICTED M=MEASURED
DATE=740328
DATE=740329
DATE=740330
DATE=740331
DATE=740401
F0F2 (MHZ) VERSUS UNIVERSAL TIME (HOURS) P=PREDICTED M=MEASURED
DATE=740402
DATE=740403
DATE=740404
DATE=740405
DATE=740406
F0F2 (MHZ) VERSUS UNIVERSAL TIME (HOURS) P=PREDICTED M=MEASURED
DATE=740407
DATE=740408
DATE=740409
DATE=740410
DATE=740411

Figure 11j.

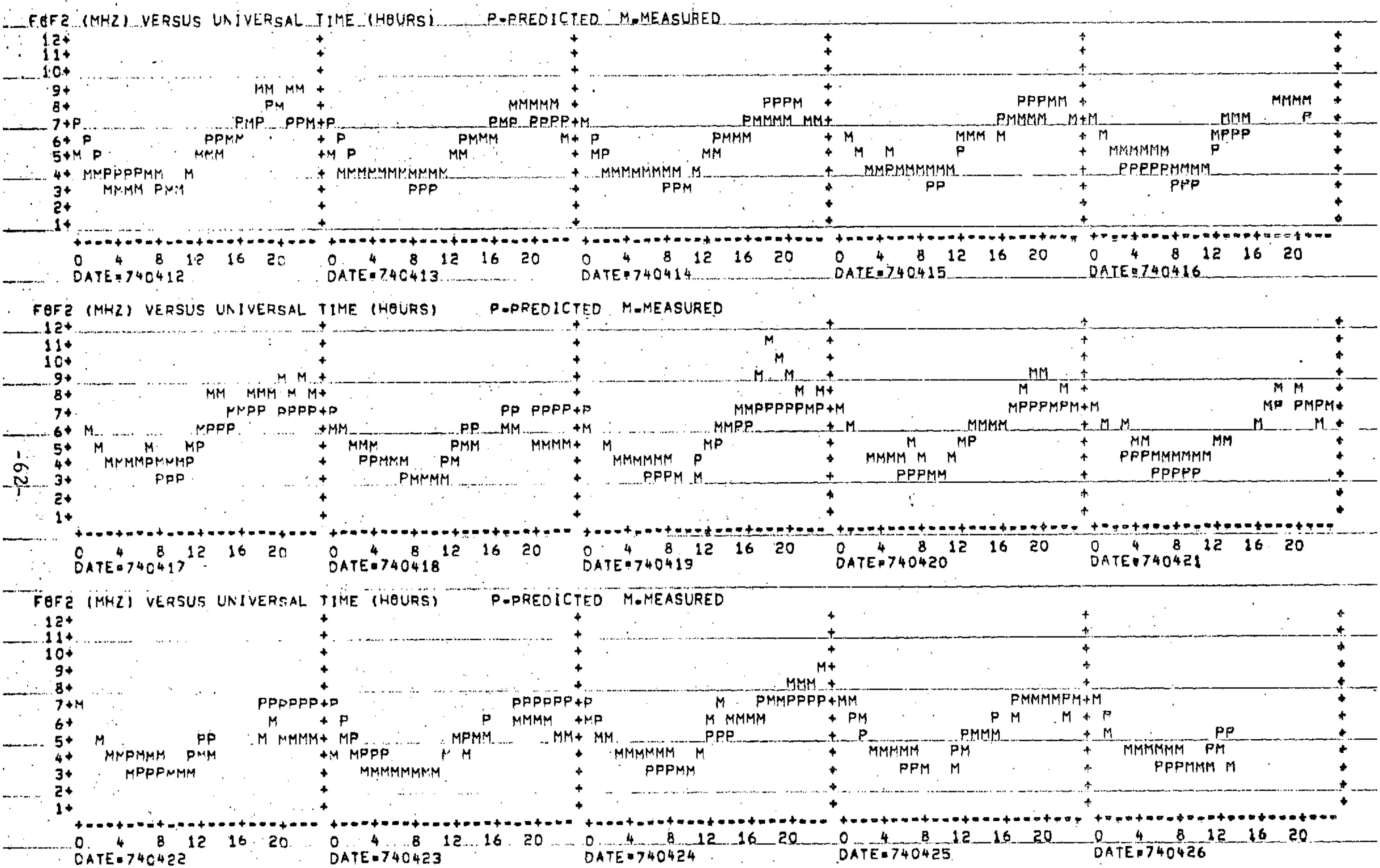
F0F2 (MHZ) VERSUS UNIVERSAL TIME (HOURS) P=PREDICTED M=MEASURED
DATE=740412
DATE=740413
DATE=740414
DATE=740415
DATE=740416
F0F2 (MHZ) VERSUS UNIVERSAL TIME (HOURS) P=PREDICTED M=MEASURED
DATE=740417
DATE=740418
DATE=740419
DATE=740420
DATE=740421
F0F2 (MHZ) VERSUS UNIVERSAL TIME (HOURS) P=PREDICTED M=MEASURED
DATE=740422
DATE=740423
DATE=740424
DATE=740425
DATE=740426

Figure 11k.

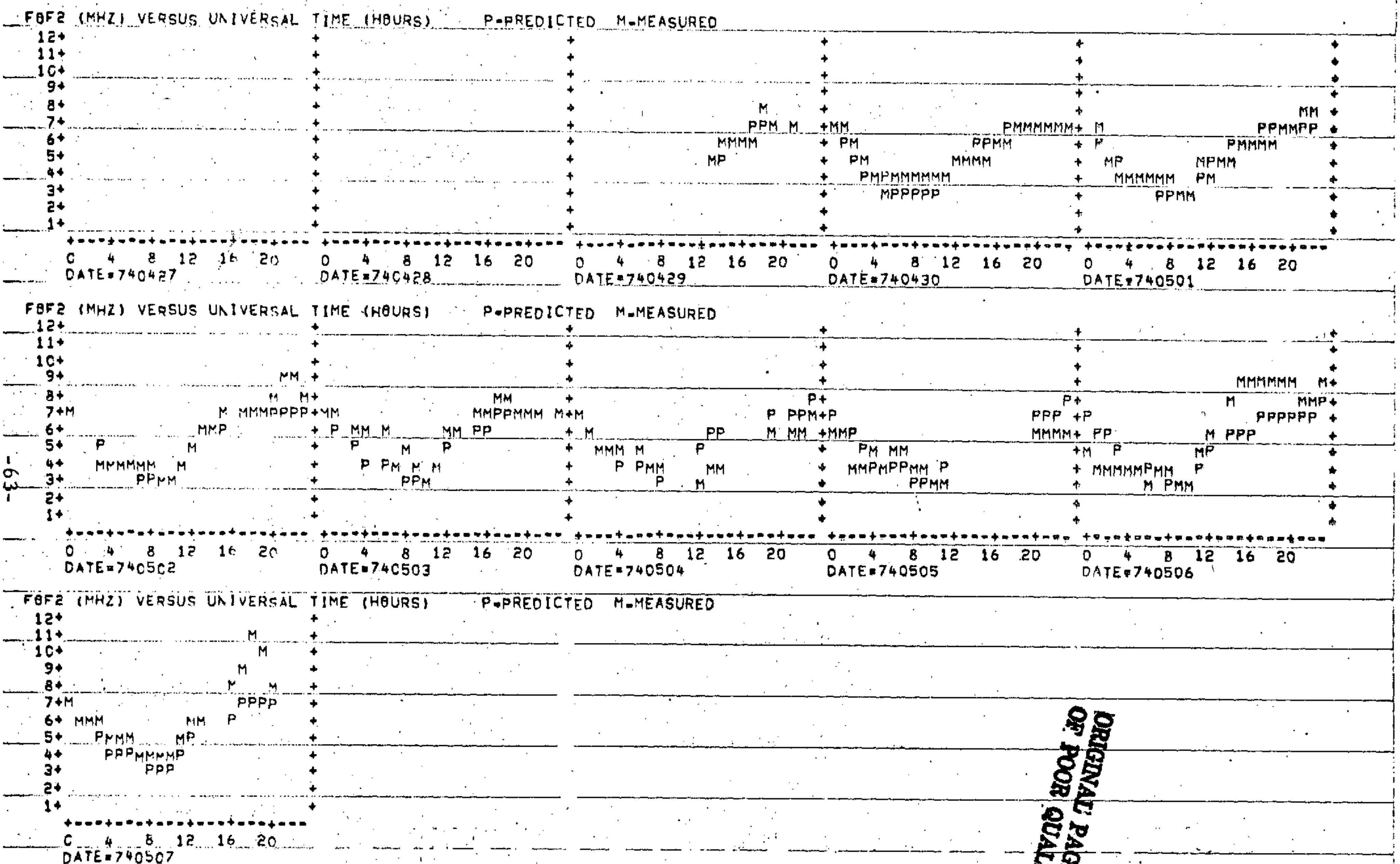
FOF2 (MHZ) VERSUS UNIVERSAL TIME (HOURS) P=PREDICTED M=MEASURED
0 4 8 12 16 20
DATE=740427
DATE=740428
DATE=740429
DATE=740430
DATE=740501
FOF2 (MHZ) VERSUS UNIVERSAL TIME (HOURS) P=PREDICTED M=MEASURED
DATE=740502
DATE=740503
DATE=740504
DATE=740505
DATE=740506
FOF2 (MHZ) VERSUS UNIVERSAL TIME (HOURS) P=PREDICTED M=MEASURED
DATE=740507

Figure 11-1.

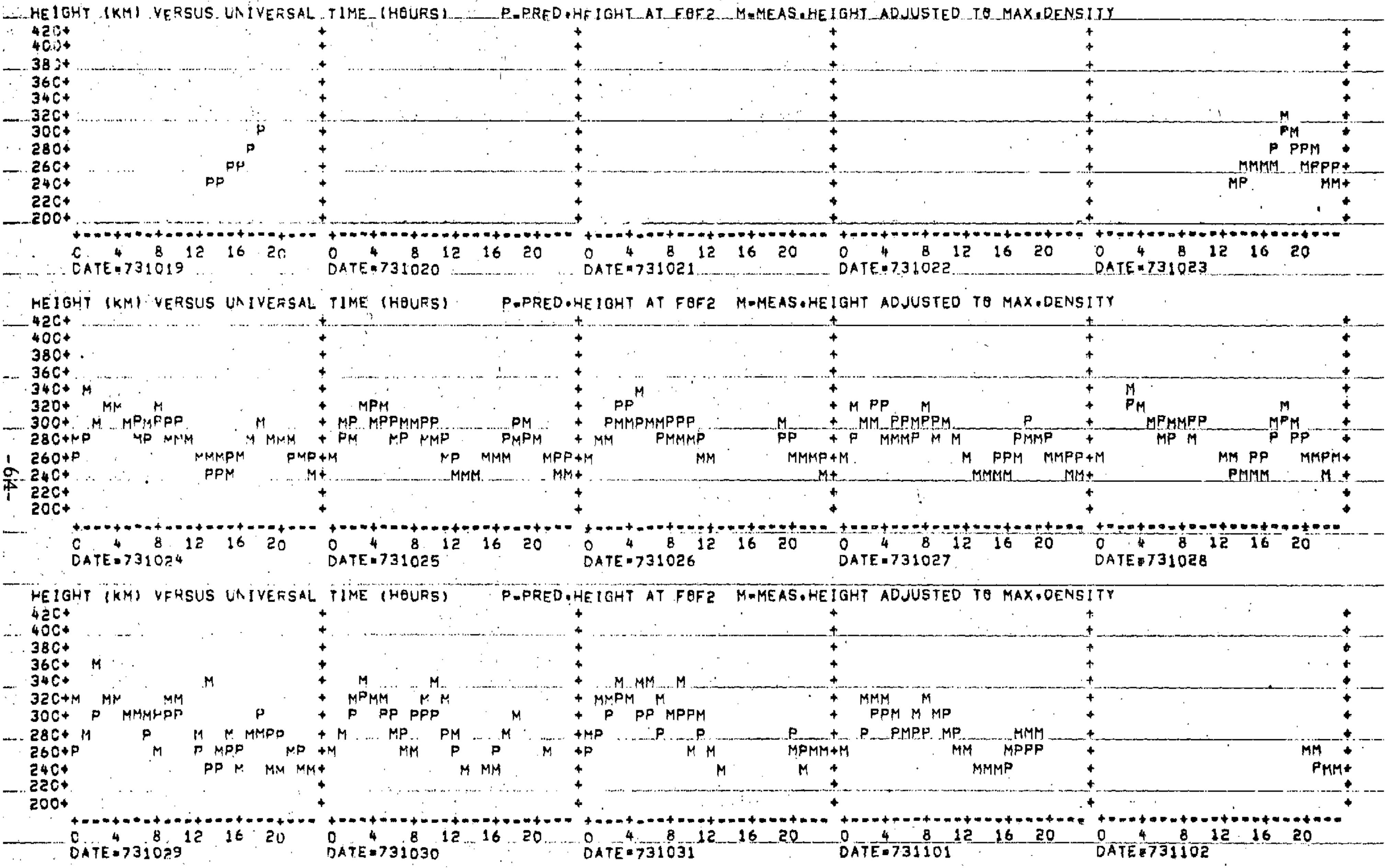
HEIGHT (KM) VERSUS UNIVERSAL TIME (HOURS)
P=PRED.HEIGHT AT FOF2
M=MEAS.HEIGHT ADJUSTED TO MAX.DENSITY
DATE=731019
DATE=731020
DATE=731021
DATE=731022
DATE=731023
DATE=731024
DATE=731025
DATE=731026
DATE=731027
DATE=731028
DATE=731029
DATE=731030
DATE=731031
DATE=731101
DATE=731102

Figure 12a.

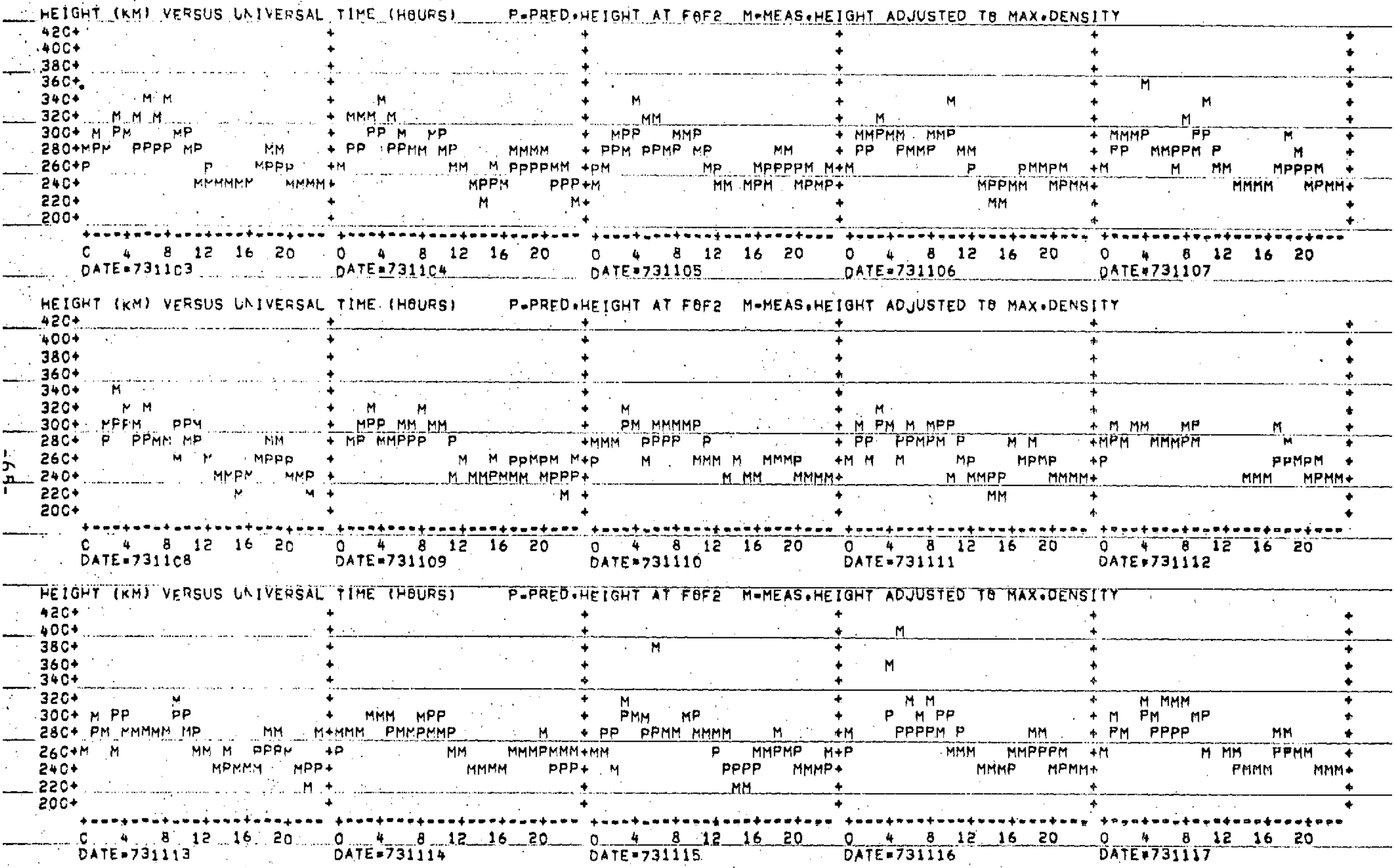
HEIGHT (KM) VERSUS UNIVERSAL TIME (HOURS) P=PRED.HEIGHT AT F0F2 M=MEAS.HEIGHT ADJUSTED TO MAX.DENSITY
DATE=731103
DATE=731104
DATE=731105
DATE=731106
DATE=731107
DATE=731108
DATE=731109
DATE=731110
DATE=731111
DATE=731112
DATE=731113
DATE=731114
DATE=731115
DATE=731116
DATE=731117

Figure 12b.

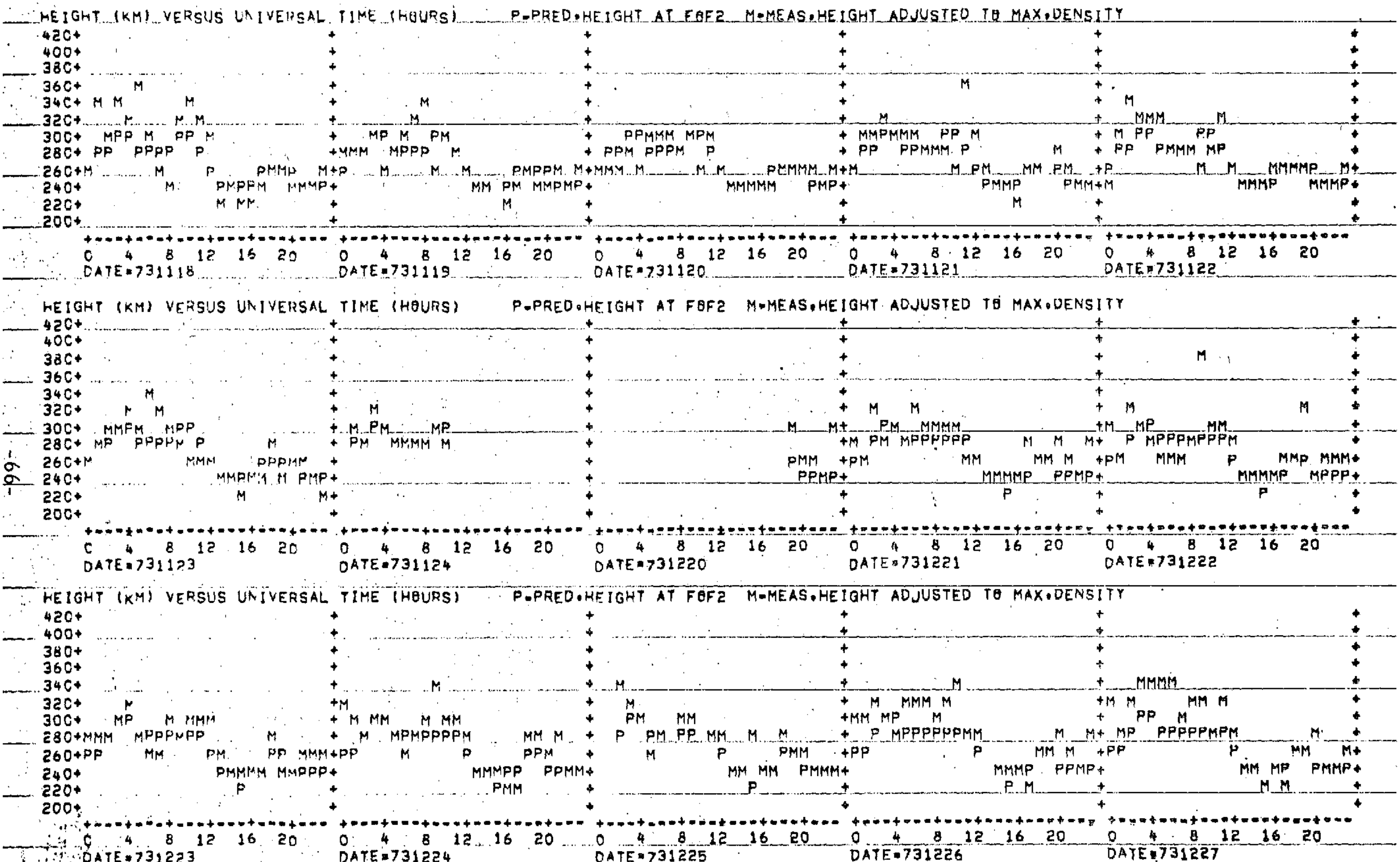
HEIGHT (KM) VERSUS UNIVERSAL TIME (HOURS) P=PRED.HEIGHT AT F0F2 M=MEAS.HEIGHT ADJUSTED TO MAX.DENSITY
420
400
380
360
340
320
300
280
260
240
220
200
0 4 8 12 16 20
DATE=731118
DATE=731119
DATE=731120
DATE=731121
DATE=731122
HEIGHT (KM) VERSUS UNIVERSAL TIME (HOURS) P=PRED.HEIGHT AT F0F2 M=MEAS.HEIGHT ADJUSTED TO MAX.DENSITY
DATE=731123
DATE=731124
DATE=731220
DATE=731221
DATE=731222
HEIGHT (KM) VERSUS UNIVERSAL TIME (HOURS) P=PRED.HEIGHT AT F0F2 M=MEAS.HEIGHT ADJUSTED TO MAX.DENSITY
DATE=731223
DATE=731224
DATE=731225
DATE=731226
DATE=731227

Figure 12c.

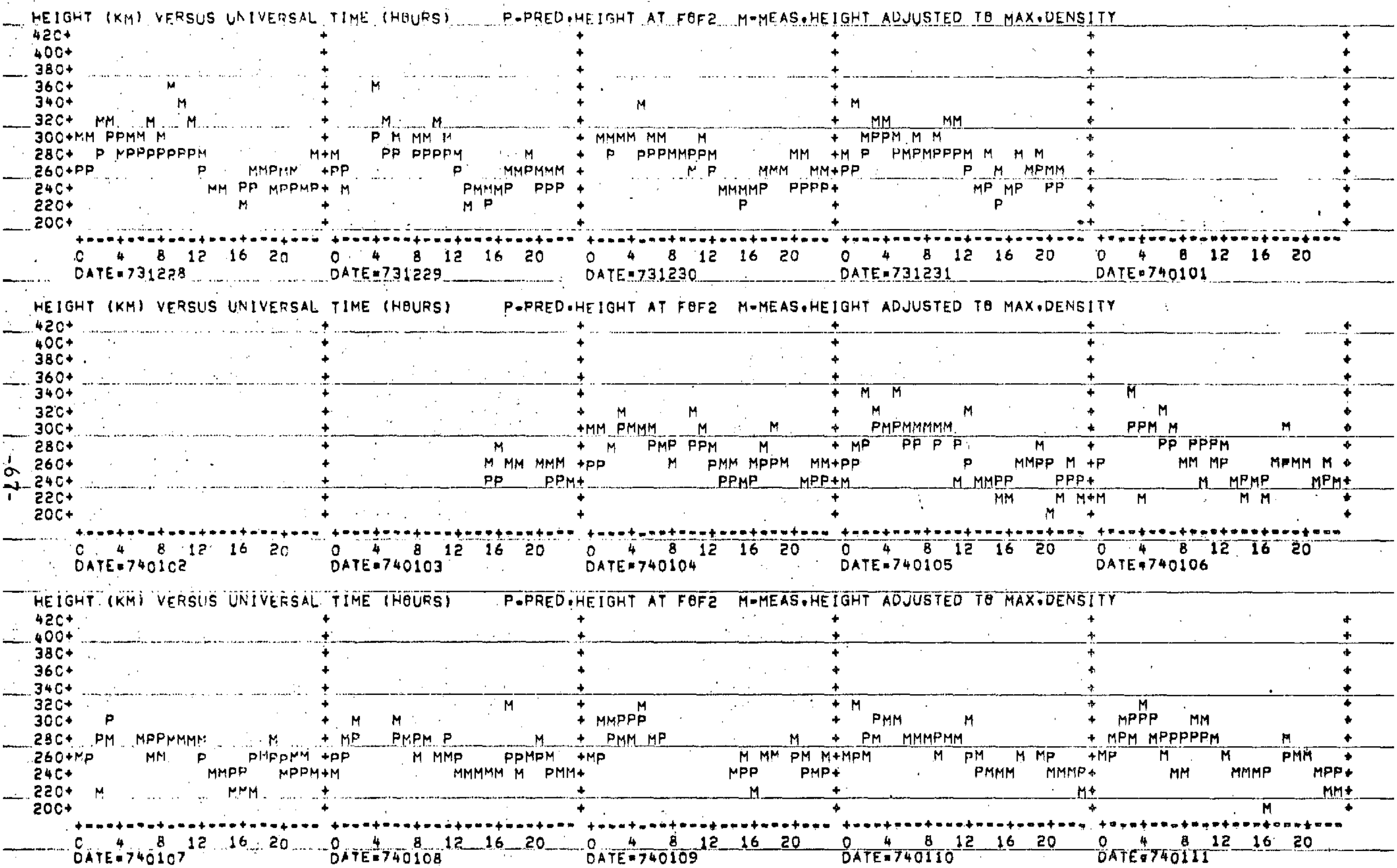
HEIGHT (KM) VERSUS UNIVERSAL TIME (HOURS)
P=PRED.HEIGHT AT F0F2 M=MEAS.HEIGHT ADJUSTED TO MAX.DENSITY
DATE=731228
DATE=731229
DATE=731230
DATE=731231
DATE=740101
HEIGHT (KM) VERSUS UNIVERSAL TIME (HOURS)
P=PRED.HEIGHT AT F0F2 M=MEAS.HEIGHT ADJUSTED TO MAX.DENSITY
DATE=740102
DATE=740103
DATE=740104
DATE=740105
DATE=740106
HEIGHT (KM) VERSUS UNIVERSAL TIME (HOURS)
P=PRED.HEIGHT AT F0F2 M=MEAS.HEIGHT ADJUSTED TO MAX.DENSITY
DATE=740107
DATE=740108
DATE=740109
DATE=740110
DATE=740111

Figure 12d.

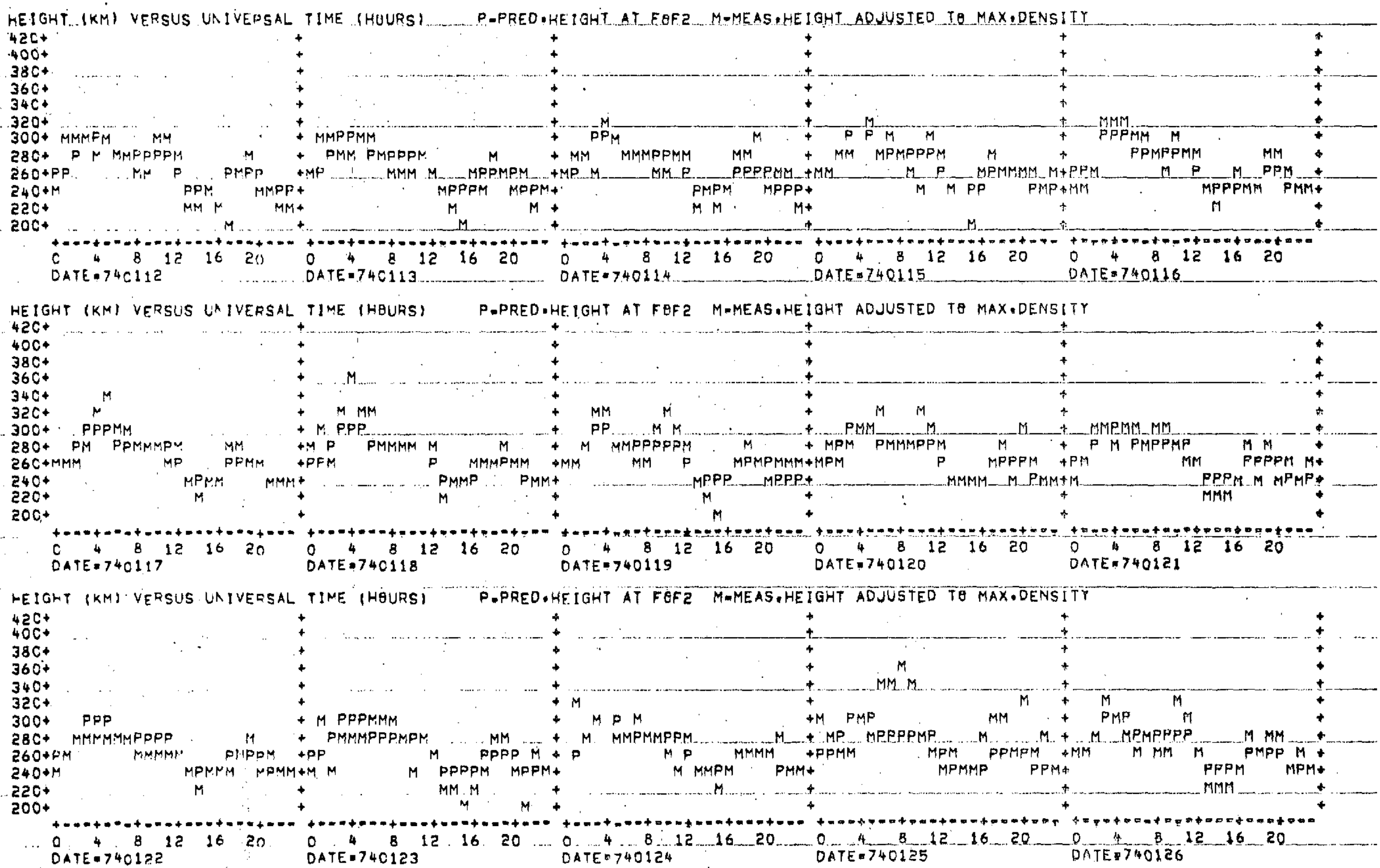
HEIGHT (KM) VERSUS UNIVERSAL TIME (HOURS) P=PRED.HEIGHT AT F0F2 M=MEAS.HEIGHT ADJUSTED TO MAX.DENSITY
DATE=740112
DATE=740113
DATE=740114
DATE=740115
DATE=740116
HEIGHT (KM) VERSUS UNIVERSAL TIME (HOURS) P=PRED.HEIGHT AT F0F2 M=MEAS.HEIGHT ADJUSTED TO MAX.DENSITY
DATE=740117
DATE=740118
DATE=740119
DATE=740120
DATE=740121
HEIGHT (KM) VERSUS UNIVERSAL TIME (HOURS) P=PRED.HEIGHT AT F0F2 M=MEAS.HEIGHT ADJUSTED TO MAX.DENSITY
DATE=740122
DATE=740123
DATE=740124
DATE=740125
DATE=740126

Figure 12e.

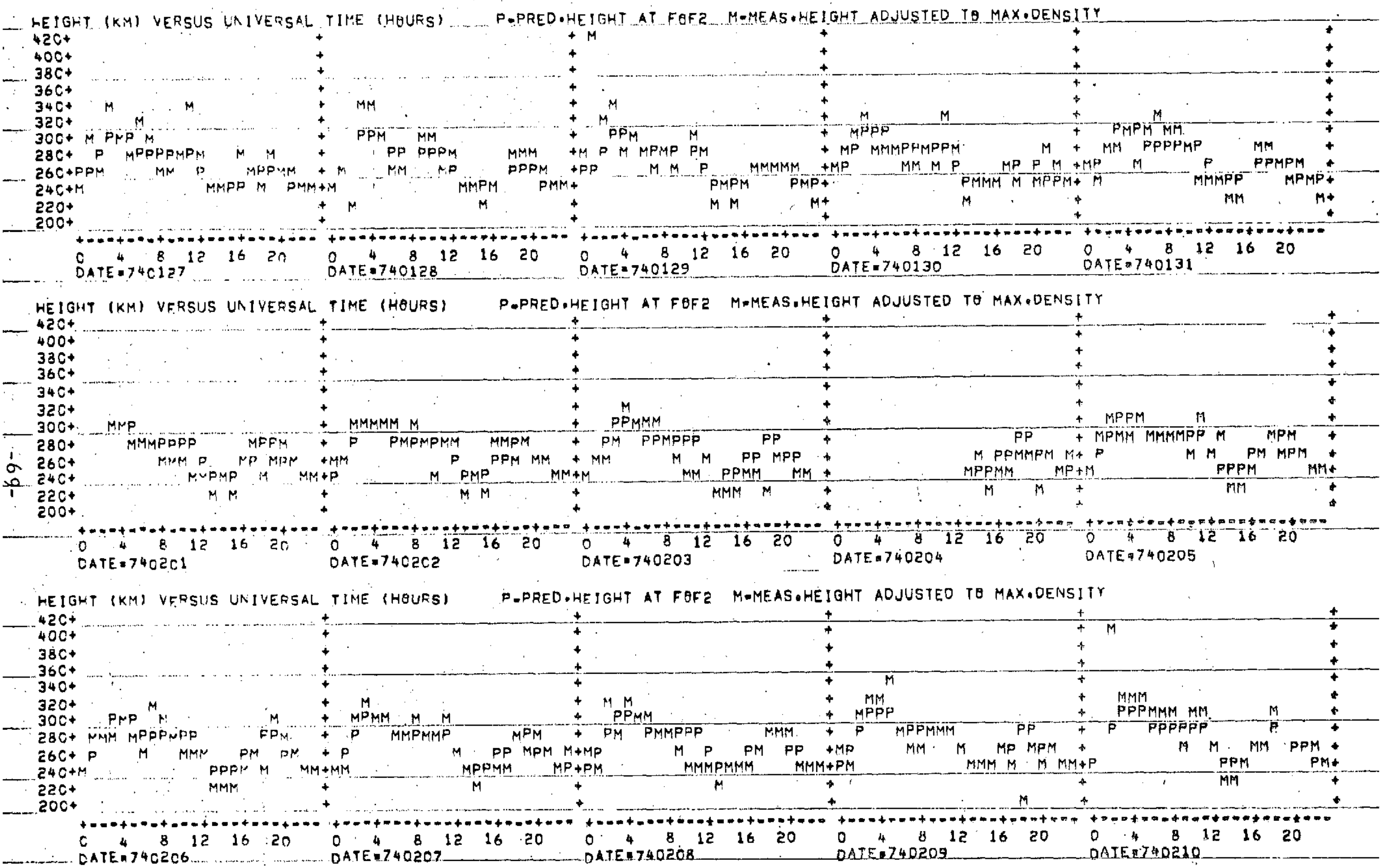
HEIGHT (KM) VERSUS UNIVERSAL TIME (HOURS) P=PRED.HEIGHT AT F0F2 M=MEAS.HEIGHT ADJUSTED TO MAX.DENSITY
DATE=740127
DATE=740128
DATE=740129
DATE=740130
DATE=740131
HEIGHT (KM) VERSUS UNIVERSAL TIME (HOURS) P=PRED.HEIGHT AT F0F2 M=MEAS.HEIGHT ADJUSTED TO MAX.DENSITY
DATE=740201
DATE=740202
DATE=740203
DATE=740204
DATE=740205
HEIGHT (KM) VERSUS UNIVERSAL TIME (HOURS) P=PRED.HEIGHT AT F0F2 M=MEAS.HEIGHT ADJUSTED TO MAX.DENSITY
DATE=740206
DATE=740207
DATE=740208
DATE=740209
DATE=740210

Figure 12f.

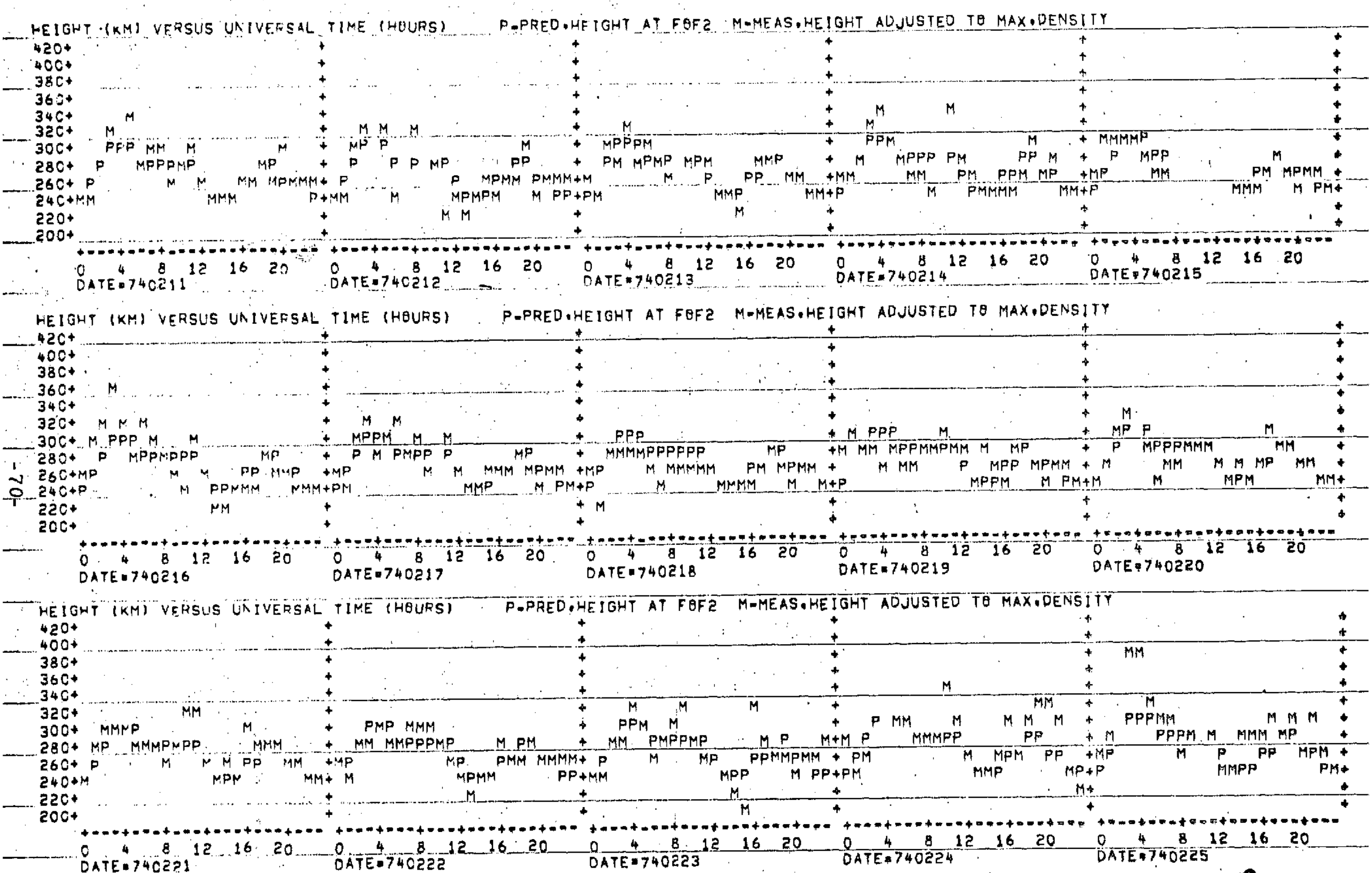

HEIGHT (KM) VERSUS UNIVERSAL TIME (HOURS) P=PRED.HEIGHT AT F0F2 M=MEAS.HEIGHT ADJUSTED TO MAX.DENSITY
420 400 380 360 340 320 300 280 260 240 220 200
0 4 8 12 16 20
DATE=740211
DATE=740212
DATE=740213
DATE=740214
DATE=740215
HEIGHT (KM) VERSUS UNIVERSAL TIME (HOURS) P=PRED.HEIGHT AT F0F2 M=MEAS.HEIGHT ADJUSTED TO MAX.DENSITY
DATE=740216
DATE=740217
DATE=740218
DATE=740219
DATE=740220
HEIGHT (KM) VERSUS UNIVERSAL TIME (HOURS) P=PRED.HEIGHT AT F0F2 M=MEAS.HEIGHT ADJUSTED TO MAX.DENSITY
DATE=740221
DATE=740222
DATE=740223
DATE=740224
DATE=740225

Figure 12g.

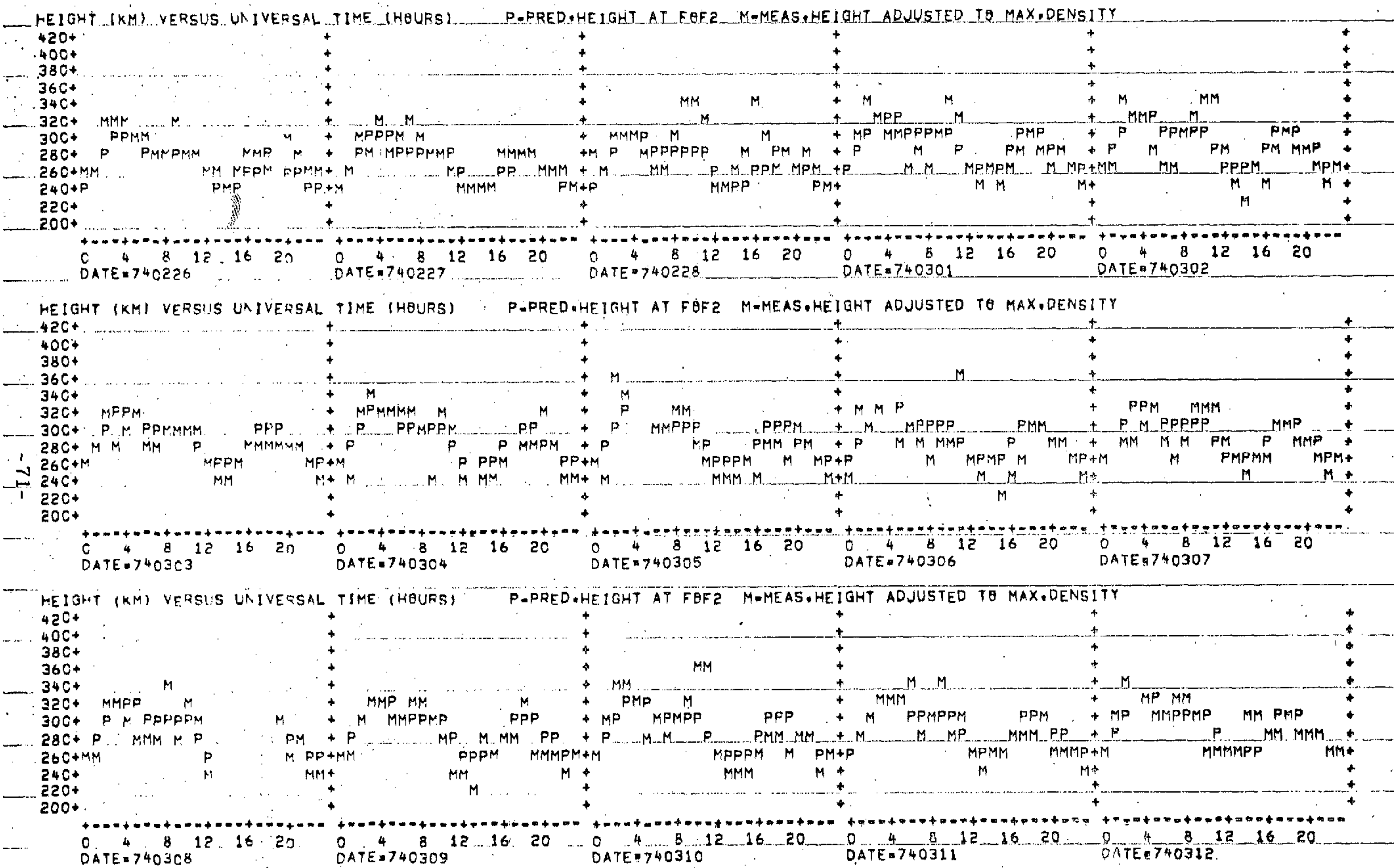
HEIGHT (KM) VERSUS UNIVERSAL TIME (HOURS) P=PRED.HEIGHT AT F0F2 M=MEAS.HEIGHT ADJUSTED TO MAX.DENSITY
DATE=740226
DATE=740227
DATE=740228
DATE=740301
DATE=740302
HEIGHT (KM) VERSUS UNIVERSAL TIME (HOURS) P=PRED.HEIGHT AT F0F2 M=MEAS.HEIGHT ADJUSTED TO MAX.DENSITY
DATE=740303
DATE=740304
DATE=740305
DATE=740306
DATE=740307
HEIGHT (KM) VERSUS UNIVERSAL TIME (HOURS) P=PRED.HEIGHT AT F0F2 M=MEAS.HEIGHT ADJUSTED TO MAX.DENSITY
DATE=740308
DATE=740309
DATE=740310
DATE=740311
DATE=740312

Figure 12h.

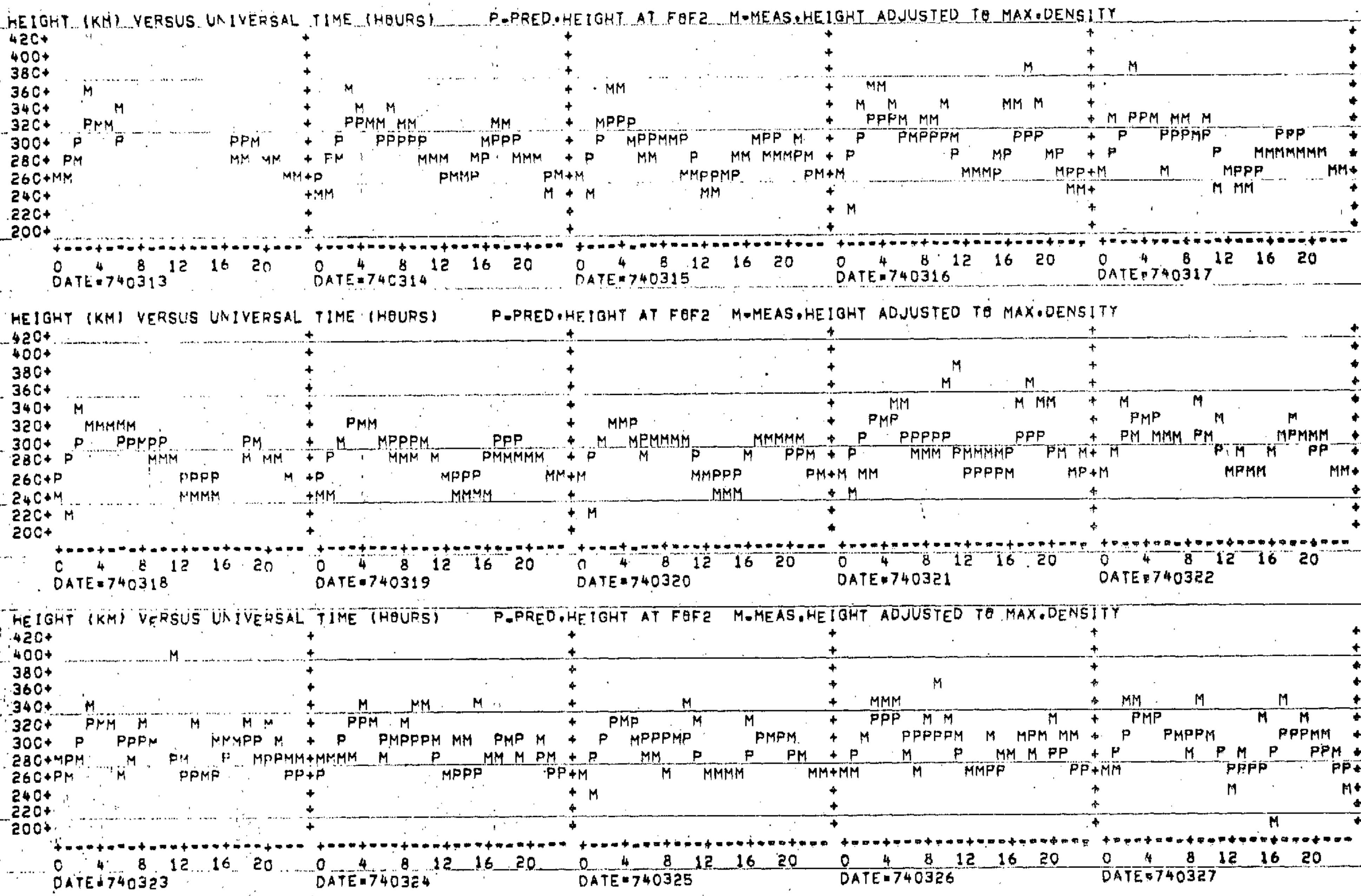
HEIGHT (KM) VERSUS UNIVERSAL TIME (HOURS)
P=PRED.HEIGHT AT F0F2
M=MEAS.HEIGHT ADJUSTED TO MAX.DENSITY
0 4 8 12 16 20
DATE=740313
DATE=740314
DATE=740315
DATE=740316
DATE=740317
DATE=740318
DATE=740319
DATE=740320
DATE=740321
DATE=740322
DATE=740323
DATE=740324
DATE=740325
DATE=740326
DATE=740327

Figure 12-1.

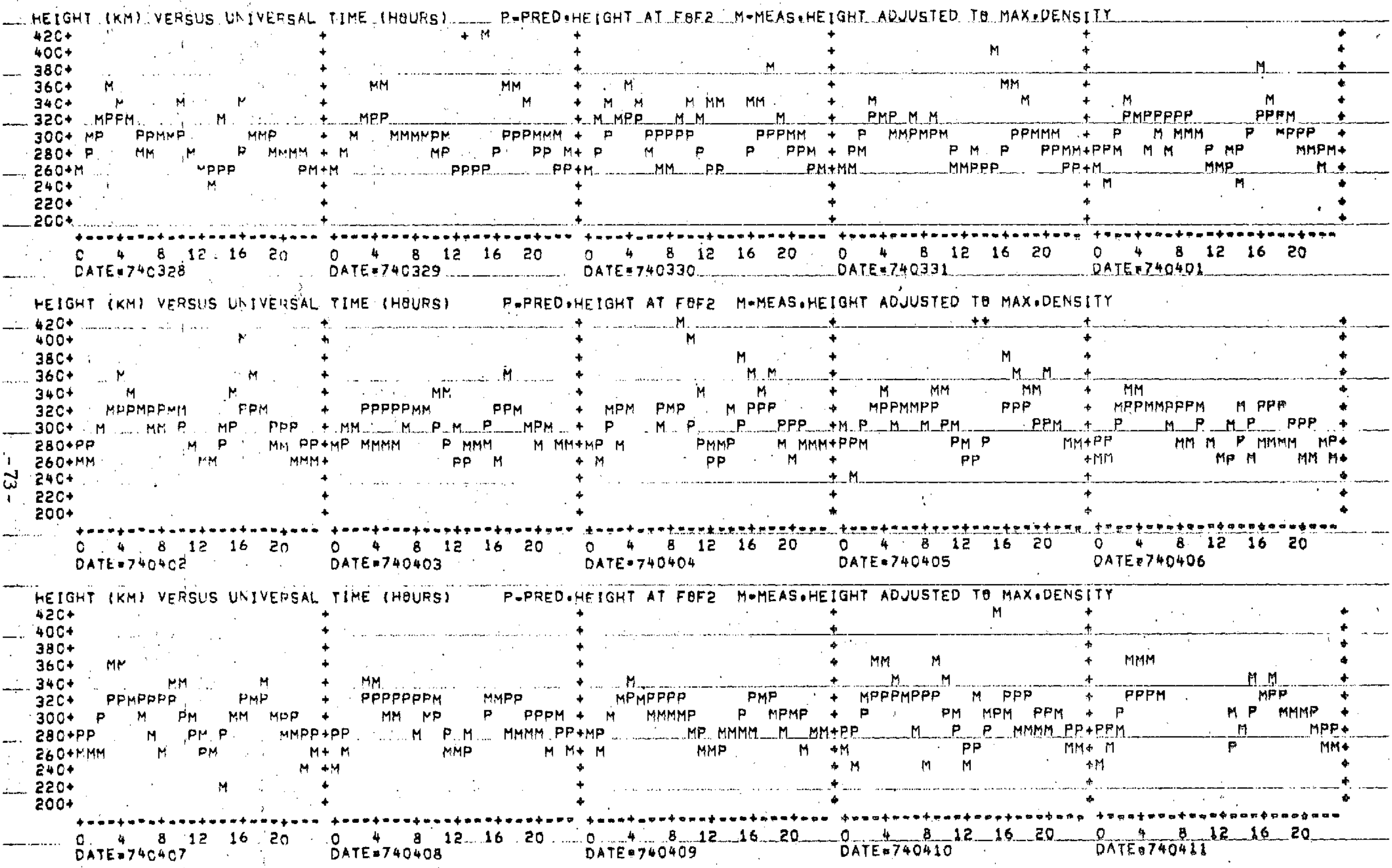
HEIGHT (KM) VERSUS UNIVERSAL TIME (HOURS) P=PRED.HEIGHT AT F0F2 M=MEAS.HEIGHT ADJUSTED TO MAX.DENSITY
DATE=740328
DATE=740329
DATE=740330
DATE=740331
DATE=740401
DATE=740402
DATE=740403
DATE=740404
DATE=740405
DATE=740406
DATE=740407
DATE=740408
DATE=740409
DATE=740410
DATE=740411

Figure 12j.

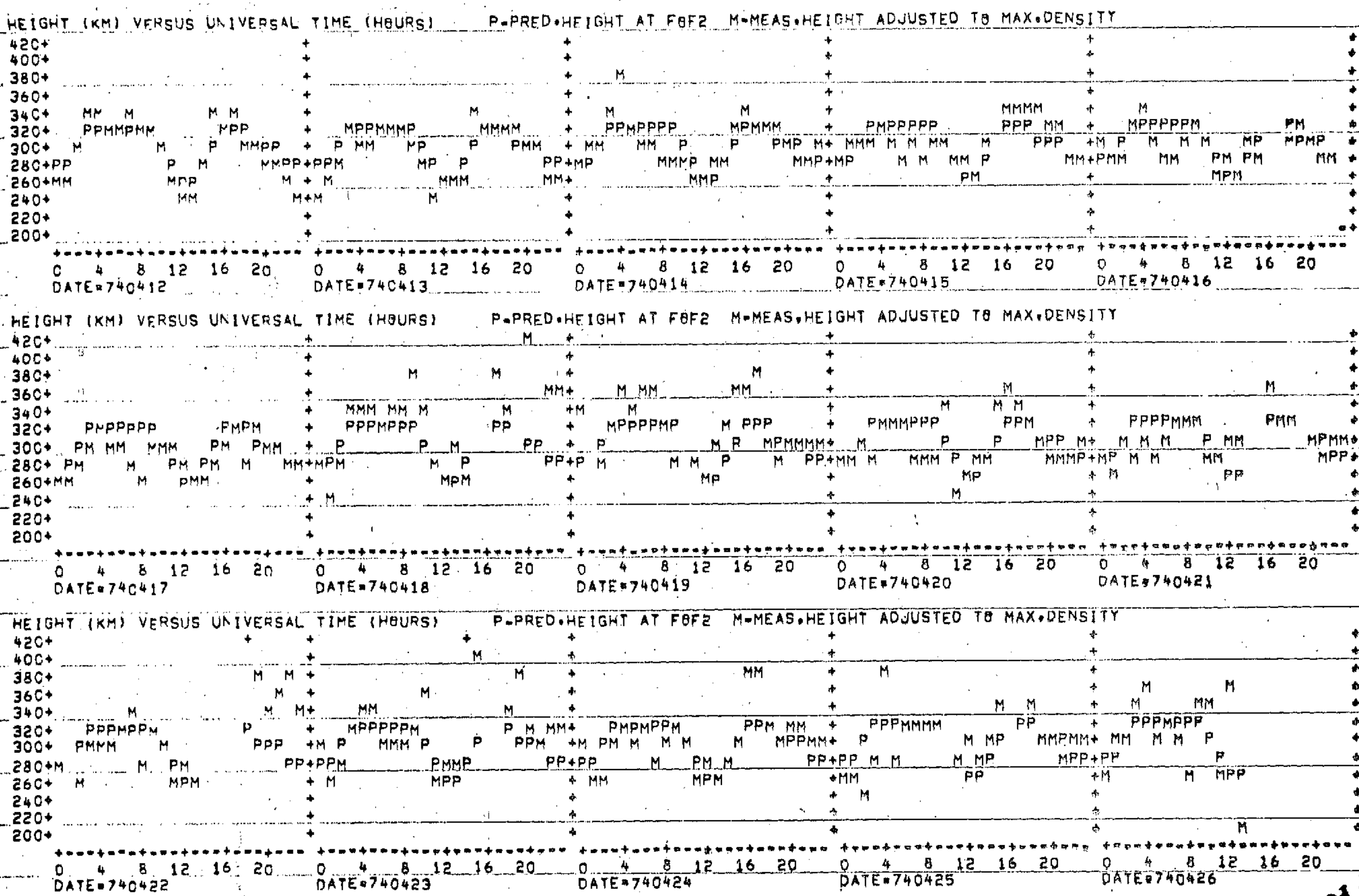
HEIGHT (KM) VERSUS UNIVERSAL TIME (HOURS) P=PRED.HEIGHT AT F0F2 M=MEAS.HEIGHT ADJUSTED TO MAX.DENSITY
DATE=740412
DATE=740413
DATE=740414
DATE=740415
DATE=740416
HEIGHT (KM) VERSUS UNIVERSAL TIME (HOURS) P=PRED.HEIGHT AT F0F2 M=MEAS.HEIGHT ADJUSTED TO MAX.DENSITY
DATE=740417
DATE=740418
DATE=740419
DATE=740420
DATE=740421
HEIGHT (KM) VERSUS UNIVERSAL TIME (HOURS) P=PRED.HEIGHT AT F0F2 M=MEAS.HEIGHT ADJUSTED TO MAX.DENSITY
DATE=740422
DATE=740423
DATE=740424
DATE=740425
DATE=740426

Figure 12k.

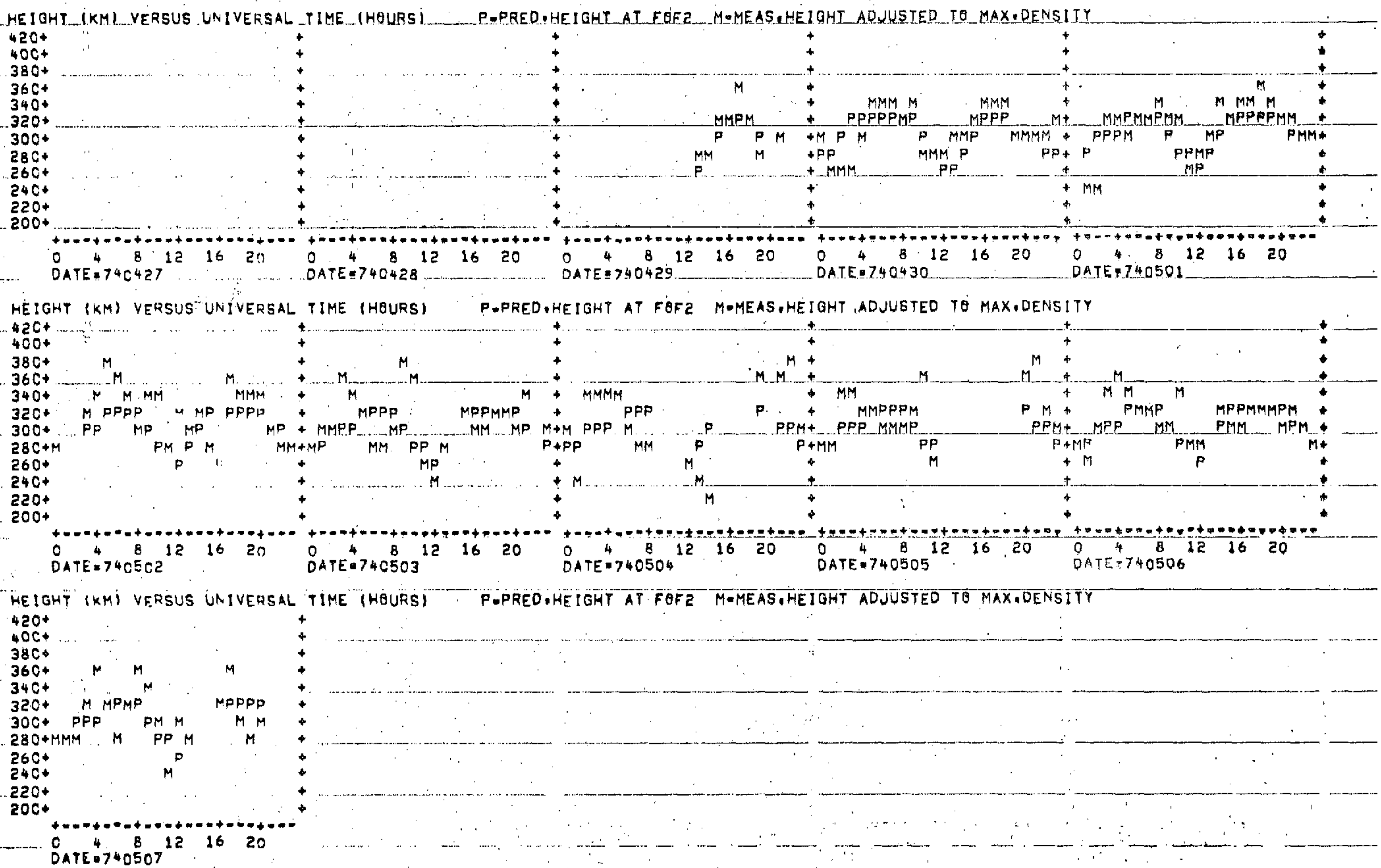
HEIGHT (KM) VERSUS UNIVERSAL TIME (HOURS)   P=PRED.HEIGHT AT F0F2 M=MEAS.HEIGHT ADJUSTED TO MAX.DENSITY
420
400
380
360
340
320
300
280
260
240
220
200
0 4 8 12 16 20
DATE=740427
DATE=740428
DATE=740429
DATE=740430
DATE=740501
HEIGHT (KM) VERSUS UNIVERSAL TIME (HOURS)   P=PRED.HEIGHT AT F0F2 M=MEAS.HEIGHT ADJUSTED TO MAX.DENSITY
DATE=740502
DATE=740503
DATE=740504
DATE=740505
DATE=740506
HEIGHT (KM) VERSUS UNIVERSAL TIME (HOURS)   P=PRED.HEIGHT AT F0F2 M=MEAS.HEIGHT ADJUSTED TO MAX.DENSITY
DATE=740507

Figure 12-1.

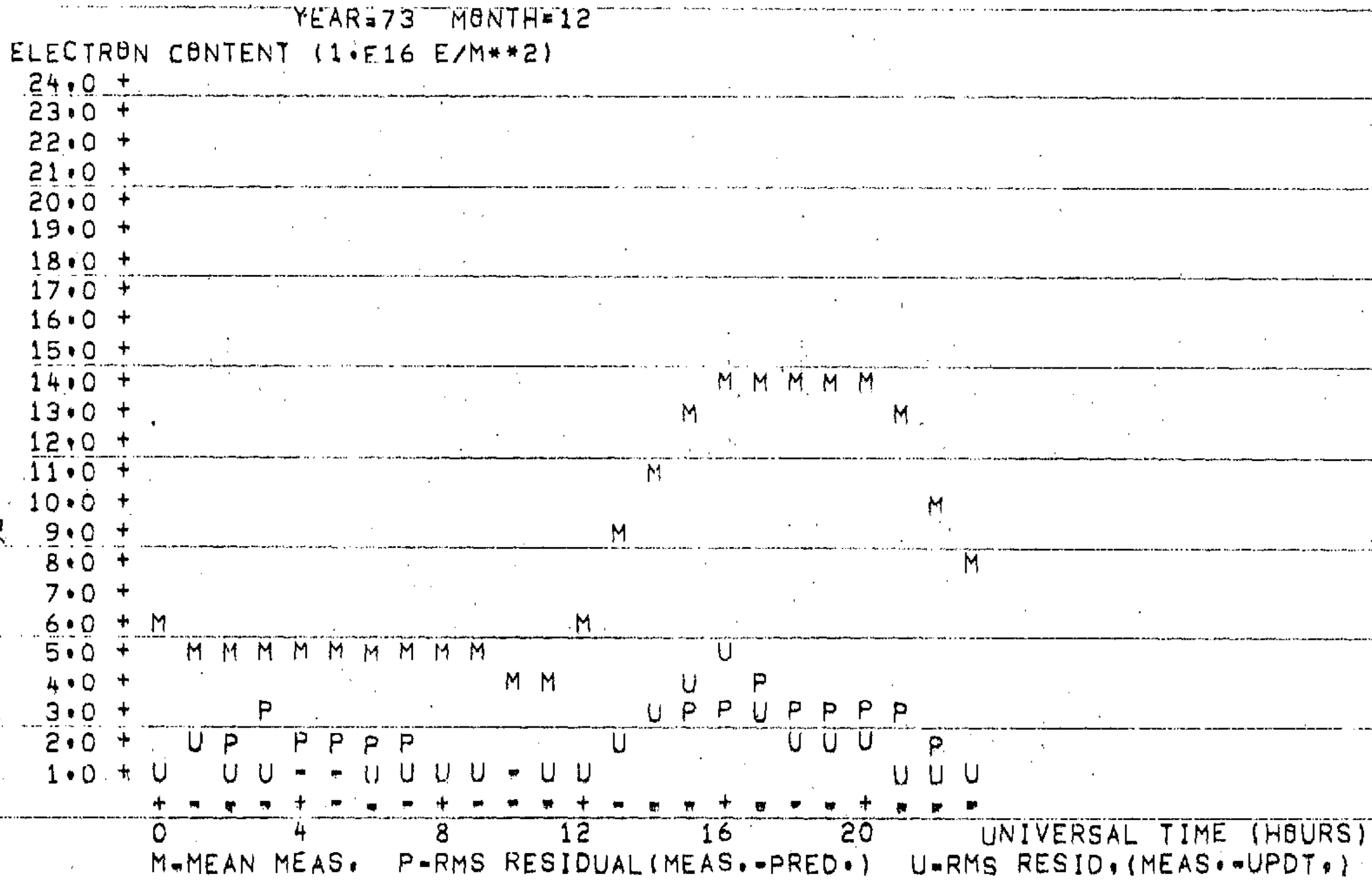

Figure 13a. Monthly Mean and Error Curves.

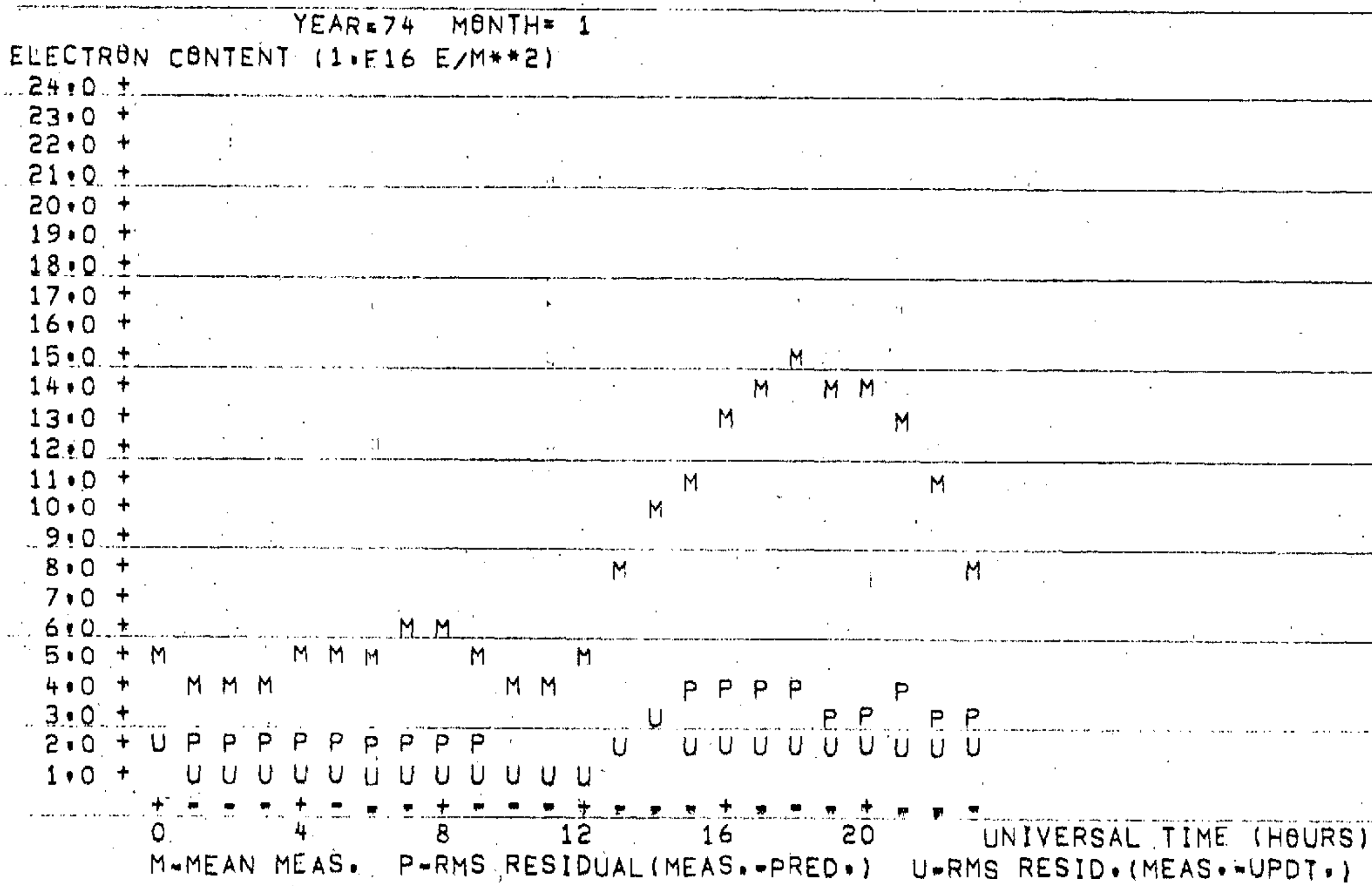

Figure 13b. Monthly Mean and Error Curves.

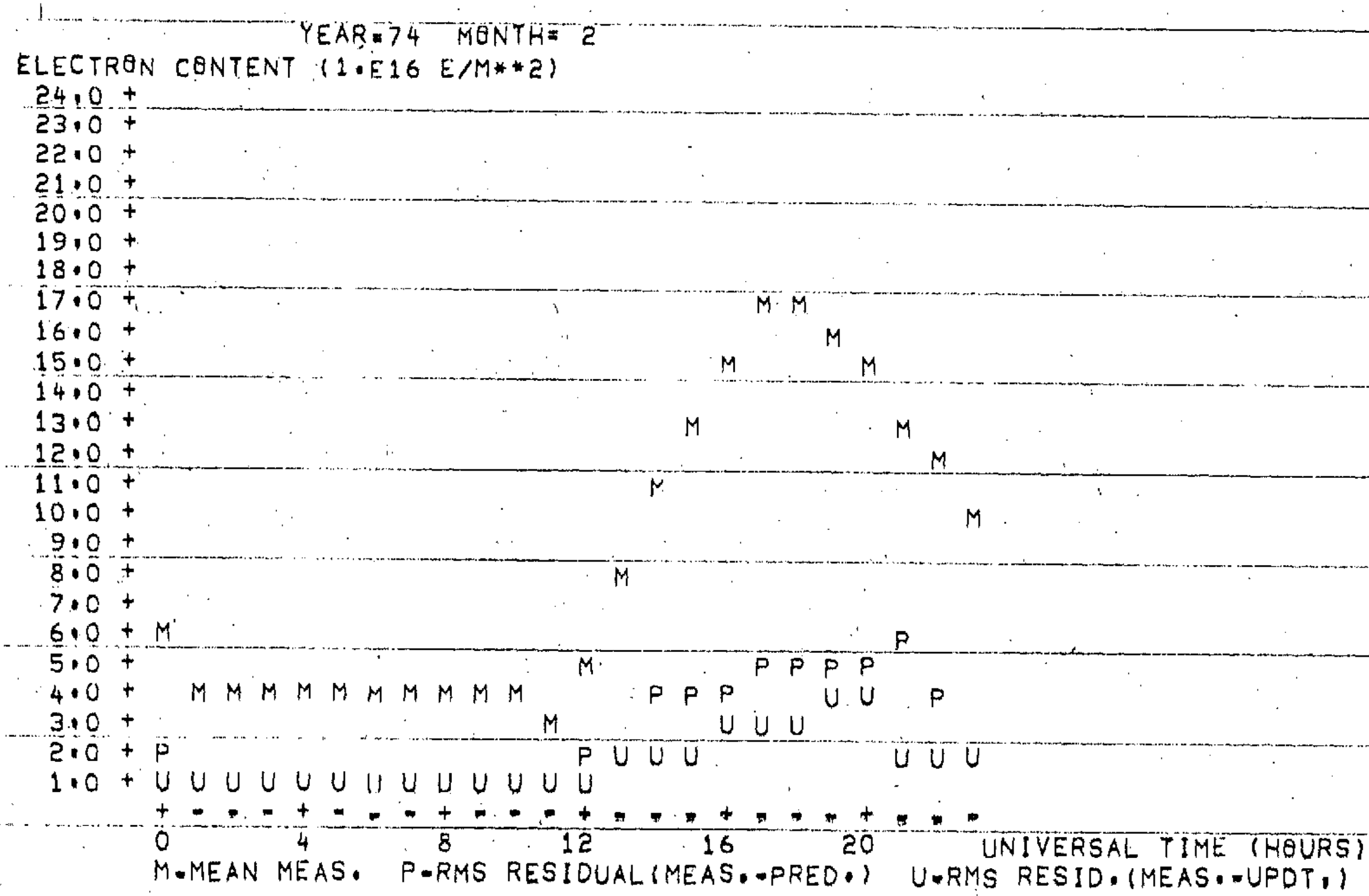

Figure 13c. Monthly Mean and Error Curves.

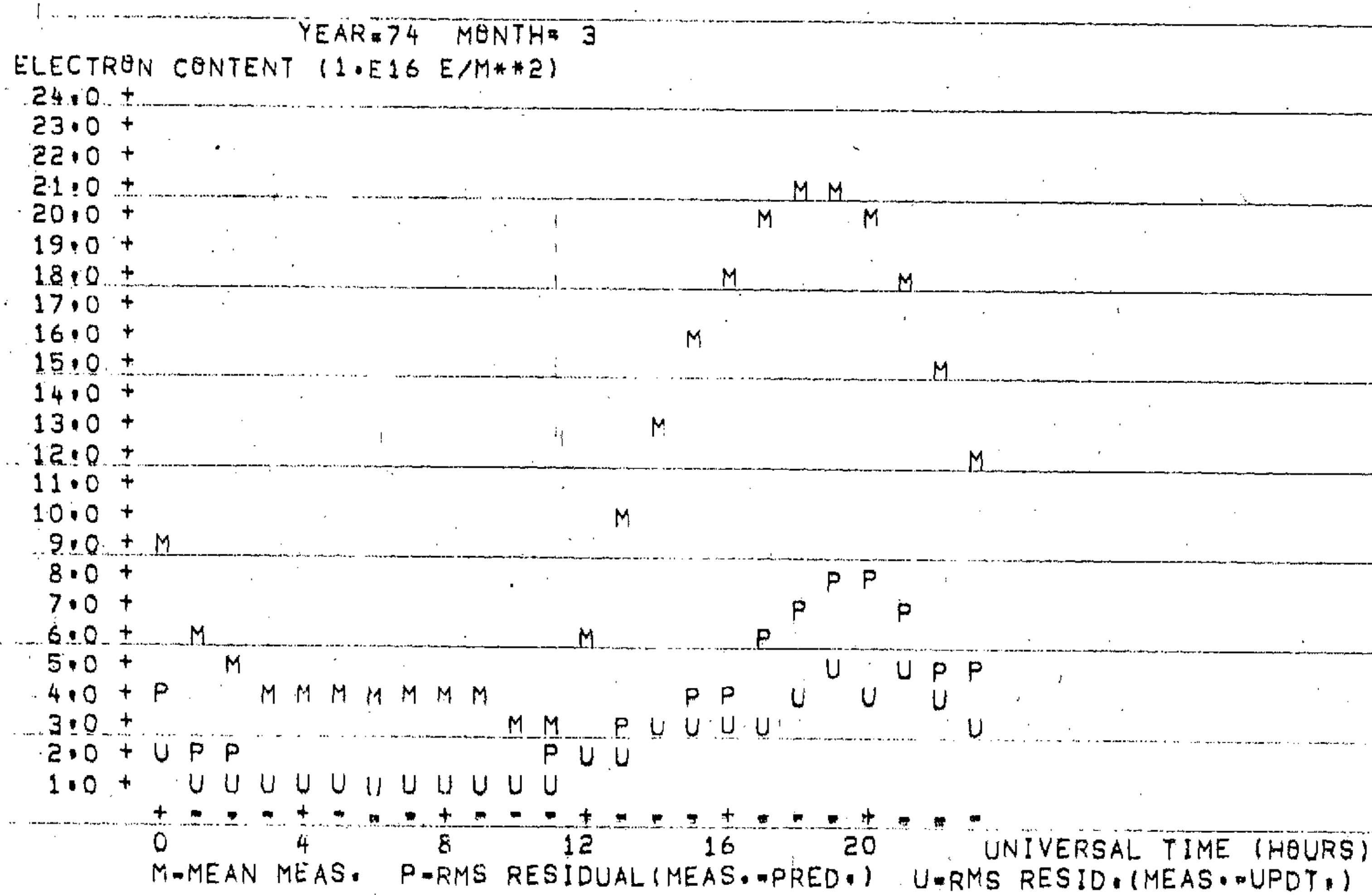

Figure 13d. Monthly Mean and Error Curves.

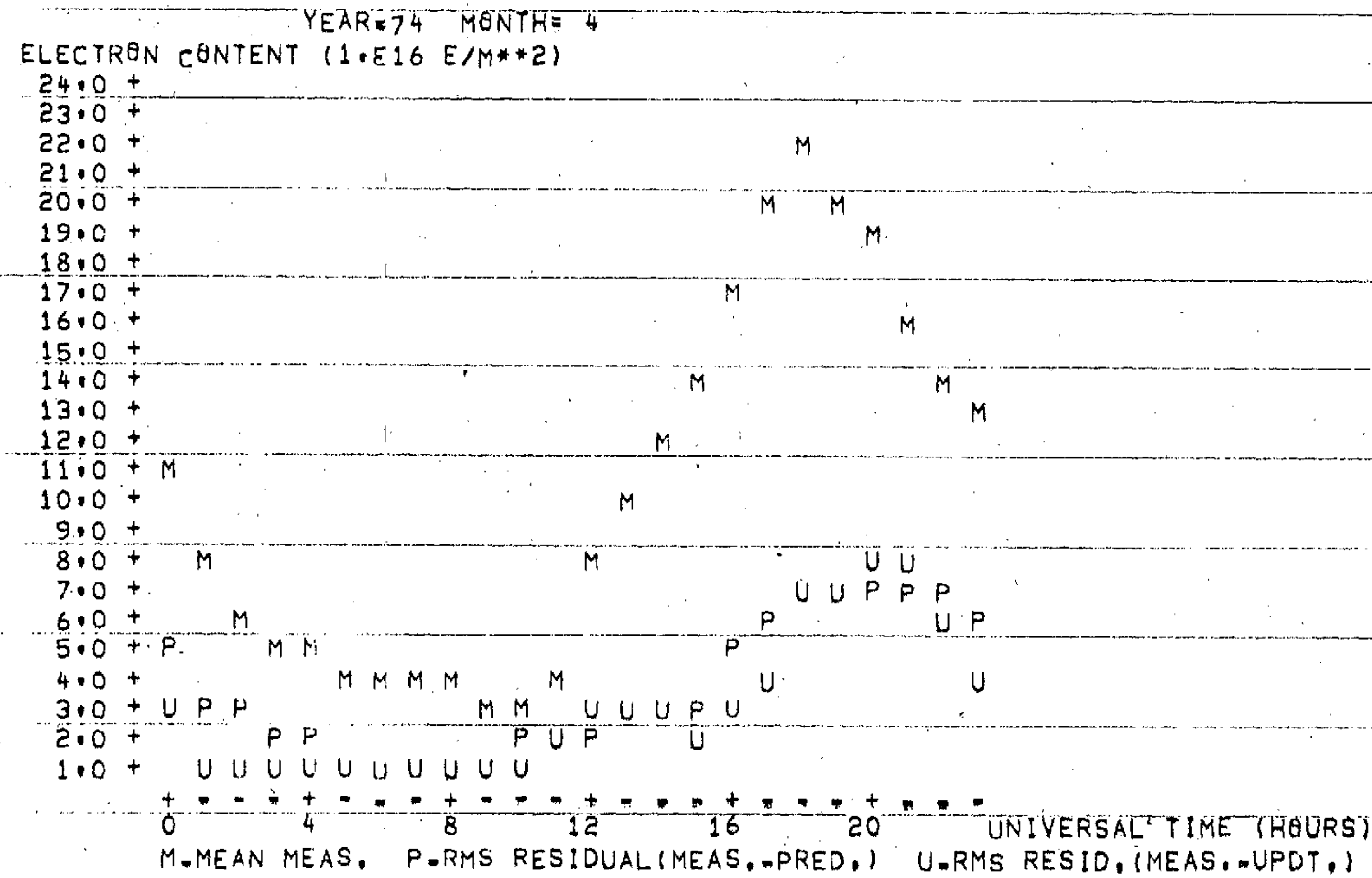

Figure 13e. Monthly Mean and Error Curves.

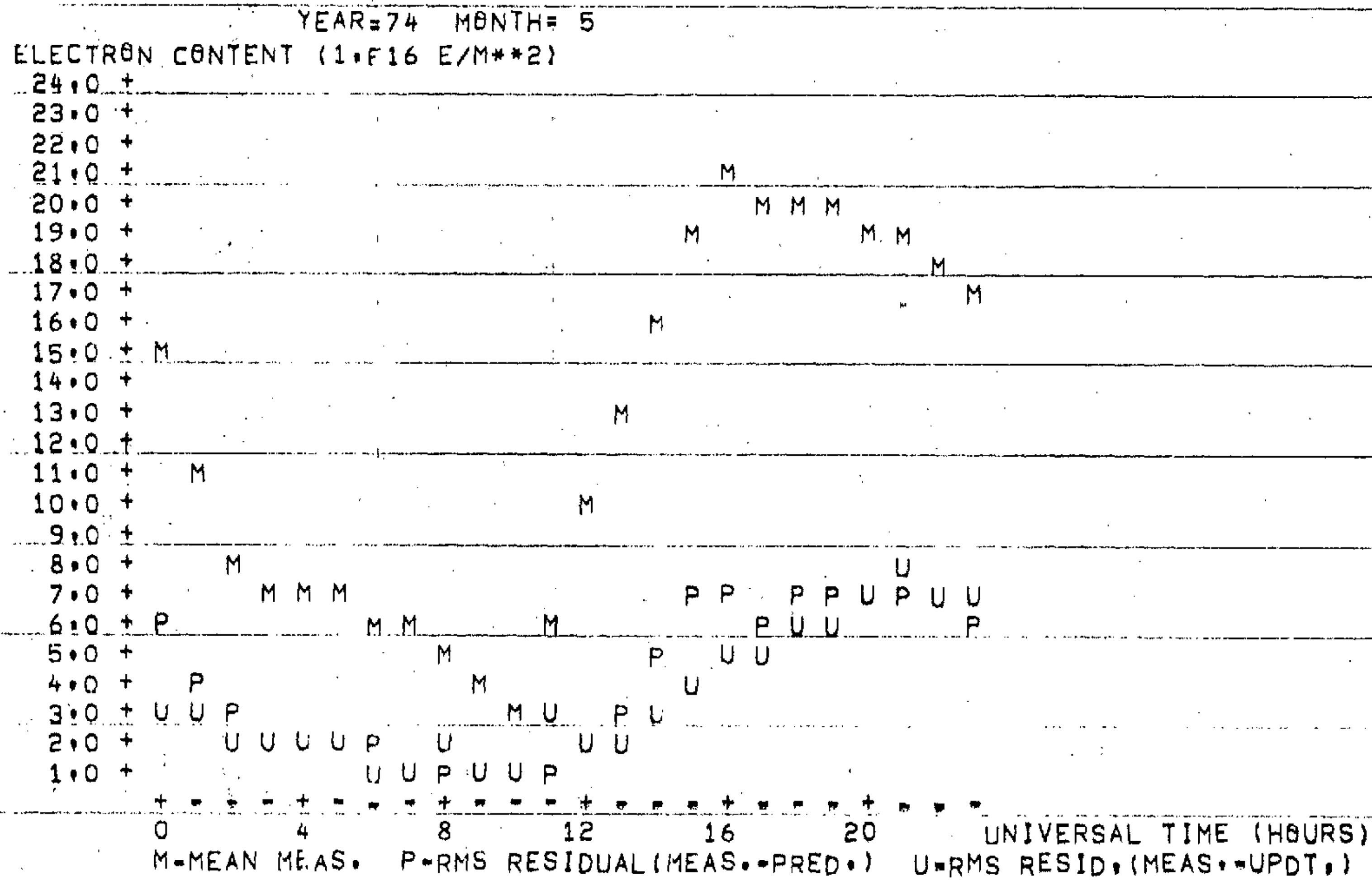

Figure 13f. Monthly Mean and Error Curves

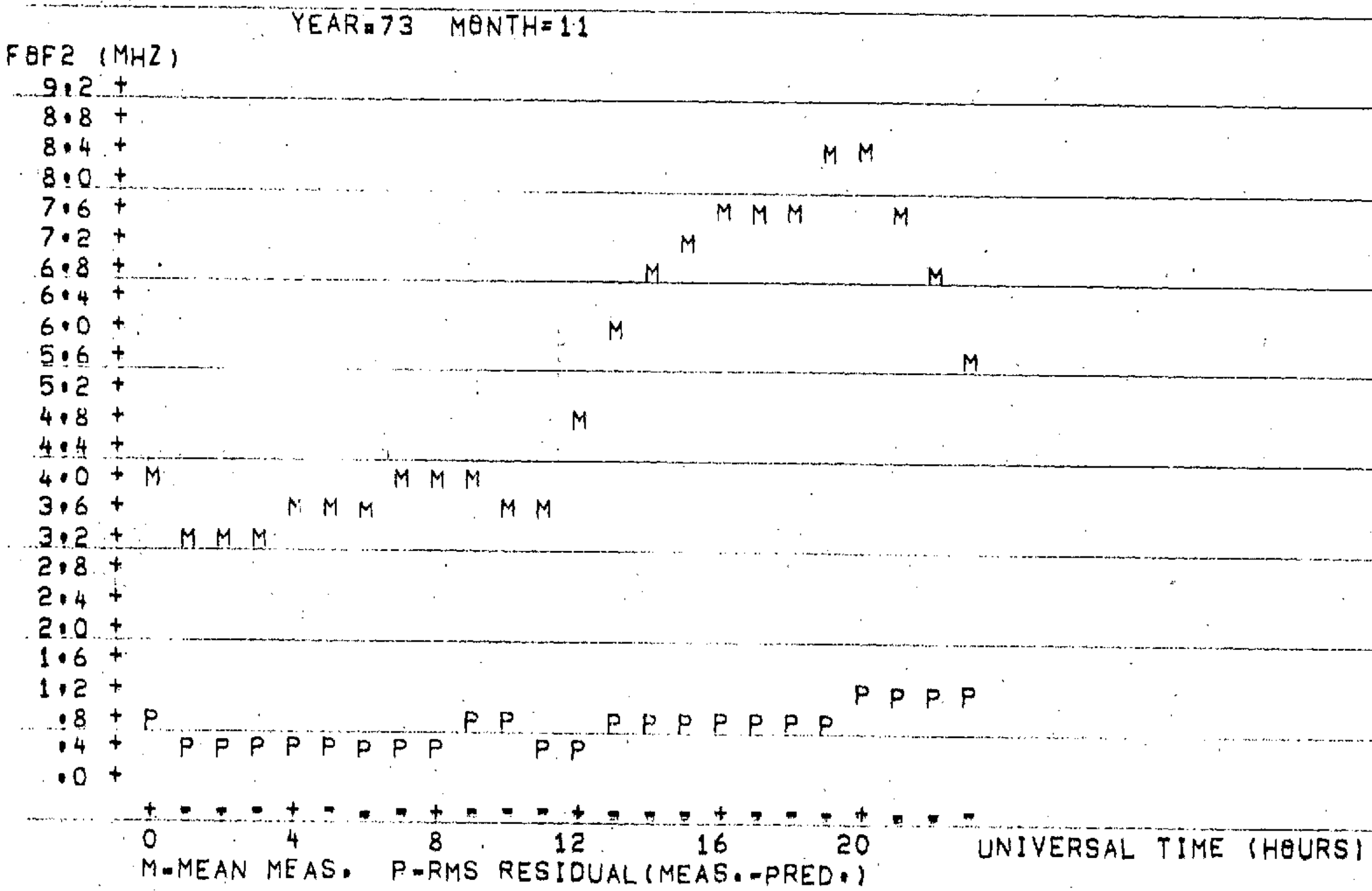

Figure 14a. Monthly Mean and Error Curves.

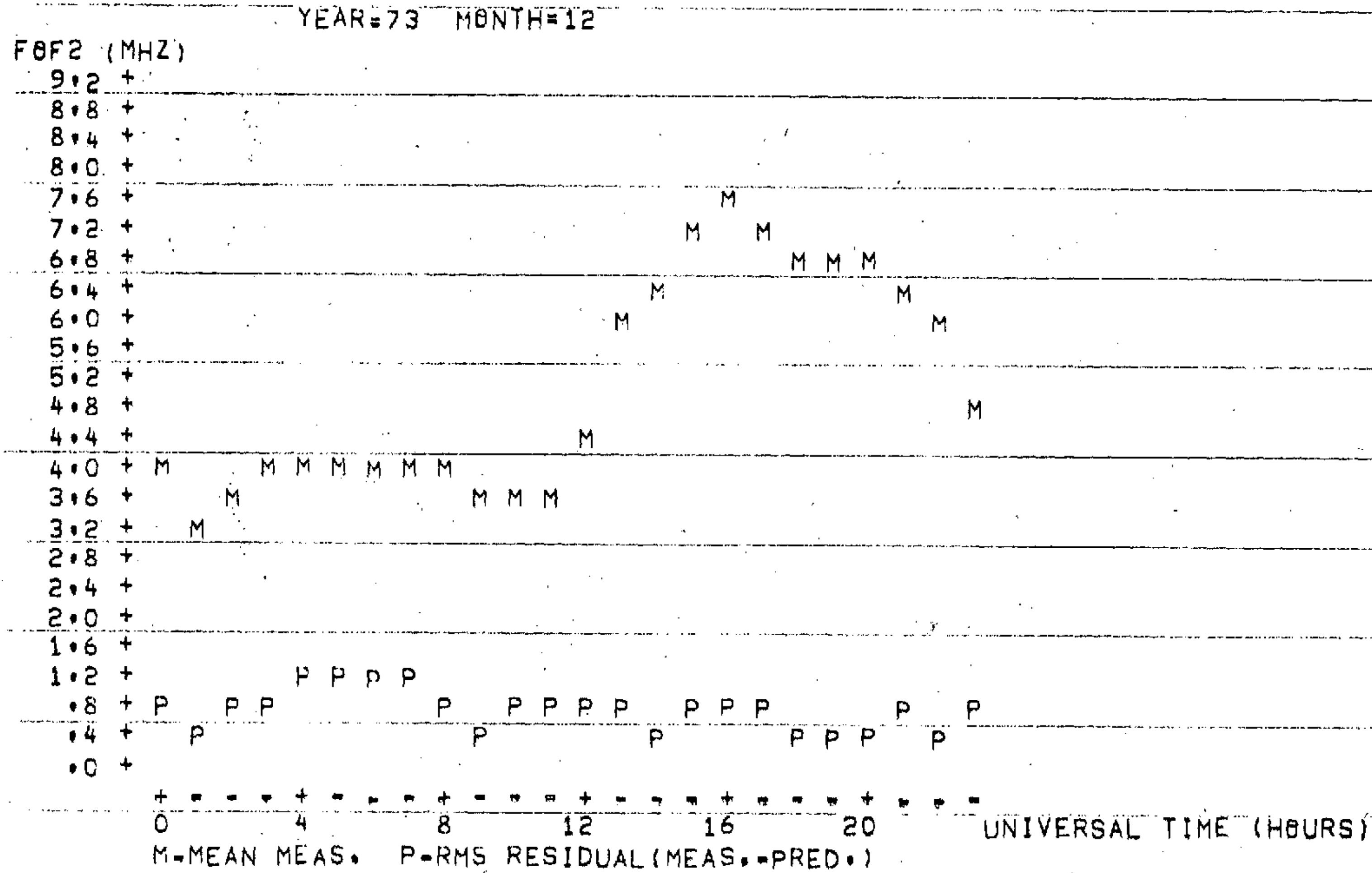

Figure 14b. Monthly Mean and Error Curves.

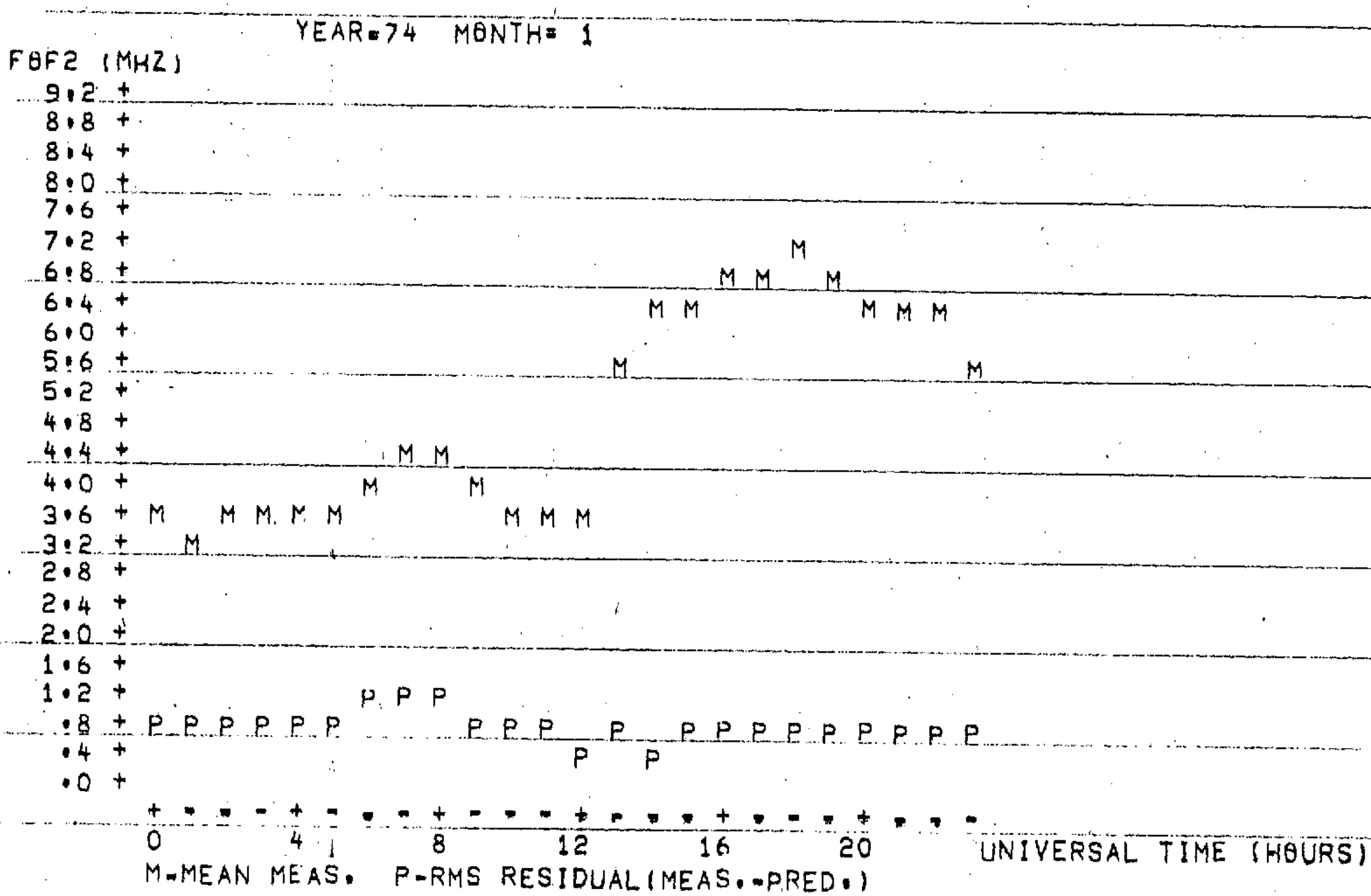

Figure 14c. Monthly Mean and Error Curves.

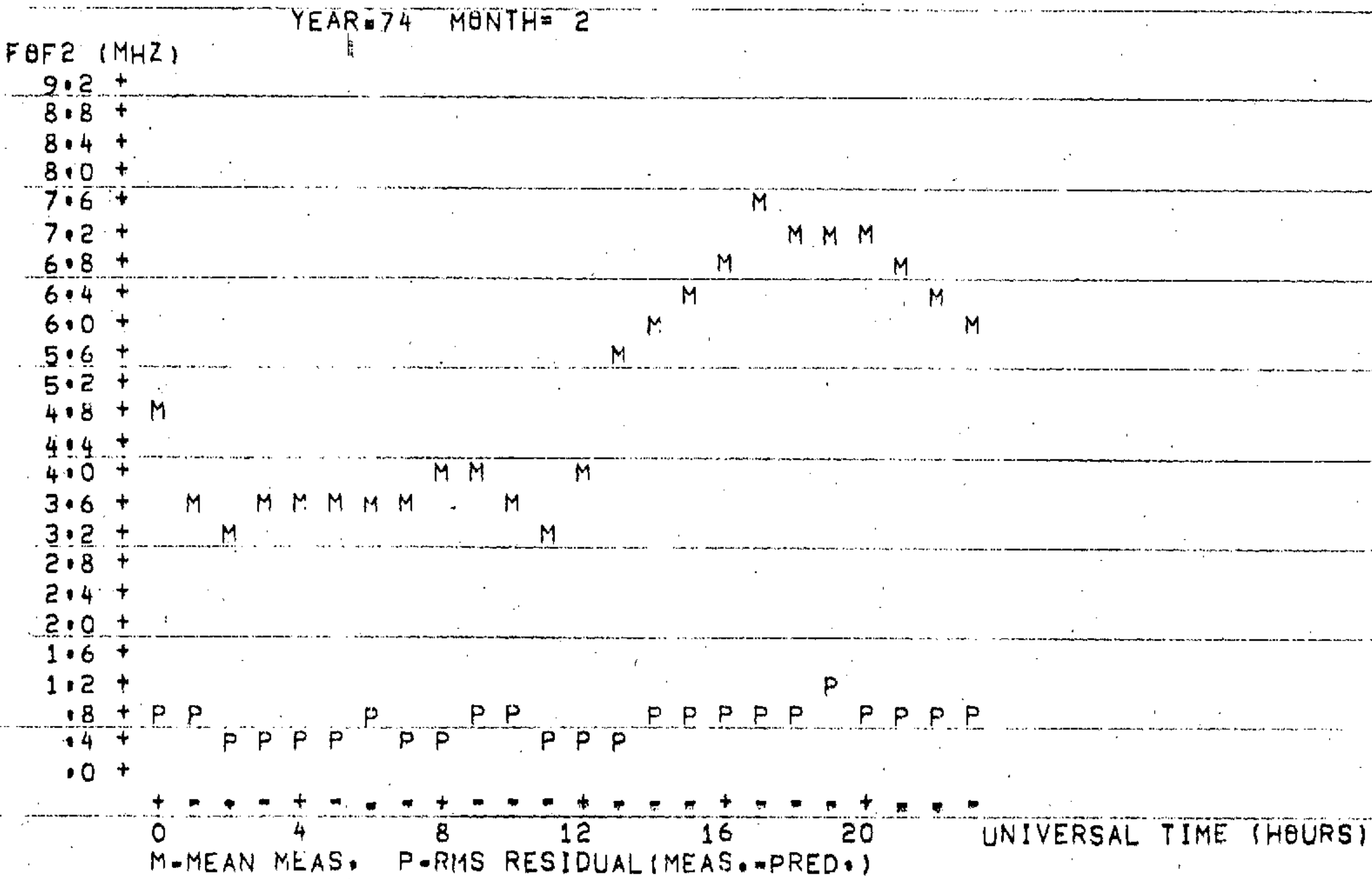

Figure 14d. Monthly Mean and Error Curves.

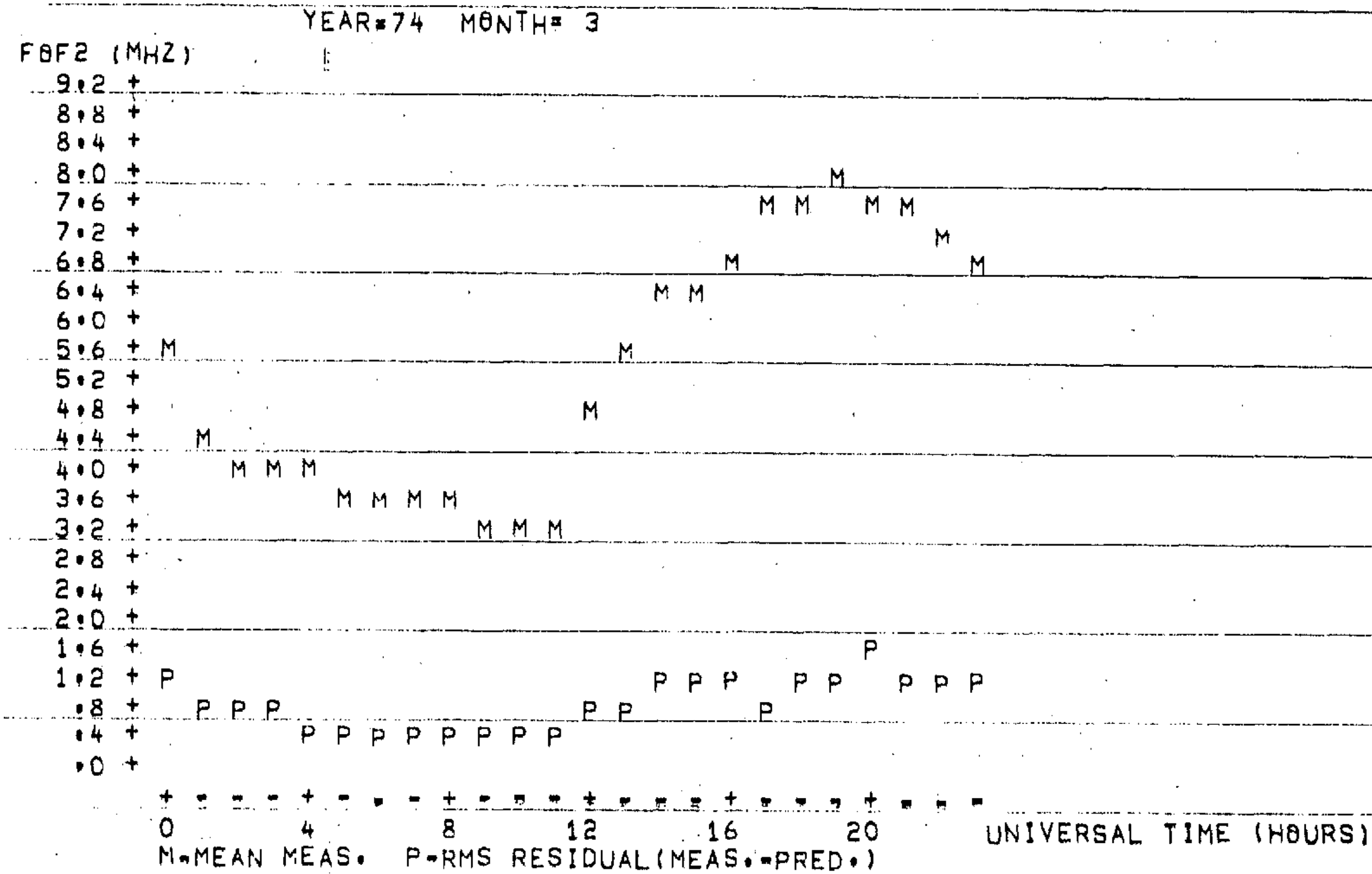

Figure 14e. Monthly Mean and Error Curves.

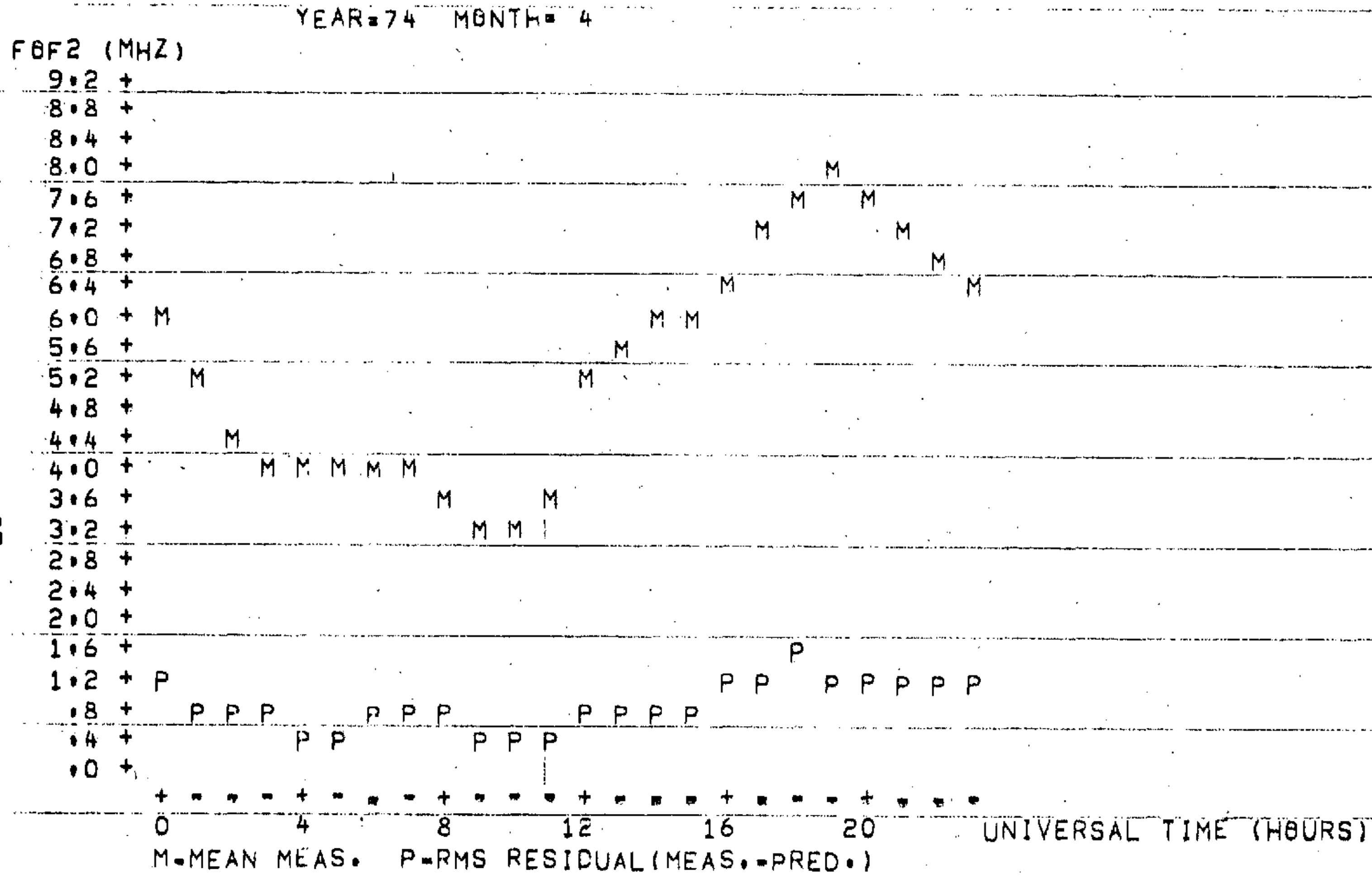

Figure 14f. Monthly Mean and Error Curves.

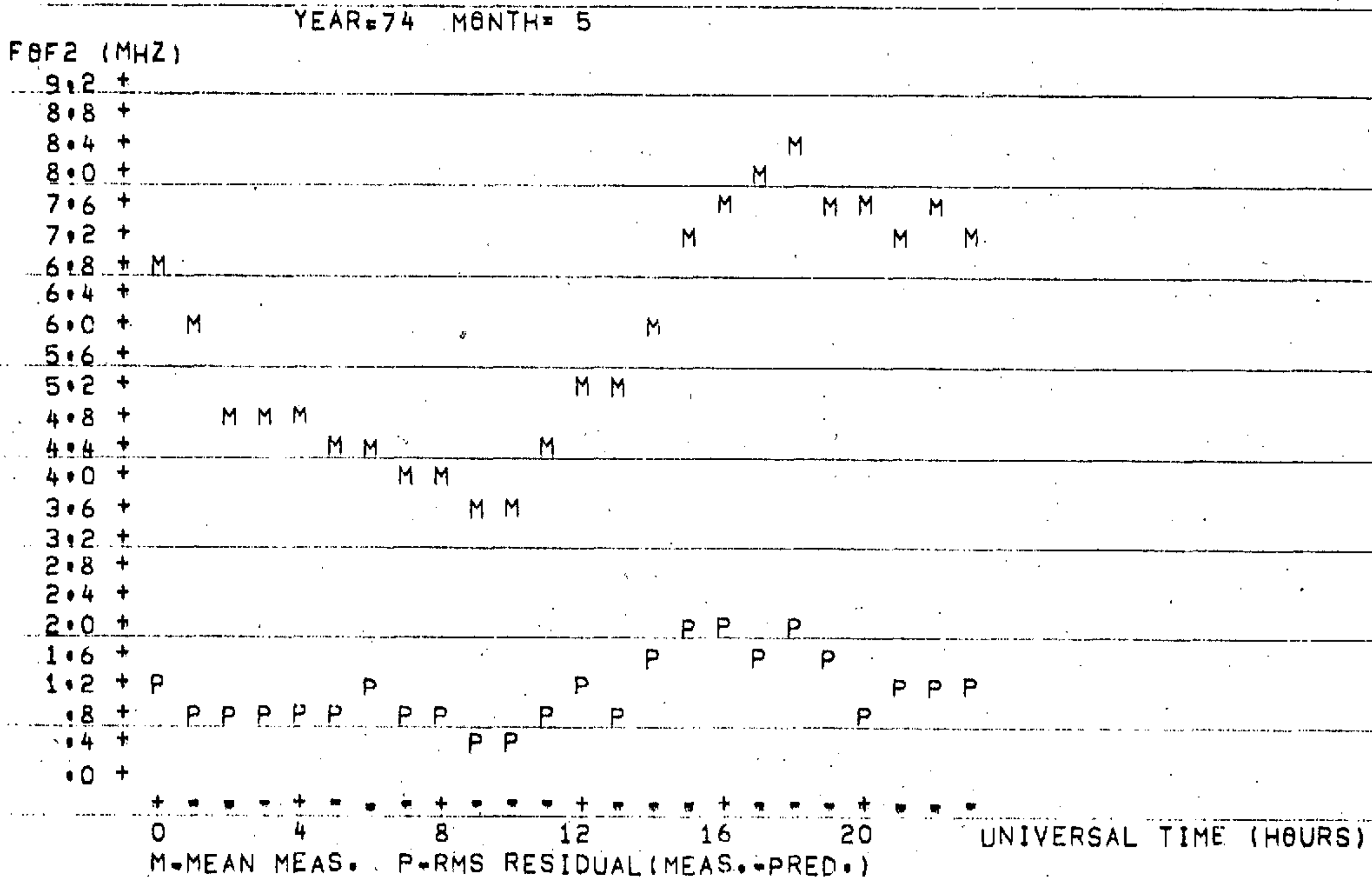

Figure 14g. Monthly Mean and Error Curves.

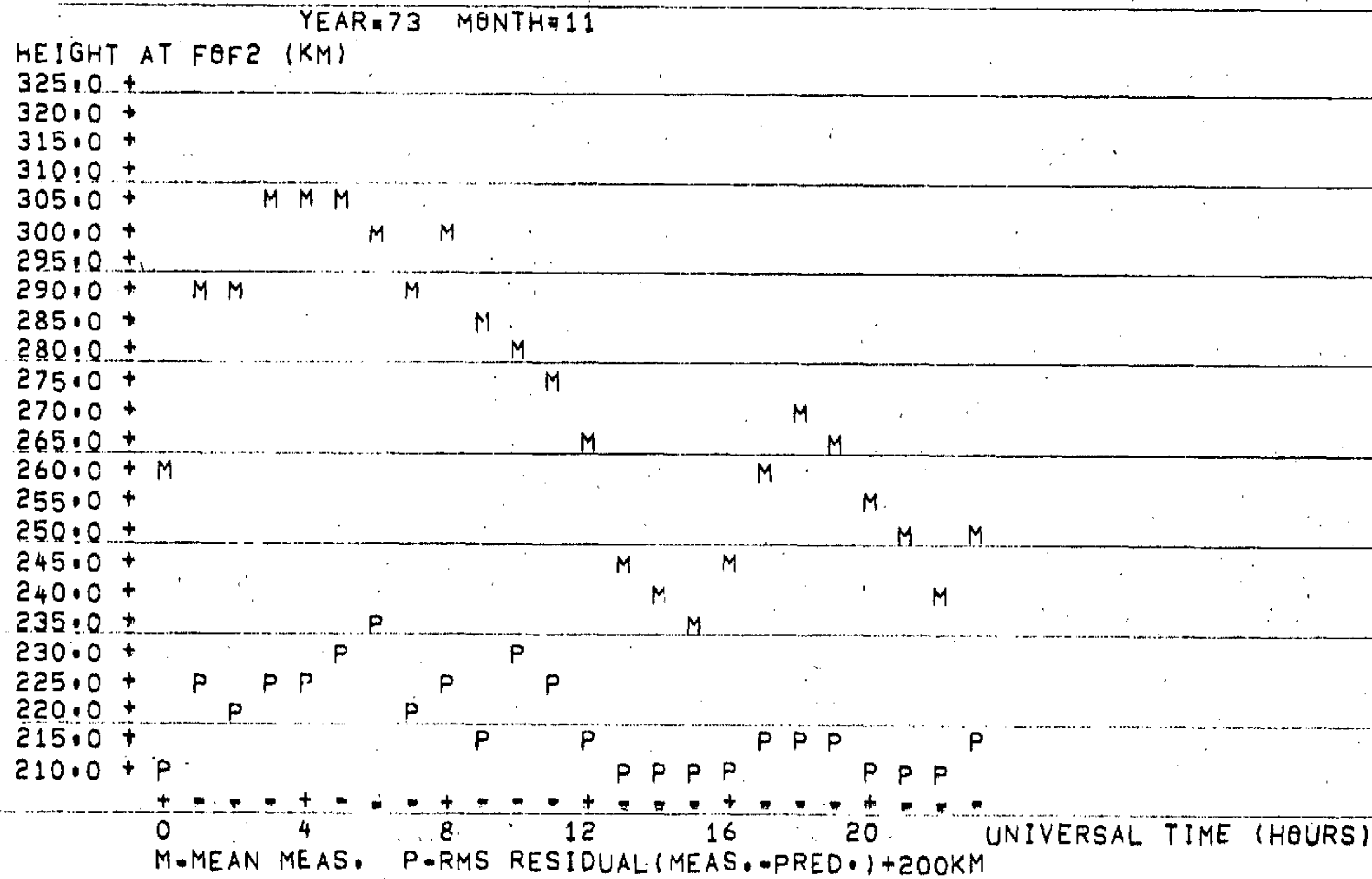

Figure 15a. Monthly Median and Error Curves.

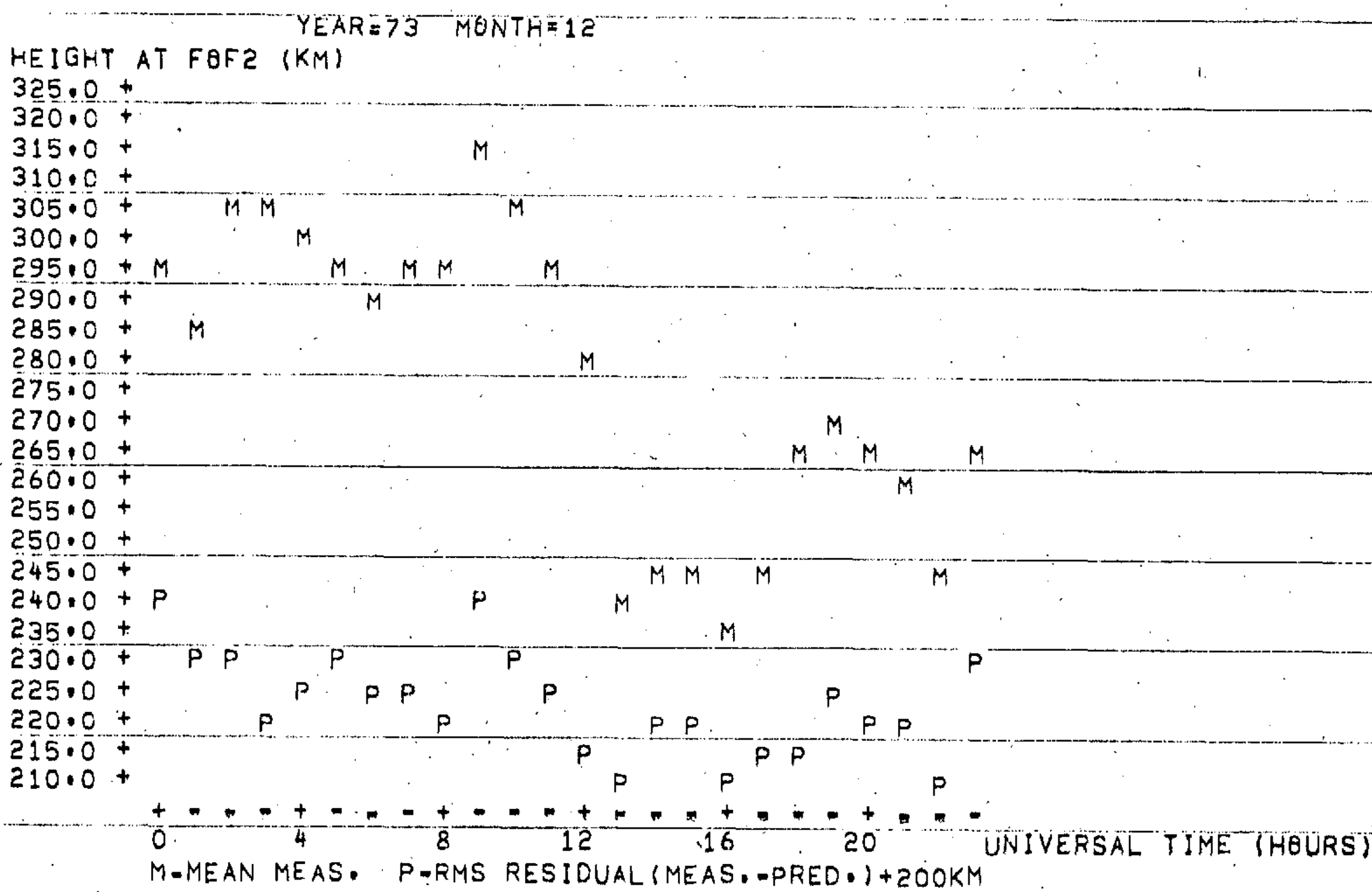

Figure 15b. Monthly Mean and Error Curves.

C-N

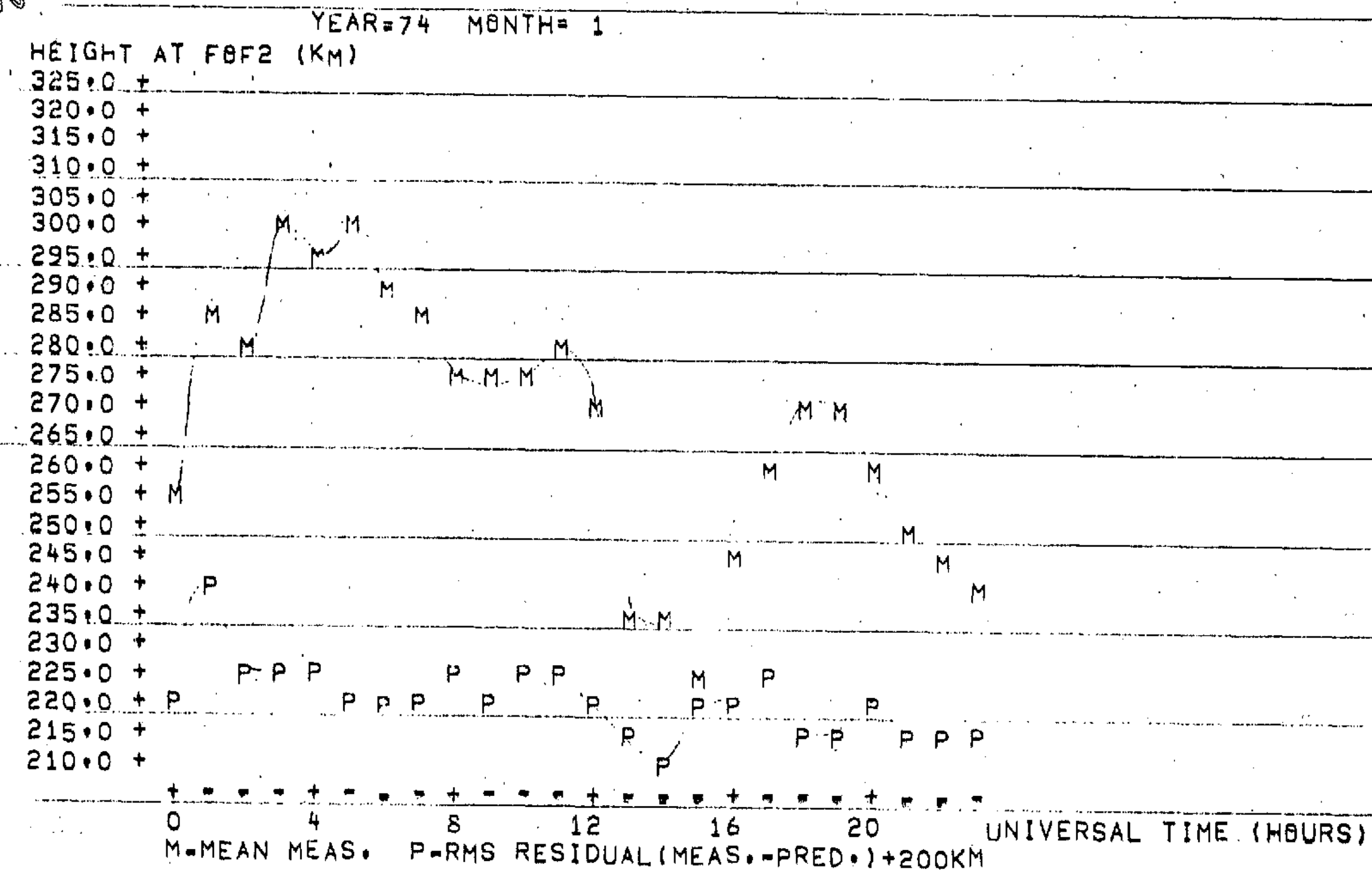

Figure 15c. Monthly Mean and Error Curves.

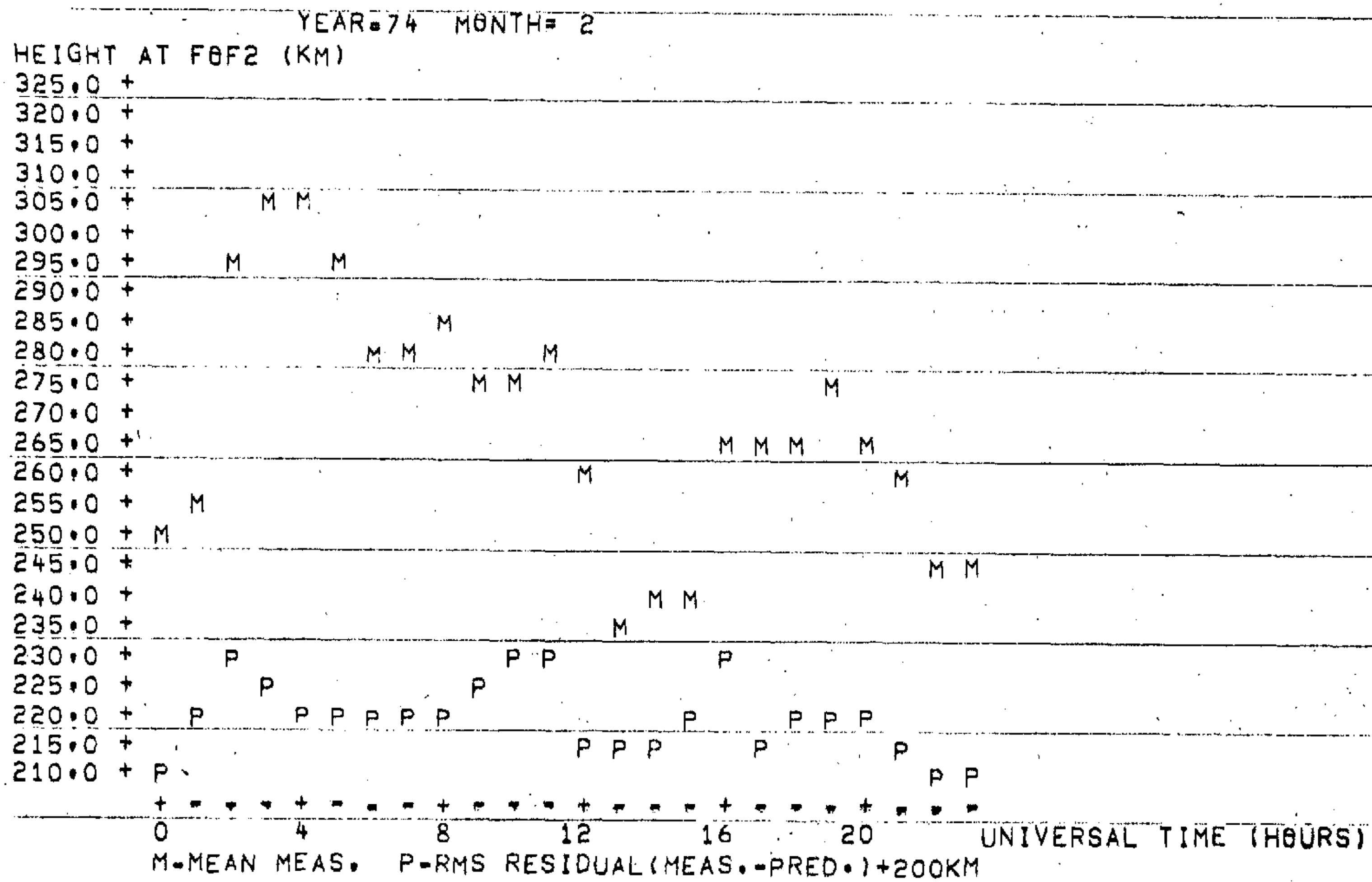

Figure 15d. Monthly Mean and Error Curves.

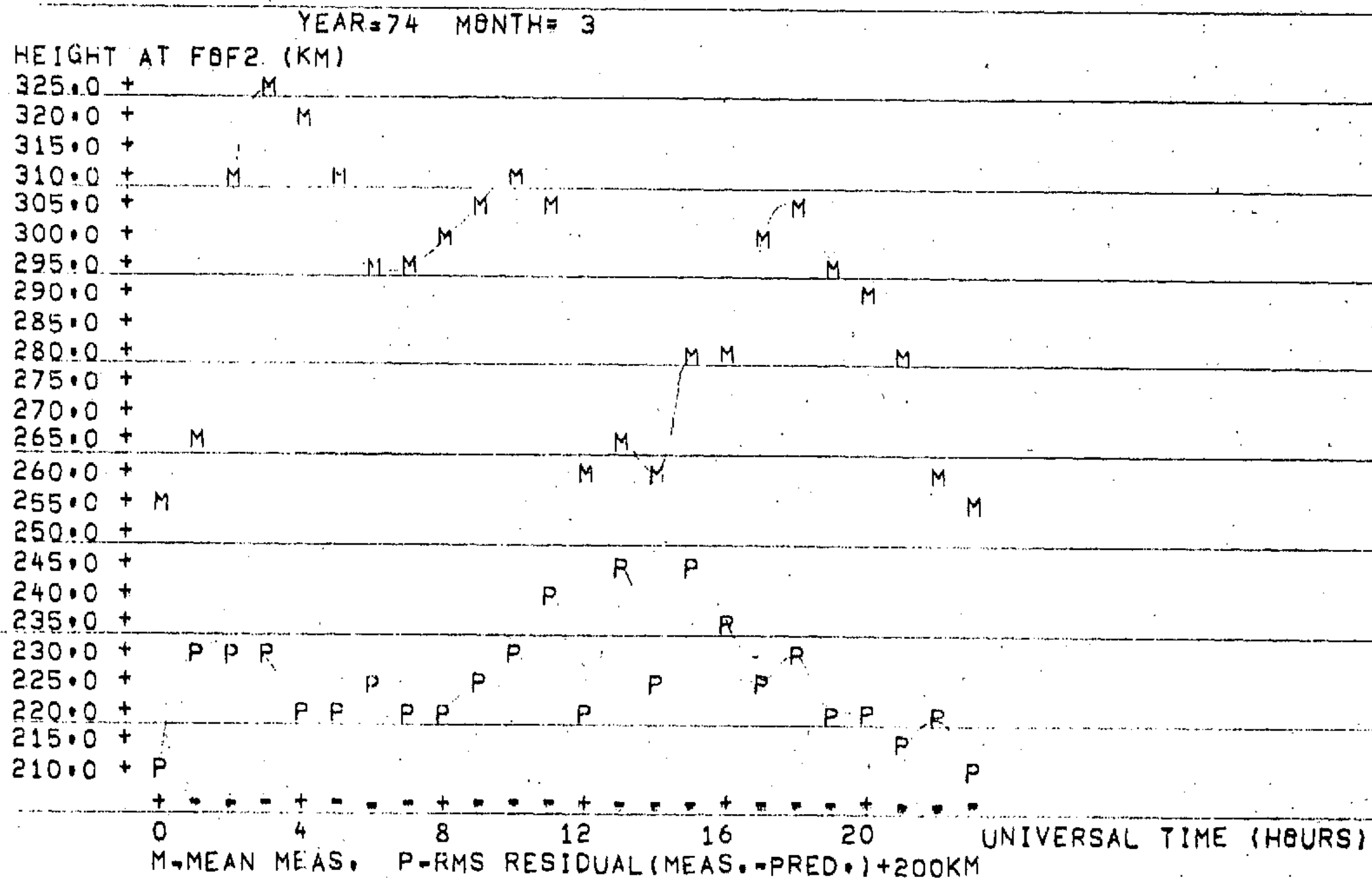

Figure 15e. Monthly Mean and Error Curves.

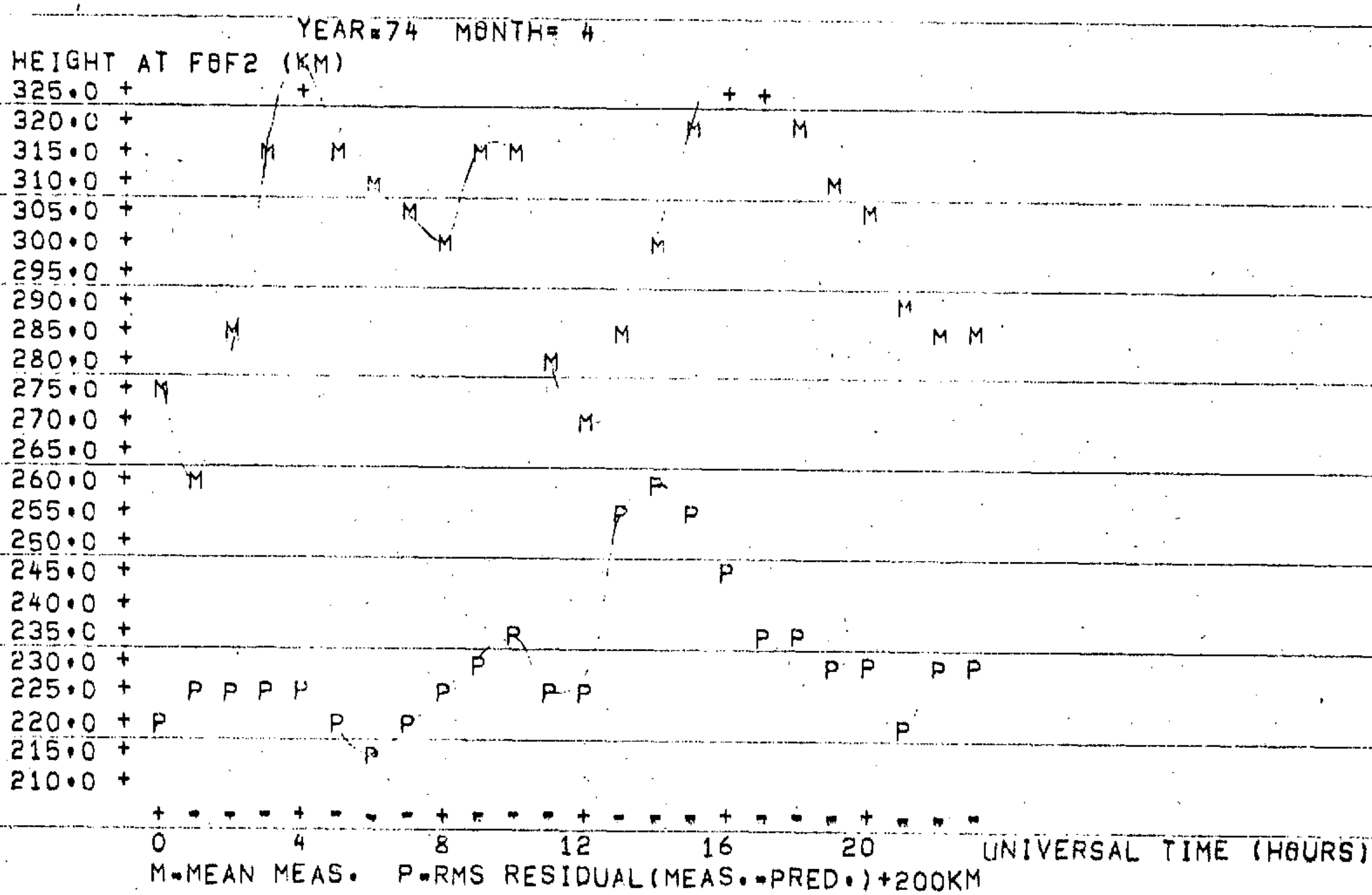

Figure 15f. Monthly Mean and Error Curves.

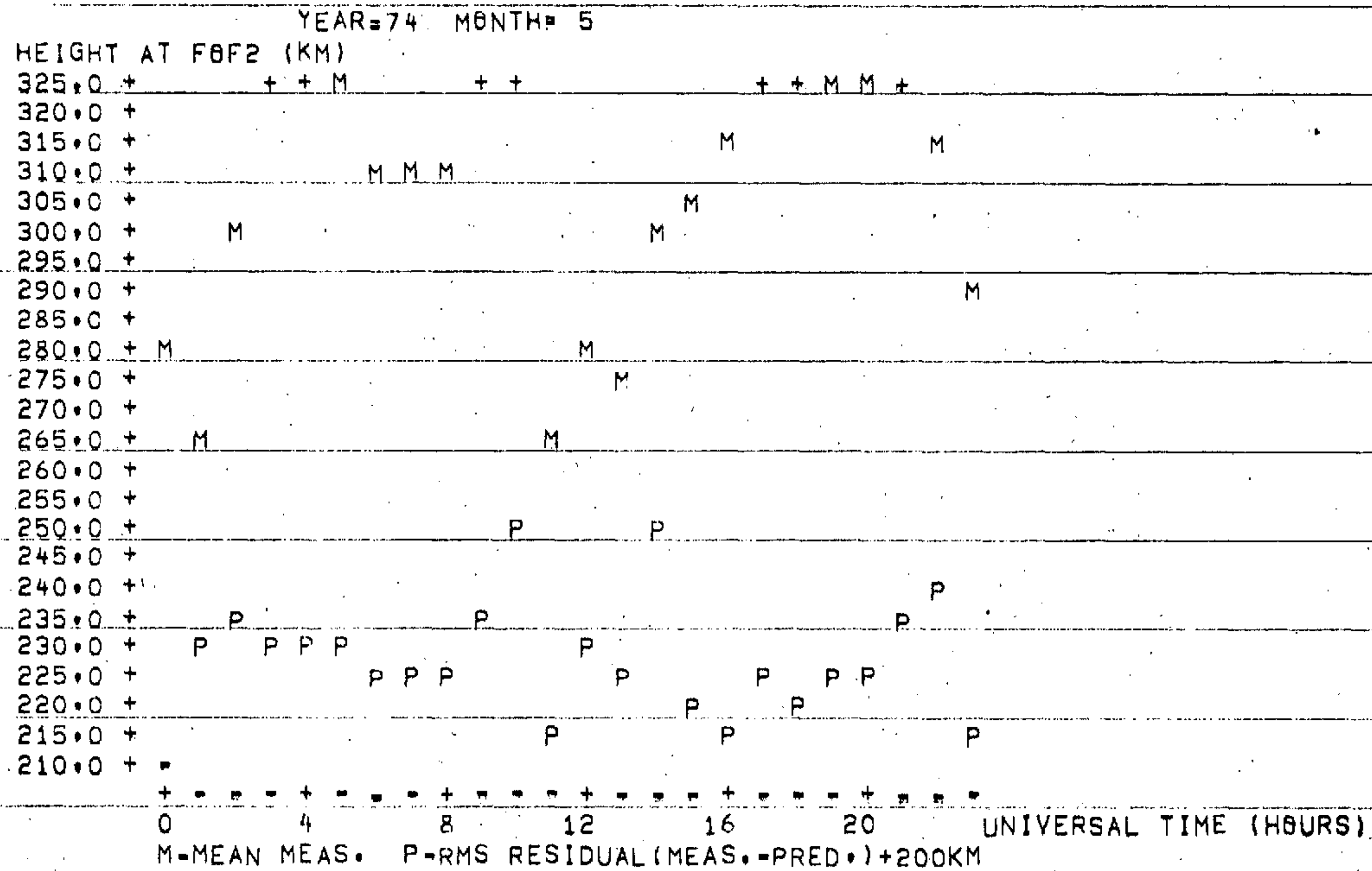

Figure 15g. Monthly Mean and Error Curves.

Table 5a. Monthly Mean Statistics.

YEAR=73 MONTH=11

UT	MEAN MEASUREMENTS NT	F0F2	HM	RMS RESIDUALS NT(PRED)	F0F2	HM	NT(UPDT)	DAYTIME RMS % ERRORS NT(P)	F0F2	HM	NT(U)	NO.POINTS			
0	.000E 00	3.88	261.0	.000E 00	.97	12.3	.000E 00					0	20	20	0
1	.000E 00	3.16	290.3	.000E 00	.56	27.4	.000E 00					0	20	20	0
2	.000E 00	3.18	289.5	.000E 00	.27	21.0	.000E 00					0	22	22	0
3	.000E 00	3.37	306.6	.000E 00	.39	22.7	.000E 00					0	21	21	0
4	.000E 00	3.46	306.5	.000E 00	.39	25.3	.000E 00					0	23	23	0
5	.000E 00	3.58	303.2	.000E 00	.50	30.8	.000E 00					0	23	23	0
6	.000E 00	3.74	301.9	.000E 00	.53	33.3	.000E 00					0	23	23	0
7	.000E 00	3.90	288.8	.000E 00	.52	21.5	.000E 00					0	23	23	0
8	.000E 00	3.91	298.6	.000E 00	.56	25.2	.000E 00					0	23	23	0
9	.000E 00	3.98	286.7	.000E 00	.91	15.6	.000E 00					0	23	23	0
10	.000E 00	3.57	280.8	.000E 00	.81	30.9	.000E 00					0	22	22	0
11	.000E 00	3.44	277.4	.000E 00	.44	27.4	.000E 00					0	20	20	0
12	.000E 00	4.88	265.6	.000E 00	.59	14.1	.000E 00					0	21	21	0
13	.000E 00	6.17	244.6	.000E 00	.98	10.2	.000E 00	.0	15.9	4.2	.0	0	20	20	0
14	.000E 00	6.85	238.6	.000E 00	.84	10.1	.000E 00	.0	12.3	4.2	.0	0	20	20	0
15	.000E 00	7.34	237.3	.000E 00	.73	11.4	.000E 00	.0	10.0	4.8	.0	0	21	21	0
16	.000E 00	7.66	246.0	.000E 00	.79	10.8	.000E 00	.0	10.3	4.4	.0	0	21	21	0
17	.000E 00	7.71	259.1	.000E 00	.78	16.6	.000E 00	.0	10.1	6.4	.0	0	22	22	0
18	.000E 00	7.70	269.1	.000E 00	.70	16.9	.000E 00	.0	9.1	6.3	.0	0	22	22	0
19	.000E 00	8.34	264.1	.000E 00	.88	14.1	.000E 00	.0	10.6	5.4	.0	0	21	21	0
20	.000E 00	8.32	253.8	.000E 00	1.05	12.1	.000E 00	.0	12.6	4.8	.0	0	22	22	0
21	.000E 00	7.72	248.3	.000E 00	1.05	9.4	.000E 00	.0	13.6	3.8	.0	0	22	22	0
22	.000E 00	6.94	239.5	.000E 00	1.21	11.7	.000E 00	.0	17.5	4.9	.0	0	21	21	0
23	.000E 00	5.54	250.4	.000E 00	1.24	12.7	.000E 00	.0	22.3	5.1	.0	0	21	21	0

Table 5b. *Monthly Mean Statistics.*

YEAR=73 MØNTH=12

	MEAN MEASUREMENTS			RMS RESIDUALS				DAYTIME RMS % ERRØRS				NØ.PØINTS			
UT	NT	FØF2	HM	NT(PRED)	FØF2	HM	NT(UPDT)	NT(P)	FØF2	HM	NT(U)				
0	.563E 17	3.82	293.5	.146E 17	.63	41.7	.119E 17					12	9	9	9
1	.507E 17	3.33	286.7	.189E 17	.43	31.0	.150E 17					12	9	9	9
2	.510E 17	3.51	305.1	.233E 17	.69	29.3	.118E 17					12	10	10	10
3	.536E 17	3.81	303.1	.263E 17	1.00	19.4	.655E 16					12	10	10	10
4	.526E 17	3.90	301.1	.244E 17	1.09	25.6	.481E 16					12	11	11	11
5	.531E 17	3.93	296.4	.232E 17	1.03	28.2	.431E 16					12	11	11	11
6	.519E 17	3.95	290.5	.226E 17	1.12	27.0	.525E 16					12	11	11	11
7	.507E 17	4.19	294.9	.178E 17	1.15	24.7	.938E 16					12	9	9	9
8	.470E 17	3.88	296.1	.116E 17	.65	21.2	.673E 16					12	11	11	11
9	.459E 17	3.76	315.2	.991E 16	.53	41.0	.904E 16					12	11	11	11
10	.445E 17	3.73	303.3	.149E 17	.72	29.4	.484E 16					12	10	10	10
11	.442E 17	3.63	297.5	.133E 17	.61	23.6	.634E 16					12	11	11	11
12	.588E 17	4.30	279.3	.113E 17	.61	16.4	.935E 16					12	11	11	11
13	.914E 17	5.97	240.4	.159E 17	.77	8.3	.233E 17	17.4	12.9	3.4	25.5	12	10	10	10
14	.113E 18	6.53	247.1	.290E 17	.47	18.5	.256E 17	25.7	7.2	7.5	22.7	12	11	11	11
15	.131E 18	7.24	244.7	.341E 17	.72	21.7	.359E 17	26.1	10.0	8.9	27.5	12	10	10	10
16	.144E 18	7.65	236.8	.316E 17	.84	8.5	.484E 17	21.9	10.9	3.6	33.5	12	11	11	11
17	.140E 18	7.07	246.7	.421E 17	.70	17.2	.316E 17	30.1	9.9	7.0	22.6	12	11	11	11
18	.141E 18	6.98	265.4	.348E 17	.55	14.5	.185E 17	24.6	7.8	5.4	13.1	12	11	11	11
19	.145E 18	6.86	267.7	.252E 17	.53	25.7	.152E 17	17.4	7.7	9.6	10.5	12	12	12	12
20	.144E 18	6.98	266.0	.263E 17	.58	21.4	.173E 17	18.2	8.2	8.1	12.0	12	12	12	12
21	.126E 18	6.50	258.4	.260E 17	.65	19.2	.974E 16	20.6	10.0	7.4	7.7	12	12	12	12
22	.102E 18	5.99	246.9	.172E 17	.40	12.1	.846E 16	16.8	6.7	4.9	8.3	12	11	11	11
23	.754E 17	4.71	267.2	.124E 17	.68	28.0	.115E 17	16.4	14.4	10.5	15.3	12	10	10	10

Table 5c. Monthly Mean Statistics.

YEAR=74 MØNTH= 1

	MEAN MEASUREMENTS			RMS RESIDUALS				DAYTIME RMS % ERRØRS							
UT	NT	FØF2	HM	NT(PRED)	FØF2	HM	NT(UPDT)	NT(P)	FØF2	HM	NT(U)	NØ.PØINTS			
0	.531E 17	3.75	255.9	.219E 17	.77	18.7	.176E 17					30	26	26	25
1	.441E 17	3.30	284.7	.190E 17	.79	38.6	.105E 17					30	26	25	25
2	.436E 17	3.46	281.1	.186E 17	.76	24.6	.569E 16					30	25	25	24
3	.438E 17	3.47	299.9	.178E 17	.74	27.4	.671E 16					31	27	27	27
4	.453E 17	3.55	295.8	.185E 17	.85	23.9	.553E 16					31	24	24	24
5	.470E 17	3.72	299.4	.184E 17	.88	19.8	.621E 16					31	24	24	24
6	.509E 17	4.02	292.3	.191E 17	1.02	19.4	.645E 16					31	28	28	28
7	.552E 17	4.40	286.4	.190E 17	1.21	20.4	.115E 17					31	28	27	28
8	.562E 17	4.47	275.1	.167E 17	1.09	23.4	.112E 17					31	24	24	24
9	.503E 17	4.11	275.6	.161E 17	1.00	21.6	.135E 17					31	26	26	26
10	.429E 17	3.65	277.4	.150E 17	.84	26.8	.605E 16					31	23	23	23
11	.394E 17	3.45	281.0	.120E 17	.71	25.2	.682E 16					31	25	25	25
12	.459E 17	3.76	271.3	.138E 17	.56	17.8	.788E 16					31	27	27	27
13	.804E 17	5.50	233.3	.162E 17	.84	13.9	.231E 17	20.2	15.3	5.9	28.7	31	27	27	27
14	.989E 17	6.25	233.2	.297E 17	.54	11.1	.253E 17	30.0	8.7	4.8	25.5	31	26	26	26
15	.111E 18	6.28	227.1	.398E 17	.74	19.7	.209E 17	35.8	11.9	8.7	18.8	30	28	28	27
16	.127E 18	6.64	243.0	.401E 17	.81	21.3	.248E 17	31.7	12.2	8.8	19.6	30	27	27	26
17	.142E 18	6.73	260.4	.408E 17	.92	24.8	.240E 17	28.8	13.7	9.5	16.9	31	26	26	26
18	.151E 18	7.06	268.6	.406E 17	.81	16.7	.234E 17	26.9	11.4	6.2	15.5	31	27	27	27
19	.144E 18	6.96	270.8	.341E 17	.70	14.3	.176E 17	23.7	10.1	5.3	12.2	31	26	26	26
20	.135E 18	6.59	261.3	.340E 17	.74	21.8	.201E 17	25.1	11.2	8.3	14.9	31	28	28	28
21	.127E 18	6.47	251.3	.354E 17	.82	15.7	.167E 17	27.9	12.7	6.3	13.2	31	29	29	29
22	.113E 18	6.29	244.8	.287E 17	.67	12.6	.212E 17	25.5	10.6	5.1	18.8	31	29	29	29
23	.847E 17	5.47	239.9	.288E 17	.97	12.6	.173E 17	34.0	17.7	5.2	20.4	31	29	29	29

Table 15d. Monthly Mean Statistics.

YEAR=74 MONTH= 2

UT	MEAN MEASUREMENTS NT	FOF2	HM	RMS RESIDUALS NT(PRED)	FOF2	HM	NT(UPDT)	DAYTIME RMS % ERRORS NT(P)	FOF2	HM	NT(U)	NO.POINTS			
0	.639E 17	4.61	251.9	.165E 17	.80	11.6	.874E 16					22	25	24	19
1	.446E 17	3.59	256.8	.149E 17	.89	22.4	.599E 16					22	23	23	18
2	.385E 17	3.38	296.3	.102E 17	.47	31.4	.542E 16					22	25	24	19
3	.384E 17	3.44	302.6	.885E 16	.40	25.7	.693E 16					22	27	26	21
4	.399E 17	3.49	305.2	.912E 16	.59	22.0	.658E 16					22	24	23	19
5	.396E 17	3.62	294.3	.106E 17	.56	17.6	.931E 16					19	27	27	18
6	.406E 17	3.72	280.6	.113E 17	.67	20.8	.774E 16					20	26	26	18
7	.433E 17	3.70	282.5	.102E 17	.47	18.9	.688E 16					22	26	26	21
8	.447E 17	3.85	284.2	.993E 16	.52	18.5	.825E 16					22	26	26	20
9	.431E 17	3.83	276.2	.118E 17	.70	25.7	.901E 16					22	24	24	19
10	.376E 17	3.50	277.0	.124E 17	.66	30.1	.639E 16					22	22	22	17
11	.323E 17	3.26	281.6	.111E 17	.48	27.7	.720E 16					22	26	25	20
12	.479E 17	3.99	257.6	.174E 17	.36	12.8	.144E 17					22	26	25	20
13	.828E 17	5.57	235.1	.239E 17	.39	17.0	.209E 17	28.9	7.0	7.2	25.2	22	26	26	20
14	.107E 18	6.07	241.7	.361E 17	.70	15.6	.250E 17	33.7	11.6	6.5	23.3	23	28	28	23
15	.132E 18	6.58	242.0	.381E 17	.63	17.8	.236E 17	28.8	9.6	7.4	17.8	23	28	27	23
16	.151E 18	6.90	266.7	.409E 17	.70	29.4	.266E 17	27.1	10.1	11.0	17.6	22	28	27	22
17	.168E 18	7.40	266.6	.465E 17	.81	17.1	.349E 17	27.8	10.9	6.4	20.8	21	28	28	21
18	.168E 18	7.02	267.4	.517E 17	.84	22.2	.346E 17	30.8	12.0	8.3	20.6	21	27	26	20
19	.163E 18	7.16	274.2	.475E 17	1.03	17.5	.373E 17	29.1	14.4	6.4	22.9	22	24	23	19
20	.152E 18	7.14	265.1	.453E 17	.73	21.1	.399E 17	29.7	10.2	8.0	26.2	22	27	25	21
21	.131E 18	6.62	259.9	.552E 17	.98	13.5	.167E 17	42.2	14.8	5.2	12.8	22	27	26	21
22	.117E 18	6.27	246.1	.393E 17	.89	10.5	.166E 17	33.7	14.2	4.3	14.2	22	26	26	21
23	.969E 17	6.07	247.4	.201E 17	.62	10.1	.173E 17	20.7	10.2	4.1	17.9	22	27	27	21

Table 15e. Monthly Mean Statistics.

YEAR=74 MONTH= 3

	MEAN MEASUREMENTS			RMS RESIDUALS				DAYTIME RMS % ERRORS				NO.POINTS			
UT	NT	F0F2	HM	NT(PRED)	F0F2	HM	NT(UPDT)	NT(P)	F0F2	HM	NT(U)				
0	.872E 17	5.58	257.0	.363E 17	1.21	9.7	.227E 17					31	30	28	30
1	.577E 17	4.39	265.1	.240E 17	.97	31.0	.118E 17					31	30	30	30
2	.456E 17	3.85	310.4	.167E 17	.63	29.3	.717E 16					31	31	29	31
3	.444E 17	3.83	326.6	.129E 17	.68	28.8	.105E 17					31	29	27	29
4	.434E 17	3.82	322.3	.109E 17	.55	17.6	.128E 17					31	29	28	29
5	.408E 17	3.79	311.6	.909E 16	.54	17.8	.113E 17					31	30	29	30
6	.407E 17	3.79	295.4	.818E 16	.50	23.3	.109E 17					31	31	30	31
7	.401E 17	3.68	294.6	.863E 16	.36	19.4	.815E 16					31	30	30	30
8	.378E 17	3.62	299.3	.904E 16	.45	21.1	.981E 16					31	29	29	29
9	.352E 17	3.35	305.4	.822E 16	.48	23.5	.798E 16					31	30	30	30
10	.329E 17	3.18	309.2	.868E 16	.58	27.7	.655E 16					31	29	29	29
11	.290E 17	3.15	302.5	.154E 17	.50	41.1	.112E 17					31	30	29	30
12	.648E 17	4.70	262.3	.165E 17	.73	20.4	.231E 17					30	30	29	30
13	.101E 18	5.76	263.6	.288E 17	.90	44.3	.244E 17	28.6	15.7	16.8	24.2	31	28	28	28
14	.131E 18	6.35	260.9	.342E 17	1.04	24.6	.305E 17	26.1	16.4	9.4	23.3	31	27	24	27
15	.156E 18	6.47	280.9	.373E 17	1.01	45.7	.262E 17	23.9	15.5	16.3	16.7	30	28	27	27
16	.185E 18	6.97	281.9	.414E 17	1.07	34.2	.314E 17	22.4	15.3	12.1	17.0	30	28	27	27
17	.204E 18	7.46	300.1	.568E 17	.97	27.4	.335E 17	27.8	13.0	9.1	16.4	30	28	27	27
18	.213E 18	7.68	305.9	.681E 17	1.14	29.7	.408E 17	32.0	14.8	9.7	19.1	31	30	29	30
19	.213E 18	7.80	293.9	.832E 17	1.19	21.2	.487E 17	39.2	15.2	7.2	22.9	30	31	30	30
20	.201E 18	7.78	291.0	.848E 17	1.40	21.2	.412E 17	42.3	18.0	7.3	20.5	31	30	30	30
21	.175E 18	7.61	280.1	.678E 17	1.27	14.5	.484E 17	38.6	16.7	5.2	27.6	31	31	31	31
22	.148E 18	7.20	262.1	.533E 17	1.05	17.8	.391E 17	36.0	14.6	6.8	26.4	31	31	31	31
23	.122E 18	6.61	256.9	.504E 17	1.29	11.7	.297E 17	41.3	19.5	4.6	24.3	31	30	28	30

Table 15f. Monthly Mean Statistics.

YEAR=74 MONTH= 4

UT	MEAN MEASUREMENTS NT	FOF2	HM	RMS RESIDUALS NT(PRED)	FOF2	HM	NT(UPDT)	DAYTIME RMS % ERRORS NT(P)	FOF2	HM	NT(U)	NO.POINTS			
0	.112E 18	6.04	274.1	.492E 17	1.10	20.8	.255E 17					29	25	25	24
1	.816E 17	5.14	262.5	.346E 17	.98	27.1	.141E 17					29	25	25	24
2	.605E 17	4.42	284.8	.259E 17	.76	24.9	.135E 17					29	23	23	22
3	.498E 17	4.19	317.2	.226E 17	.66	26.8	.130E 17					29	27	27	26
4	.458E 17	4.03	330.9	.186E 17	.55	24.9	.124E 17					29	27	27	26
5	.442E 17	3.90	314.2	.141E 17	.55	21.1	.941E 16					29	26	26	25
6	.428E 17	3.93	308.6	.127E 17	.61	17.5	.104E 17					29	26	26	25
7	.424E 17	3.90	306.8	.127E 17	.63	21.1	.116E 17					29	26	25	25
8	.396E 17	3.76	298.4	.126E 17	.64	26.6	.132E 17					29	26	26	25
9	.339E 17	3.34	317.4	.125E 17	.58	32.4	.921E 16					29	25	25	24
10	.300E 17	3.16	315.3	.152E 17	.51	32.9	.803E 16					29	24	24	23
11	.398E 17	3.64	277.6	.217E 17	.45	24.7	.155E 17					29	26	26	25
12	.789E 17	5.07	272.2	.211E 17	.68	23.0	.267E 17					29	26	26	25
13	.104E 18	5.59	282.9	.299E 17	.97	54.6	.298E 17	28.9	17.4	19.3	28.8	29	28	28	27
14	.122E 18	5.92	301.1	.292E 17	.93	59.9	.309E 17	23.9	15.8	19.9	25.4	29	24	24	23
15	.145E 18	6.18	319.7	.339E 17	.89	52.5	.238E 17	23.4	14.4	16.4	16.4	29	22	22	22
16	.168E 18	6.59	336.1	.462E 17	1.04	42.9	.314E 17	27.5	15.8	12.8	18.7	27	22	22	20
17	.200E 18	7.24	336.4	.561E 17	1.23	34.1	.444E 17	28.0	16.9	10.1	22.1	29	24	23	23
18	.216E 18	7.75	321.8	.682E 17	1.43	33.2	.730E 17	31.6	18.4	10.3	33.8	29	26	26	25
19	.202E 18	7.88	308.1	.748E 17	1.21	28.8	.741E 17	37.0	15.4	9.3	36.6	29	25	25	24
20	.187E 18	7.68	302.8	.722E 17	1.22	32.4	.762E 17	38.6	15.9	10.7	40.8	29	26	26	25
21	.164E 18	7.38	288.8	.729E 17	1.11	18.9	.755E 17	44.5	15.0	6.5	46.1	29	27	26	26
22	.144E 18	6.96	287.3	.714E 17	1.14	29.8	.594E 17	49.6	16.4	10.4	41.2	29	25	25	24
23	.134E 18	6.55	286.7	.603E 17	1.25	29.4	.409E 17	44.9	19.1	10.3	30.5	29	25	25	24

Table 15g. Monthly Mean Statistics.

YEAR=74 MONTH= 5

UT	MEAN MEASUREMENTS NT	FOF2	HM	RMS RESIDUALS NT(PRED)	FOF2	HM	NT(UPDT)	DAYTIME RMS % ERRORS NT(P)	FOF2	HM	NT(U)	NO.POINTS			
0	.147E 18	6.62	278.0	.582E 17	1.13	7.2	.306E 17					7	6	6	6
1	.108E 18	6.10	266.9	.441E 17	.95	28.6	.297E 17					7	6	6	6
2	.789E 17	4.96	298.1	.340E 17	.96	34.1	.218E 17					7	5	5	5
3	.697E 17	4.71	330.9	.219E 17	.77	31.2	.170E 17					7	7	7	7
4	.683E 17	4.66	336.6	.210E 17	.83	32.2	.155E 17					7	7	7	7
5	.660E 17	4.36	326.9	.223E 17	.75	29.7	.174E 17					7	5	5	5
6	.626E 17	4.43	309.8	.248E 17	1.13	24.2	.145E 17					7	7	7	7
7	.565E 17	4.13	308.1	.134E 17	.72	24.7	.124E 17					7	7	7	7
8	.498E 17	4.11	309.8	.834E 16	.84	25.6	.204E 17					7	7	7	7
9	.393E 17	3.58	330.2	.728E 16	.40	34.0	.117E 17					7	6	6	6
10	.342E 17	3.45	331.3	.149E 17	.26	50.3	.118E 17					7	6	6	6
11	.611E 17	4.38	264.2	.145E 17	.69	16.2	.263E 17					7	6	6	6
12	.101E 18	5.22	279.5	.248E 17	1.01	28.7	.244E 17					7	6	6	6
13	.134E 18	5.32	275.9	.325E 17	.93	25.5	.221E 17	24.2	17.6	9.2	16.5	7	5	5	5
14	.161E 18	6.00	300.6	.470E 17	1.64	47.8	.277E 17	29.2	27.4	15.9	17.2	7	4	4	4
15	.187E 18	7.20	306.7	.662E 17	1.92	18.4	.438E 17	35.4	26.7	6.0	23.4	7	4	4	4
16	.207E 18	7.80	316.6	.718E 17	2.02	16.4	.456E 17	34.7	25.9	5.2	22.1	7	4	4	4
17	.203E 18	7.84	337.7	.634E 17	1.72	23.7	.458E 17	31.2	22.0	7.0	22.6	6	5	5	4
18	.204E 18	8.30	328.0	.716E 17	2.01	18.3	.555E 17	35.0	24.2	5.6	27.2	6	5	5	4
19	.204E 18	7.73	326.0	.726E 17	1.49	26.0	.621E 17	35.6	19.3	8.0	30.5	6	6	6	5
20	.195E 18	7.47	324.3	.739E 17	.98	25.8	.682E 17	37.9	13.1	8.0	35.0	6	6	6	5
21	.186E 18	7.27	330.1	.749E 17	1.10	35.3	.810E 17	40.2	15.2	10.7	43.5	6	6	6	6
22	.179E 18	7.44	314.9	.749E 17	1.18	37.8	.739E 17	41.8	15.9	12.0	41.2	6	5	5	5
23	.171E 18	7.40	291.7	.640E 17	1.05	14.6	.679E 17	37.5	14.2	5.0	39.8	6	5	5	5

Table 6. Daytime RMS Percent Errors (for 8-18 hours local time).

Time Period	Daytime RMS Percent Errors and Number of Observations for							
	N_T Predicted	No.	N_T Updated	No.	f_oF2	No.	h_m	No.
Nov 73	--	0	--	0	13.7	233	5.0	233
Dec 73	21.8	132	19.7	121	9.9	121	7.3	121
Jan 74	28.4	339	19.1	300	12.5	302	6.9	302
Feb 74	30.7	242	20.3	232	11.6	296	7.0	289
Mar 74	33.3	337	22.1	318	16.0	322	10.3	312
Apr 74	35.5	317	32.7	263	16.5	274	13.0	272
May 74	34.9	70	31.4	51	20.8	55	9.0	55
Nov 73 - May 74	31.5	1437	24.0	1285	14.2	1603	8.6	1584
Jan 74- Mar 74	30.9	918	20.6	850	13.6	920	8.3	903

APPENDIX B

Brief Plan Regarding the Collection, Intercomparison, and Analysis of the INTASAT Worldwide Data

The NASA Space Science Data Center is not at present, scheduled to receive any polarimeter data from INTASAT. It is suggested that the NSSDC request this data from the worldwide users of INTASAT in the same way that they do with many other international satellite experiments. The format should be compatible with the NSSDC computers and be on magnetic tapes or punched cards.

The data should be collected from users throughout the world and could provide a unique data base for many ionospheric investigations. It has been suggested that the data could be used for modeling the total electron content (TEC) on a worldwide basis, but we do not recommend this because much larger and more comprehensive data bases of f_oF2 already exist from which TEC can be deduced.

The data could be used for investigating traveling ionospheric disturbances or sudden ionospheric disturbances. Such areas of research are of particular interest at the present time for the development of two global navigation satellite systems, GPS and AEROSAT. In these areas the behavior and movement of ionospheric disturbances are important. If two or more INTASAT users are simultaneously recording Faraday data from INTASAT, then the disturbances can be monitored along these two or more different paths through the ionosphere as the satellite moves across the sky. These results will provide a unique analysis tool for such effects.

Comparisons of INTASAT data from its low orbit could also be made with similar Faraday satellites and two frequency satellites such as ATS-F and Timation II at highter orbits. Analysis of TEC above 1500 km could be undertaken along with the investigation of Faraday factor errors using group delay and Faraday techniques.

The unmodeled part of the ionosphere just above the height of the maximum of the F2 layer in the Bent model could also be investigated in detail around the world rather than at the few sites on the continental United States reported in the model description.

REFERENCES

1. R. B. Bent, S. K. Llewellyn, M. K. Walloch, "Description and Evaluation of the Bent Ionospheric Model", SAMSO TR-72-239, October, 1972.

2. S. Chapman & J. Bartels, "Geomagnetism," Vol II, Oxford at the Clarendon Press (1962).

3. D. C. Jensen & J. C. Cain, "Iterim Geomagnetic Field," J. Georgr. Res., No. 9, 3568-3569 (August, 1962).

4. J. A. Klobuchar, M. J. Mendillo, "Model Studies of the Conversion of Faraday Rotation Measurements from a Geostationary Satellite to Total Electron Content," JSSG Report No. 4, October, 1971.